

Analysis of Mating Circuitry in The Fungal Pathogen *Candida albicans*

Yuan Sun

A Thesis
in
The Department
of
Biology

Presented in Partial Fulfillment of the Requirements
for the Degree of
Doctor of Philosophy (Biology) at
Concordia University
Montreal, Quebec, Canada

October 2016

© Yuan Sun, 2016

CONCORDIA UNIVERSITY
School of Graduate Studies

This is to certify that the thesis prepared

By: Yuan Sun

Entitled: Analysis of Mating Circuitry in The Fungal Pathogen *Candida albicans*

and submitted in partial fulfillment of the requirements for the degree of

Doctor of Philosophy (Biology)

complies with the regulations of the University and meets the accepted standards with respect to originality and quality.

Signed by the final Examining Committee:

_____	Chair
<i>Chair's name</i>	
_____	External Examiner
<i>Examiner's name</i>	
_____	External to Program
<i>Examiner's name</i>	
_____	Examiner
<i>Dr. A. Piekny</i>	
_____	Examiner
<i>Dr. C. Brett</i>	
_____	Thesis Supervisor
<i>Dr. M. Whiteway</i>	

Approved by _____
Dr. G. Brown (Graduate Program Director)

_____ 2016 _____
Dr. A. Roy (Dean of Faculty of Arts and Science)

Abstract

Analysis of Mating Circuitry in The Fungal Pathogen *Candida albicans*

Yuan Sun, Ph.D.

Concordia University, 2016

It has been proposed that the ancestral fungus was mating competent and homothallic. However, many mating competent fungi were initially classified as asexual because their mating capacity was hidden behind layers of regulation. For efficient *in vitro* mating, the essentially obligate diploid ascomycete pathogen *Candida albicans* has to homozygose its mating type locus from *MTLa/α* to *MTLa/a* or *MTLα/α*, and then undergo an environmentally controlled epigenetic switch from the white form to the mating competent opaque form (white opaque switch). These requirements greatly reduce the potential for *C. albicans* mating. In this thesis, I used a mutant library to screen genes involved in white to opaque switching in the *MTLa/α* background, which allowed us to focus on the barriers of mating in *C. albicans* (Chapter 2 to 5). Construction of the mutant library is described as an appendix. Heterotrimeric G proteins are an important class of eukaryotic signaling molecules that have been identified as central elements in the pheromone response pathways of many fungi. As well, I did genetic studies on G proteins of the mating pheromone pathway in *C. albicans* (Chapter 6).

Chapter 2 discusses how deletion of the YciI domain gene *OFRI* allows the bypass of the need for *C. albicans* cells to homozygose the mating type locus prior to switching to the opaque form and mating, and allows homothallic mating of *MTL* heterozygous strains. Transcriptional profiling of *ofr1* mutant cells shows that in addition to regulating cell type and mating circuitry, Ofr1 is needed for proper regulation of histone and chitin biosynthesis gene expression. It appears that *OFRI* is a key regulator in *C. albicans*, and functions in part to maintain the cryptic mating phenotype of the pathogen. Chapter 3 describes the gene termed *OFR2*, which affects the formation of lipid droplets, white opaque switching and mating. Chapter 4 discusses how the different transcripts of *ORF19.7060* in white and opaque states play a role in white opaque

switching and mating. Chapter 5 describes how the F1-ATPase chaperon *ATP12* regulates white opaque switching and carbon metabolism.

In Chapter 6, disruption of the *STE18* gene which encodes a potential γ subunit of a heterotrimeric G protein was shown to cause sterility of *MTLa* mating cells and to block pheromone-induced gene expression and shmoo formation; deletion of just the C-terminal CAAX box residues is sufficient to inactivate Ste18 function in the mating process. Intriguingly, ectopic expression behind the strong *ACT1* promoter of either the $G\alpha$ or the $G\beta$ subunit of the heterotrimeric G protein is able to suppress the mating defect caused by deletion of the $G\gamma$ subunit and restore both pheromone-induced gene expression and morphology changes.

Acknowledgments

I would like to thank my supervisor, Dr. Malcolm Whiteway, for his guidance, encouragement, support, and patience during the entire course of the research and thesis work. He is always willing to provide me help and guidance to move the research forward. I would also like to thank Dr. Alisa Piekny and Dr. Christopher Brett for serving on my thesis committee and for their valuable comments. I would like to extend my special thanks to the Whiteway lab research group members, including former group members Dr. Pierre Cote, Yaolin Chen and Dr. Hannah Regan, in the discussions with them, many problems during my thesis research are solved. I am grateful for the professors, staffs and students from the Biology department. Without them, graduate life would have never been the same. Finally, I express my gratitude to my parents, my friends especially Qingchuan Zhao and Junfeng Gao, my boyfriend Yi Zhang and my dog Fubao and Wiggles for their love, support, encouragement and loyalty during my life.

Table of contents

List of Figures	viii
List of Tables	ix
List of abbreviations.....	x
Chapter 1: Introduction	1
1.1 A brief introduction of <i>Candida albicans</i>	1
1.1.1. Phenotype switching in <i>Candida albicans</i>	3
1.2 Mating in <i>Candida albicans</i>	5
1.3 <i>C. albicans</i> laboratory strains and lineages.....	8
Chapter 2: Deletion of a Yci1 domain protein of <i>Candida albicans</i> allows homothallic mating in <i>MTL</i> heterozygous cells.....	10
2.1 Introduction	10
2.2 Materials and Methods.....	12
2.3 Results.....	20
2.4 Discussion.....	35
Chapter 3: Ofr2 regulates white opaque switching and lipid droplets.....	39
3.1 Introduction	39
3.2 Materials and Methods.....	40
3.3 Results.....	45
3.4 Discussion.....	50
Chapter 4: Transcripts of <i>ORF19.7060</i> modulate white opaque switching.....	53
4.1 Introduction	53
4.2 Materials and Methods.....	54
4.3 Results.....	60
Chapter 5: ATPase chaperone Atp12 is involved in white opaque switching of <i>Candida albicans</i>	4
5.1 Introduction	4
5.2 Materials and Methods.....	4
5.4 Discussion.....	5
Chapter 6: Ste18p is a positive control element in the mating process of <i>Candida albicans</i>	7

6.1 Introduction	7
6.2 Materials and Methods.....	9
6.3 Results.....	15
6.4 Discussion.....	21
Chapter 7: Conclusions and Future work.....	24
Appendix: Construction of new strain library.....	28
Construction of GRACE version 1.0 library	28
Chapter 8: References.....	31

List of Figures

Figure 1.1 Signal pathway response to environmental factors leading to hyphal specific gene expression.	4
Figure 1.2 White- opaque switching circuitry	6
Figure 1.3 The switch from white-to-opaque responds to environmental factors through regulated pathways.....	7
Figure 1.4 Mating in <i>Candida albicans</i>	8
Figure 1.5 The lineages of <i>C. albicans</i> strains used in this study	9
Figure 2.1 <i>ofr1</i> mutants undergo white-opaque switching on YCB-GlcNAc.....	21
Figure 2.2 Bioinformatics analysis of OFR1.....	22
Figure 2.3 Microscopy.....	24
Figure 2.4 Mating ability of <i>ofr1</i> mutant	29
Figure 3.1 White opaque switching of <i>ofr2</i> null mutant.....	46
Figure 3.2 Mating ability of <i>ofr2</i> mutant	48
Figure 3.3 Protein sequence alignments among Ofr2, Ast1 and Ast2	49
Figure 3.4. Fluorescence microscopy of lipid droplets	50
Figure 4.1. White-opaque switching with mutated OFR3	61
Figure 4.2. Mating ability of <i>ofr3</i> mutant.....	1
Figure 5.1 White opaque switching of <i>atp12</i> null mutant	1
Figure 5.2. Growth curve of <i>atp12</i> compared with WT	5
Figure 6.1 Alignment of candidate G protein γ subunit sequences encoded by 14 species of ascomycete yeasts	16
Figure 6.2 <i>Ste18</i> null mutant strains are sterile.....	17
Figure 6.3 Transcriptional response to pheromone treatment.....	18
Figure 6.4 Strains with C termini of CaG γ subunits (CCTIV) deleted are sterile	19
Figure 6.5 Ectopic expression the <i>STE4</i> gene in a <i>ste18</i> Δ strain reverts the sterile phenotype.....	20
Figure 6.6 Ectopic expression of the <i>CAG1</i> gene in a <i>ste18</i> Δ strain reverts the sterile phenotype	20
Figure A.1 Strain arrangement of GRACE 1.0 collection.	30

List of Tables

Table 2.1 Strains used in this study.....	14
Table 2.2 Primers used in this study.	16
Table 2.3 Ratio of white-opaque switching	26
Table 2.4 Quantitative mating assays	28
Table 2.5 Highlighted significant genes in white cells of the <i>ofr1</i> null mutant compared with white cells of the wild-type reference strain	32
Table 2.6 Highlighted significant genes in opaque cells compared with white cells of the <i>ofr1</i> null mutant	35
Table 3.1 Strains used in this study.....	41
Table 3.2 Primers used in this study.	42
Table 3.3 Ratio of white to opaque switching of <i>ofr2</i> null mutant.....	47
Table 3.4 Ratio of opaque to white switching of <i>ofr2</i> null mutant.....	47
Table 4.1 Strains used in this study.....	55
Table 4.2 Primers used in this study.	57
Table 4.3 Ratio of white to opaque switching of <i>ofr3</i> null mutant.....	62
Table 4.4 Ratio of opaque to white switching of <i>ofr3</i> null mutant.....	63
Table 5.1 Strains used in this study.....	5
Table 5.2 Primers used in this study.	7
Table 5.3 Ratio of white to opaque switching of <i>atp12</i> null mutant.....	2
Table 5.4 Ratio of opaque to white switching of <i>atp12</i> null mutant.....	2
Table 6.1 <i>C. albicans</i> strains used in this study.....	10
Table 6.2 Oligonucleotides used in this work	11
Table 6.3 Quantitative mating of wild-type strain 3294 and mutant strains	21
Table A.1 Loss of heterozygosity of GRACE 1.0 library.	29

List of abbreviations

5-fluoroorotic acid	5FOA
Cyclic AMP- protein kinase A	cAMP-PKA
Clustered regularly interspaced short palindromic repeats	CRISPR
Endoplasmic reticulum	ER
Green fluorescent protein	GFP
Gene replacement and conditional expression	GRACE
N-Acetylglucosamine	GlcNAc
Loss of heterozygosity	LOH
Mitogen-activated protein kinase	MAPK
Mating type-like	MTL
Nourseothricin	NAT
Phosphate-buffered saline	PBS
Polymerase chain reaction	PCR
Room temperature	RT
Tetracycline	TET
Total internal reflection fluorescence	TIRF
Transcripts per million	TPM
Scanning electron microscope	SEM
Wild-type	WT
Yeast extract, peptone, dextrose	YPD

Chapter 1: Introduction

1.1 A brief introduction of *Candida albicans*

Based on Linnaean taxonomy, *Candida albicans* is from domain Eukarya, Kingdom Fungi, Division Ascomycota, Class Saccharomycetes, Order Saccharomycetales, Family Debaryomycetaceae and Genus *Candida* [1].

Candida albicans represents the most prevalent opportunistic fungal pathogen colonizing humans [2]. As a commensal yeast, *C. albicans* colonizes niches of the majority of the healthy people such as the tegumental, oral, gastrointestinal, and genital areas without causing any pathogenesis [3]. However, as an opportunist, it can cause annoying localized Candidiasis arising from growth of *C. albicans* due to the interrupted balance between the immune system of the host and the fungi [4]. Further, the fungi can cause systematic *Candida* infection in immunosuppressed people such as patients undergoing organ transplantation, people undergoing cancer chemotherapy, and AIDS patients [5]. Most women suffer from vaginal *Candidiasis* at least once in their lifetime [6]. Patients who suffer from systematic *Candida* infections are usually those who received intensive medical treatment such as invasive surgery [7]. Systematic *Candidiasis* is very dangerous; up to 40% of these infections may lead to the death of the patients. Even among survivors, *Candida albicans* will remain in niches of different organs and thus retain the opportunity to reinfect, and patients frequently have to be rehospitalized [7].

As a commensal yeast, *C. albicans* presents challenges for antifungal therapy [2]. Finding drug targets is an efficient way of obtaining better antifungal therapies and for testing new antifungal medicines. A library of mutants of *Candida albicans* is important for conducting such research. During the start of my research on this important human pathogen, I constructed a collection of mutant strains for easy and convenient assaying of antifungal drugs as well as for fundamental research.

As a pathogen, it is also important to understand the basics of the organism. The intriguing characteristics of its mating system and its ability for morphological switching that are the focus of my study can provide a better understanding of the evolution of ascomycetes and the strategies for adaptation to its host environment. These include white-opaque switching, a

distinct, spontaneous, reversible cell morphological transition of *C. albicans*, which is the essential prerequisite for gamogenesis of this fungus [8, 9].

Analysis of the mating pathway in *Candida albicans* has provided a series of high-impact papers, starting with the identification of the *MTL* locus derived from genome sequencing in 1999 and the proof of mating in derived *MTL* homozygotes in a pair of 2000 papers in Science [10, 11]. Further work has led to the establishment that the previously enigmatic opaque cell form represented the mating competent state of the pathogen [12], that the transcriptional control of the opaque epigenetic state involved a *Wor1* regulated circuit [13, 14], and that same-sex mating could occur in the pathogen [15].

A continuing puzzle in this interesting story has been the way the complex signaling process required for mating is apparently hidden behind layers of regulation. To unlock the mating potential first requires a cell to be homozygous at the *MTL* locus. However, the vast majority of clinical isolates of *C. albicans* are *MTL* heterozygotes, and thus they must first undergo a rare homozygosis event. After this event, the standard white cell form then has to switch to the opaque state, another low frequency event that is made even less likely by the fact that the process is inhibited at the temperature of the pathogen's mammalian host. Even if a *C. albicans* cell enters the mating competent opaque state, it has to await the chance meeting of a mating competent partner of the opposite type generated by the same rare combination of events. So the *C. albicans* cell seems to have developed circuitry that makes the use of its mating machinery infrequent under natural conditions. Why maintain a complex mating system that the cell seems unlikely to be able to use? Perhaps the most likely answer is we really do not know all the key details of how mating is actually controlled.

To decode the mating mysteries of this fungal pathogen, I have focused on two major themes. In the first, I have made use of recently developed collections of mutant strains that allow cellular processes in *C. albicans* to be probed genetically. I looked for mutants that would allow the *MTL* heterozygous form of the pathogen to switch to the opaque state, in effect bypassing one of the normal blocks to mating. In the second, I studied details of the G protein coupled pheromone response MAPK pathway in *C. albicans*.

1.1.1. Phenotype switching in *Candida albicans*

Candida albicans faces multiple variations in host niches and threats from the ambient environment and has to make frequent cell decisions by responding to signals to ensure population survival [16]. As a pathogen, its success stems not only from its ability to generate an opportunistic infection when the host physiological environment and habitat niche change, but also from its capacity to grow and transition to different morphological forms including unicellular yeast, pseudohyphae and elongated hyphae [17]. In certain conditions, communities of *C. albicans* can also form biofilms [18]. As well, *C. albicans* has a specific cell phenotypic transition within the yeast form termed white opaque switching [19]. This transition is crucial for its gamogenesis [12]. The phenotypic transitions of yeast-hypha, white-opaque and even biofilm formation play critical roles in host adaptation, sexual reproduction, and virulence.

White opaque switching was first identified in a *C. albicans* isolate WO-1, isolated from a clinical patient who died of systematic infection after organ transplantation [19]. White and opaque phases have a variety of different properties, including differences in cellular morphology, staining with phloxine B, systemic and cutaneous infection, adhesion, surface antigenicity and specific gene expression profiles [20]. Under the optical microscope, white cells appear round or ovoid and opaque cells are elongated with a large vacuole and are bigger than white cells [21]. Based on transmission electron microscopy observations, opaque cells have unique pimples on the surface of the cell walls with channels traversing them from the plasma membrane [22]. On agar medium, white cell phase colonies appear white and smoother, while opaque cells form gray and flatter colonies [20]. When Phloxine B is added into the agar medium, opaque colonies become very distinguishable, forming pink colonies while white cell colonies stay white because of permeability differences of their cell walls [19, 23]. Usually, the white-opaque transition is regulated by Wor1, which is itself under $\alpha 1$ - $\alpha 2$ repression [13, 14]. Opaque cell filamentation has recently been discovered; this does not occur under the hyphal inductive conditions characteristic of white cells but can occur during growth on sorbitol, SLAD or GlcNAc medium at 25 °C, or can be induced by organic acids [24, 25]. Opaque cell filamentation is regulated through the cAMP-PKA pathway, the pH sensing pathway and by other transcription factors such as Bcr1, Nrg1, and Rfg1 [25].

The most frequent phenotype switching in *Candida albicans* is the morphological transition between yeast and hyphae [2]. This process has been well studied because it has been suggested that the yeast form allows *C. albicans* to spread easily through the blood stream to quickly occupy important organs while the fast transition to hyphal forms allows invasive growth within deep niches of the organs, causing difficulties and challenges for clinical treatment [26]. Both phenotypes are important for virulence. In response to various environmental factors, *C. albicans* can regulate hyphal-specific gene expression through several pathways; the two major being the cAMP-PKA (shown in Fig.1.1 black arrow pathway) and MAPK (see green and blue arrow pathway in Fig.1.1) pathways, as well as through a series of transcription factors [17, 27].

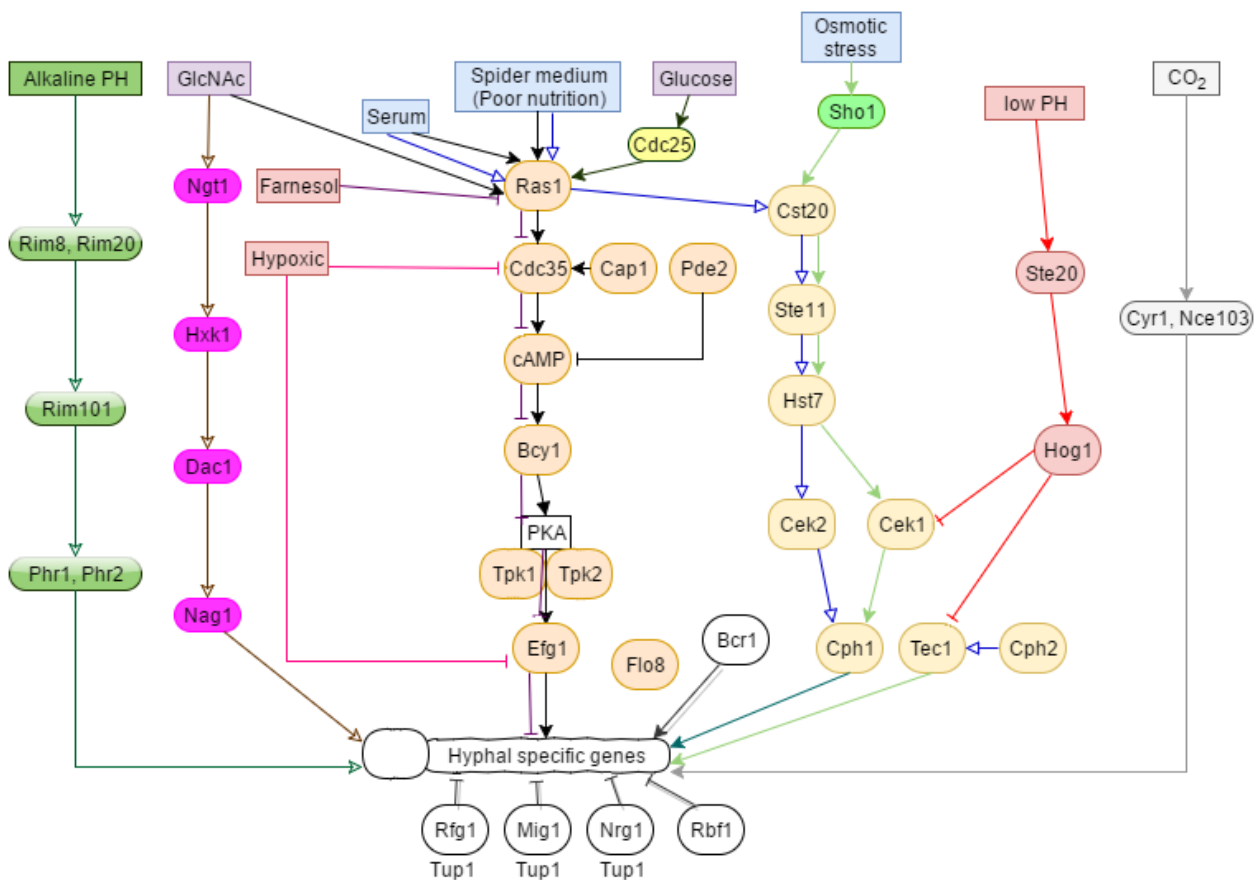


Figure 1.1 Signal pathway response to environmental factors leading to hyphal specific gene expression. The arrows represent activation and the bars represent repression. Different pathways are coloured with different lines. Proteins with the white background are transcription factors.

1.2 Mating in *Candida albicans*

1.2.1. Mating type of *C. albicans*

Cells of *Candida albicans* are natural diploids [28]. The mating type of *C. albicans* is controlled by the *MTL* (mating type-like) locus. The *MTL* locus, located on chromosome 5, contains two alleles, *MTL \mathbf{a}* and *MTL α* . Typically, *C. albicans* is a diploid heterozygous at this mating type locus (*MTL \mathbf{a}/α*) [10]. Each locus contains a set of genes that include transcription regulators termed **a1**, **a2** (at *MTL \mathbf{a}*), and $\alpha 1$, $\alpha 2$ (at *MTL α*) respectively. $\alpha 1$ and **a2** are homeodomain proteins [29]. The $\alpha 1$ protein activates the α -specific genes, while **a2** is the positive regulator of the **a**-specific genes. As well, the two homeodomain proteins **a1**- $\alpha 2$ form a heterodimer to repress the expression of homozygous-specific genes, such as mating-related genes and white-to-opaque transition-related genes (Fig. 1.3) [13]. Though it is thought that *Candida albicans* shared a common ancestor with *Saccharomyces cerevisiae* about 100 to 800 million years ago, and they share the three homologs of **a1**, $\alpha 1$, and $\alpha 2$, *C. albicans* encodes an extra transcriptional regulator **a2** at *MTL \mathbf{a}* , as well as the non-mating related genes *PAP*, *PIK* and *OBP* at the *MTL* locus (Fig. 1.3) [30].

1.2.2. A strategy for *C. albicans* to mate efficiently: switch from white to opaque

Wor1 was identified as a key regulator of white-to-opaque switching that was controlled by **a1**- $\alpha 2$ repression [14]. Deletion of *WOR1* blocks the transition to opaque cells in *MTL* homozygotes and ectopic expression of *WOR1* can induce white-to-opaque switching in the *MTL \mathbf{a}/α* background [13, 14]. *WOR1* is in a bistable expression loop that is driven by feedback regulation (Fig. 1.2). The positive feedback loop makes opaque cells stable after several cell divisions, and the negative feedback loop makes the white-to-opaque transition easily reversible due to the influence of environmental factors [14]. Other potential regulators may participate in the feedback loops to strengthen bistable expression of *WOR1*. To mate, diploid **a**/ α cells must homozygose *MTL* by either gene conversion or chromosome loss followed by duplication of the retained copy [20]. The switching is a unique step inserted before pheromone response in the mating process in *C. albicans* and its relatives *C. dubliniensis* and *C. tropicalis* [31, 32]. Even rare haploid strains of *C. albicans* selected through forced homozygosis of several loci still have to switch to the opaque phase to mate, and thus opaque represents the necessary mating competent state [33]. Only when environmental cues and conditions trigger the cells to enter the opaque phase

can cells of the opposite mating types undergo mating. There is no similar switching required for mating among other species of ascomycetes.

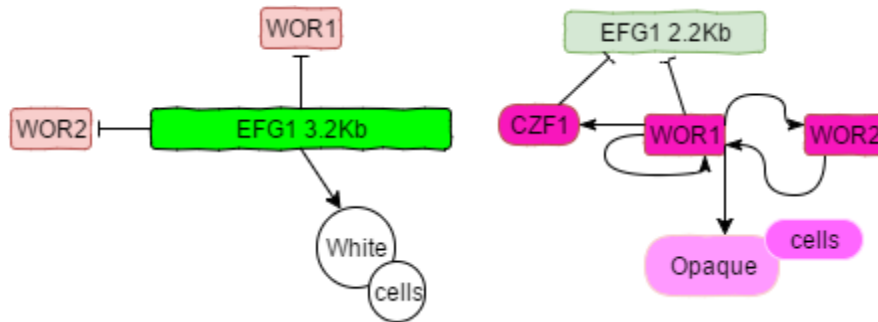


Figure 1.2 White- opaque switching circuitry. *EFG1* expresses two forms of transcripts in white and opaque cells. In white cells, *EFG1* produces the 3.2 Kb long form, which can repress the expression of master regulator *WOR1* as well as *WOR2* (white-opaque regulator 2). In opaque cells, *EFG1* expresses the 2.2 Kb short version of the transcript and the expression of *EFG1* is repressed by both *WOR1* and *CZF1*. *WOR1* can activate the expression of both *WOR2* and *CZF1*. *WOR1* and *WOR2* also strengthen the expression of *WOR1* [27, 34].

Switching of the white and opaque states can be affected by a series of environmental cues such as CO₂, carbon source, temperature, pH, and various stresses [17]. Opaque formation is favoured by room temperature (25°C), GlcNAc as the carbon source, 5% CO₂, low pH and low oxidative stress [27]. Even when cells of *C. albicans* are *MTL* homozygous they usually remain in the white phase except for spontaneous response to environmental factors through regulated pathways by activating the expression of *WOR1* (Fig. 1.4) [17, 27]. Efficient white-to- opaque switching will provide efficient mating.

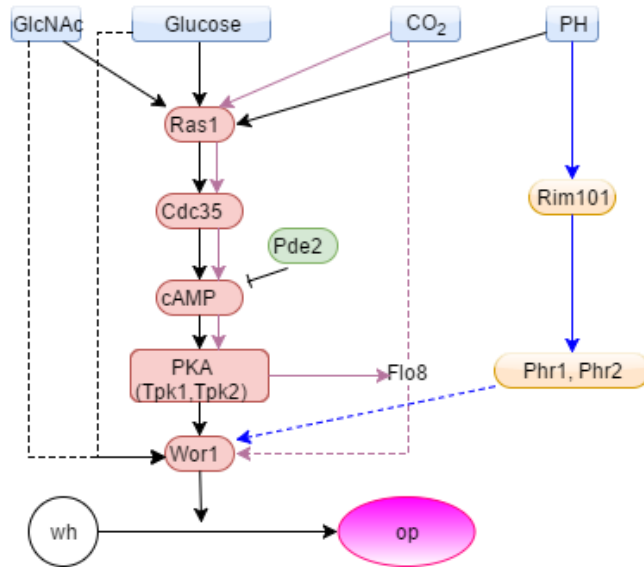


Figure 1.3 The switch from white-to-opaque responds to environmental factors through regulated pathways. The well-known pathway that regulates white-to-opaque switching is the cAMP-PKA pathway. GlcNAc, CO₂, and lower pH are environmental inducers of white-to-opaque switching; other regulatory pathways have not yet been clarified.

1.2.3. Pheromone response signalling: G protein and MAPK pathway

Candida albicans and *Saccharomyces cerevisiae* are both able to respond to sex pheromones and to mate; this mating process is directed by pheromone-mediated signalling in both organisms. In both these species, the presence of the sex pheromone from the opposite sex is transmitted to the cell nucleus through a signalling system consisting of a receptor-G protein module linked to a MAP kinase module [35]. Ste2/Ste3 are transmembrane pheromone receptors; Ste2 is the α pheromone receptor while Ste3 is the \mathbf{a} pheromone receptor [36]. The signal of the pheromone binding the receptor can be transduced to a heterotrimeric G protein comprised of the three subunits, G α , G β , and G γ [37]. The G protein activation transfers the signal to the MAPK pathway involving a MAP kinase module Cst20, Ste11, and Hst7 and the downstream Cek1/Cek2 and then Cph1 to regulate gene expression involved in pheromone response and mating (Fig. 1.3) [38]. *MFAl*, located on chromosome 2, encodes the \mathbf{a} pheromone precursor [39] and is highly expressed in response to the α pheromone. The α -factor precursor is encoded by *MFalpha* localized on chromosome 1 and is processed by Kex2 to create the active peptide [40, 41].

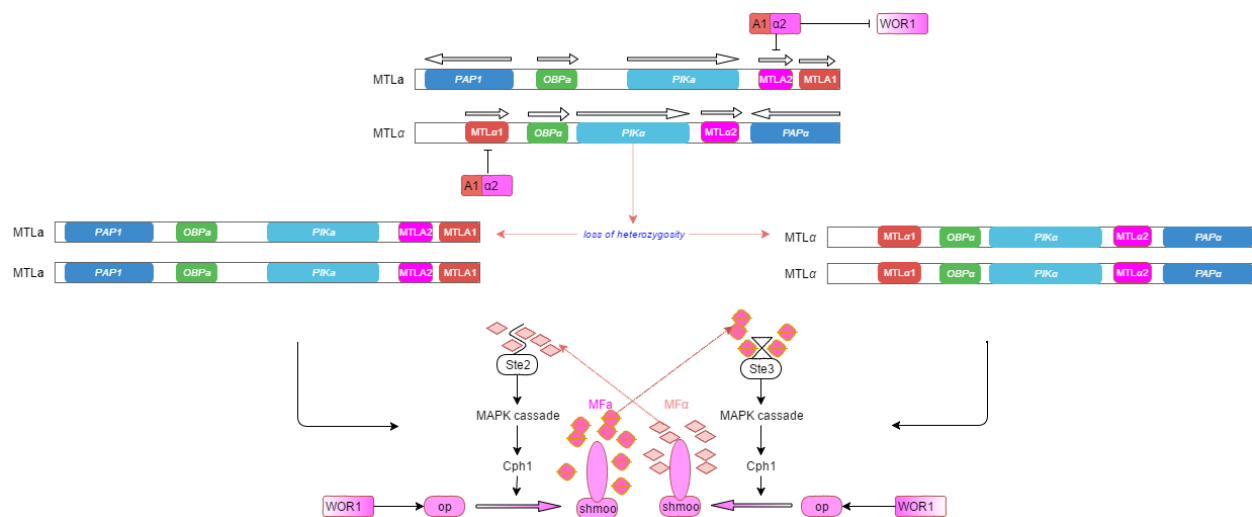


Figure 1.4 Mating in *Candida albicans*. *Wor1* is the master regulator of white-opaque switching. The expression of *WOR1* is repressed by the $\alpha 1$ - $\alpha 2$ corepressor. As well, $\alpha 1$ - $\alpha 2$ suppresses the expression of *MTL* homozygous specific genes activated by $\alpha 2$ and $\alpha 1$, such as *STE2*, *MFA1*, *STE3*, and *MF α* . After loss of heterozygosity at the *MTL* locus, *C. albicans* can no longer generate the $\alpha 1$ - $\alpha 2$ repressor. Then, *WOR1* is expressed to promote white-to-opaque switching and at the same time, the pheromone response pathway is turned on. In this way, opaque cells of *C. albicans* can undergo shmooing and mating. Non mating-related genes *PAP*, *PIK*, and *OBP* are also located at the mating type locus of *C. albicans*. As well as there being varied arrangements of these genes at the *MTL_a* and *MTL_α* loci, they share lower similarities of their DNA sequences (about 58% to 66%) than is typical for classical alleles in *C. albicans*.

1.3 *C. albicans* laboratory strains and lineages

1.3.1. *C. albicans* laboratory strain lineages

The lineages of strains used in this study are shown in Figure 1.5.

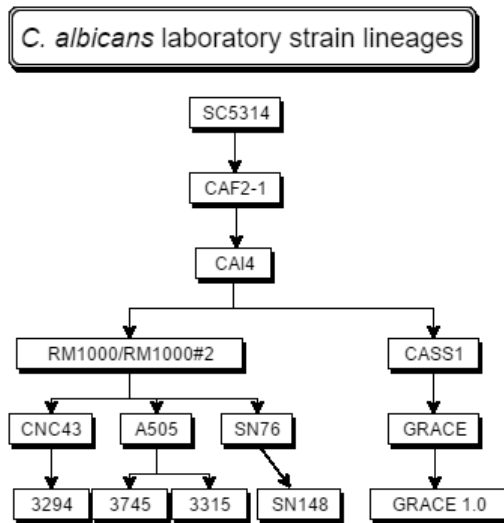


Figure 1.5 The lineages of *C. albicans* strains used in this study. *SC5314* is wild-type strain belonging to the predominant *C. albicans* clade that represents 40% of all clinical isolates worldwide. It is also the strain sequenced as the reference sequence. Wild-types used in this study are all standard laboratory strains derived from *SC5314*.

1.3.2. GRACE library

The GRACE (gene replacement and conditional expression) library is a non-redundant conditional mutant library that contains a total of 2357 different mutants [42]. The wild-type strain for the collection is CASS1 [43]. The GRACE strains have been designed with one copy of each regulated gene replaced and the other copy of the gene under tetracycline promoter-regulated transcriptional repression [42](Fig. 1.5).

Chapter 2: Deletion of a Yci1 domain protein of *Candida albicans* allows homothallic mating in *MTL* heterozygous cells

This Chapter was published as a manuscript in the journal mBio (Sun Y, Gadoury C, Hirakawa MP, Bennett RJ, Harcus D, Marcil A, Whiteway M. 2016. Deletion of a Yci1 domain protein of *Candida albicans* allows homothallic mating in *MTL* heterozygous cells. mBio 7(2):e00465-16. doi:10.1128/mBio.00465-16.). I am responsible for all the tables and figures except Figure 3.3(B) in this Chapter.

2.1 Introduction

Most eukaryotes, from yeasts to humans, are sexual, and gametogenesis has evolved to increase diversity and improve species survival. Within the ascomycete fungi the regulatory circuitries controlling mating are broadly similar, but the propensity for mating varies considerably. For fungi like *Saccharomyces cerevisiae*, heterothallic haploid cells are stable and mating is essentially constitutive for cells that are propagating vegetatively, so these cells couple mating to good environments [44, 45]. For fungi such as *Schizosaccharomyces pombe*, mating is linked to nutrient limitation or other stressful conditions; these cells initiate mating in response to negative conditions in the environment [46]. Other fungi such as *Candida albicans* successfully hid their sexuality until the genomic era [8]; in these fungi regulatory circuits demand very specific conditions for mating. Typically, *C. albicans* are diploid cells with the mating type \mathbf{a}/α . These cells must first undergo loss of the heterozygosity at the *MTL* locus to become \mathbf{a}/\mathbf{a} and α/α , and subsequently undergo an epigenetic switch to mating competency [9, 47]. This limits *C. albicans* mating under laboratory conditions to specific genetic constitutions and environments; it is less clear what the situation is under natural conditions.

C. albicans represents the most prevalent opportunistic fungal pathogen colonizing humans. As a commensal yeast, it presents challenges for antifungal therapy due in part to its morphological diversity and flexibility [2]. This flexibility includes the spontaneous and reversible cell morphological transition termed white-opaque switching, which is a prerequisite for gametogenesis and mating [20, 48]. The white and opaque phases have differing properties in various aspects of the pathogen's function, including its cellular morphology, staining with

phloxine B, roles in systemic and cutaneous infections, adhesion, surface antigenicity and specific gene expression profiles [20].

The mating type of *C. albicans* is controlled by the *MTL* (mating type-like) locus. This locus, located on chromosome 5, contains two alleles designated *MTLa* and *MTL α* [11]. Each locus contains a set of genes that include transcription regulators; **a1** and **a2** at *MTLa*, and *α 1* and *α 2* at *MTL α* . The *α 1* protein activates the *α* -specific genes, while **a2** activates the **a**-specific genes [30]. Furthermore, **a1** and *α 2* combine to form a complex that represses the expression of various mating-related genes as well as white-to-opaque switching genes [12]. *Wor1* was identified as the key regulator of white-to-opaque switching controlled by **a1**- *α 2* repression. Deletion of *WOR1* blocks the transition to opaque cells in *MTL* homozygotes whereas ectopic expression of *WOR1* can induce white-to-opaque switching in the *MTLa*/ *α* background. *WOR1* is in a bistable expression loop that is driven by feedback regulation; the positive feedback loop makes opaque cells stable after several cell divisions and the negative feedback loop makes the white-to-opaque transition easily reversible due to the influence of environmental factors [14, 49, 50].

Other potential regulators may participate in the feedback loops to strengthen the bistable expression of *WOR1*. Mating requires diploid **a**/ *α* cells to homozygose the *MTL* by either gene conversion or chromosome loss followed by duplication of the retained copy [20]. This switching circuit is a unique step inserted before pheromone response in the mating process in *C. albicans* and its relatives *C. dubliniensis* and *C. tropicalis* [32, 50, 51]. Even rare haploid strains selected through forced homozygosis of several loci still have to switch to the opaque phase to mate [33], and thus the opaque state represents the “mating competent” state. Only when environmental cues and conditions trigger the cells to enter the opaque phase can cells of the opposite sex then undergo mating. There is no similar switching required for mating among species of the *Saccharomyces* clade such as *S. cerevisiae*, *Kluyveromyces lactis* and *Saccharomyces paradoxus*; these strains appear constitutively mating competent.

Various conditions have been identified that reduce the requirement for *MTL* homozygosity in the activation of the opaque state. Repression of the hemoglobin response gene *HBRI*, which is the activator of the mating type locus gene *α 2*, allowed the mutant strains in the **a**/ *α* background to undergo white-opaque switching and mating as a type cells [52]. Recently,

some clinical *MTLa/α* isolates were identified that were capable of switching to opaque under specific conditions of 5% CO₂ with *N*-acetylglucosamine (GlcNAc) as the carbon source. Deletion of the transcriptional factors Brg1, Rfg1 and Efg1, which are involved in repressing the positive feedback loop of *WOR1*, also allow white-to-opaque switching in the 5% CO₂ /GlcNAc conditions [53]. As well, specific conditions have identified alternative states, termed grey and gut cells. Grey cells were first discovered from a clinical isolate that when grown on YPD plates generated smooth grey colonies, distinguishable from white and opaque colonies [54]. Grey cells were subsequently identified in different clinical isolates and shown to represent a third morphological type generated by a white-grey-opaque tristable switch controlled by Efg1 and Wor1. These grey cells have distinctive transcription profiles, but have similar cell morphologies to the opaque haploids. As well, gut cells were found in genetically engineered strains that constitutively overexpressed *WOR1* after cell passage through the murine gut; these cells have a transcriptome compatible with the conditions found in the digestive tract, but a morphology similar to opaque cells [55].

We have investigated further controlling elements of mating in *C. albicans*. Here we identified white-opaque switching cells from a library of *MTL a/α* strains that were mutant in non-conditional, non-essential genes and grown on GlcNAc agar medium. A strain defective in *orf19.5078* was identified as permitting efficient switching of *MTLa/α* cells to the opaque state. *ORF19.5078*, which we have designated *OFRI* for opaque formation regulator, has not previously been characterized and has no ortholog in *S. cerevisiae*. By reconstructing the *ofr1* null mutant (*ofr1Δ/Δ*), we established that the complete deletion mutant also has the ability to bypass normal regulation and undergo white-opaque switching on GlcNAc medium when in the *MTLa/α* state. These opaque cells are fully mating competent, and thus *OFRI* functions, in an environmentally dependent manner, to maintain the cryptic mating state of *C. albicans*.

2.2 Materials and Methods

2.2.1 Strains, media and culture conditions

A collection of 887 non-conditional strains inactivated for non-essential genes, termed the GRACE version 1.0 library (see appendix), was derived from the GRACE library of regulated disruptions [42] by identifying, through growth on 5-FOA medium [56], derivatives that had lost the transactivator cassette. This library was used to identify colonies that could undergo white to

opaque switching in the a/α background. The entire library collection was suspended in 20% glycerol-supplemented YPD medium and stocked in 96-well microtiter plates. Fully defrosted stock plates were mixed well on a microplate mixer and then robotically pinned to rectangular plates of GlcNAc agar medium containing phloxine B to identify dark-staining opaque cell sectors. The original GRACE library versions of candidates were then tested with and without tetracycline to confirm any mutants that triggered inappropriate white to opaque switching. Subsequently *C. albicans* strain SN148 was used as the parent strain to construct the complete *ofr1* Δ/Δ null mutant strain (See Table 2.1).

Table 2.1 Strains used in this study.

Strain	Parent	Mating type	Description	Source
SN148	SN76	<i>a/α</i>	<i>arg4/arg4; leu2/leu2; his1/his1; ura3 imm434/ura3 imm434; iro1 imm434/iro1 imm434</i>	Noble/Johnson
SN148a	SN148	<i>a/a</i>	<i>arg4/arg4; leu2/leu2; his1/his1; ura3 imm434/ura3 imm434; iro1 imm434/iro1 imm434</i>	Renjie Tang
GRACE version 1.0 library	GRACE library	<i>a/α</i>		Whiteway
GRACE library	CASS1	<i>a/α</i>		Merck
3315	A505	<i>α/α</i>	<i>trp1/trp1; lys2/lys2</i>	Magee
3745	A505	<i>a/a</i>	<i>trp1/trp1; lys2/lys2</i>	Magee
CAI4 <i>MTLa</i>	CAI-4	<i>a/a</i>	<i>ura3 ::imm434/ ura3 ::imm434</i>	Doreen Harcus
CAI4 <i>MTLa</i>	CAI-4	<i>α/α</i>	<i>ura3 ::imm434/ ura3 ::imm434</i>	Doreen Harcus
CP29-17CK13	CP29-1-7L4	<i>a/a</i>	<i>ura3/ura3 cpp1 ::hisG/cpp1 ::hisG; CEK1/cek1 ::hisGURA3-hisG</i>	Csank
<i>ys01</i>	SN148	<i>a/α</i>	<i>ofr1::HIS1/OFR1; arg4/arg4; leu2/leu2; ura3 imm434/ura3 imm434; iro1 imm434/iro1 imm434</i>	This study
<i>ys02</i>	<i>ys01</i>	<i>a/α</i>	<i>ofr1::HIS1/ofr1::URA3; arg4/arg4; leu2/leu2; iro1 imm434/iro1 imm434</i>	This study
<i>ys04</i>	<i>ys02</i>	<i>a/a</i>	<i>ofr1::HIS1/ofr1::URA3; arg4/arg4; leu2/leu2; iro1 imm434/iro1 imm434</i>	This study
<i>ys05</i>	<i>ys02</i>	<i>α/α</i>	<i>ofr1::HIS1/ofr1::URA3; arg4/arg4; leu2/leu2; iro1 imm434/iro1 imm434</i>	This study

For cultivation, YCB-media with glucose (2%) or GlcNAc (1.25%) were used. Plate cultures were grown at a density of 40-120 colonies per 90 mm plate. Other carbon sources, including galactose, fructose and mannitol, were used at 2%. For opaque colony identification, Phloxine B (5µg ml⁻¹) was added to the agar media. For routine liquid cultivation, YPD (1% yeast extract, 2% peptone and 2% glucose) was used.

2.2.2 Strain construction

OFRI was deleted by standard two-step disruptions using PCR products [35]. The markers *HIS1* and *URA3* were amplified by PCR from plasmids pFA-CaHIS1 and pFA-CaURA3 using primers that provided homology to the flanking regions of *OFRI*. The *HIS1* and *URA3* markers were sequentially transformed to the parent strain SN148 and transformants were selected on SD-*his*⁻ and SD-*ura*⁻ agar plates. Successful transformants were further confirmed by PCR. One pair of long oligonucleotides for deletion and three pairs of short oligonucleotides for confirmation were used for the PCR reactions (See Table 2.2).

Table 2.2 Primers used in this study.

Name	Description	Sequence (5' to 3')	Source
<i>OFRI</i> _F	<i>OFRI</i> deletion PCR cassette forward primer	ACAACCAGCTGAAAATTAGCATAAAGGAAAAGAAAGACAA AAGAGGGGATTCAAATCGAACACATAATGGTTGGTATAGA CGCAGCTAGTGCATTTGgaagcttcgtacgtgcaggtc	This study
<i>OFRI</i> _R	<i>OFRI</i> deletion PCR cassette reverse primer	AGAGACACAATGAACAATAAGTGTGGAGAGTTTGTACAAG CCATACAATCAGCAACTTCGGGATTTAAGAAGAATTTGCAA CAGCAATAACACCTtctgatcatcgtgaattcgag	This study
<i>OFRI</i> _ex_F	<i>OFRI</i> external forward primer	AGAGATGAACAATATGAGAG	This study
<i>OFRI</i> _ex_R	<i>OFRI</i> external reverse primer	TGGTGACCACGTTTGACAG	This study
<i>OFRI</i> _in_F	<i>OFRI</i> internal forward primer	TGACTTTACGATCATTGAGG	This study
<i>OFRI</i> _in_R	<i>OFRI</i> internal reverse primer	TAGATTCGTCAACACCATCC	This study
HIS1- F	<i>HIS1</i> forward primer	TTTAGTCAATCATTTACCAGACCG	This study
HIS1R	<i>HIS1</i> reverse primer	TCTATGGCCTTTAACCAGCTG	This study
URA3 -F	<i>URA3</i> forward primer	TTGAAGGATTAACACAGGGAGC	This study
URA3 -R	<i>URA3</i> reverse primer	ATACCTTTTACCTTCAATATCTGG	This study
MTLa F	<i>MTLa1</i> forward primer	TTGAAGCGTGAGAGGCAGGAG	Magee
MTLa R	<i>MTLa1</i> reverse primer	GTTTGGGTCCTTCTTTCTCATTC	Magee
MTLa F	<i>MTLa2</i> forward primer	TTCGAGTACATTCTGGTCGC	Magee
MTLa R	<i>MTLa2</i> reverse primer	TGTAACATCCTCAATTGTACCCG	Magee

2.2.3 Phenotype switching

White and opaque cells were all selected from single colonies on YCB-GlcNAc medium after five days at room temperature. Cells then were suspended in water, the cell concentration was adjusted, and the suspensions plated on agar media containing 5 $\mu\text{g ml}^{-1}$ phloxine B and different carbon sources. Plates were incubated at either 24°C or at 25°C with 5% CO₂. Data were collected and plates were scanned on the 7th day and the frequency of sectorized colonies calculated by standard statistical methods.

2.2.4 Microarrays

The wild-type SN148 and the *ofr1* Δ/Δ null mutant were selected from single colonies and grown in either YCB-glucose or YCB-GlcNAc liquid medium overnight at RT and then were diluted to OD₆₀₀=0.1 in fresh YCB-glucose or YCB-GlcNAc liquid medium. Cells were grown at RT until the culture reached an OD₆₀₀ between 0.8 and 1.2, harvested, and stored at -80°C until RNA extraction. Total RNA was isolated by the hot phenol method as described elsewhere [35] and mRNA was purified using the New England Biolabs polyA Spin mRNA isolation kit, then reverse transcription for cDNA production was followed by indirect cDNA labeling with amino-allyl dUTP for dye addition. Arrays were obtained from the NRC-BRI Microarray Facility; hybridization protocols were as described [35]. The microarray data are available in the Gene Expression Omnibus (GEO) with accession number GSE75780.

2.2.5 Microscopy and imaging

Optical microscopic images of cells were captured using a Nikon Eclipse TS100. Immunofluorescence microscopic images were visualized and photographed using Nikon Eclipse TiE with 400x magnification with settings: Objective: 100x Oil, Filter: TxRed-560/40, Dichroic beam splitter: bs585, Emission: 630/75, Ex wavelength: 555 nm using Multi-laser Heliophor and Camera: Photometrics Evolve. Images of plates and colonies were scanned at 800pi by an Epson Perfection v500 photo scanner.

2.2.6 Immunofluorescence

Cells from single colonies cultured for five days on SD agar medium at RT were pre-grown in SD liquid medium overnight at RT, 220 rpm shaking and then diluted in fresh SD liquid

medium for another 12 h incubation at RT, 220 rpm. Cells were fixed with 1/10 the volume of 37% formaldehyde (Fisher Scientific) in 1x PBS for 45 min at RT. The cells were pelleted and washed in 1 mL of 1xPBS twice for 45 mins and stored in PBS at 4°C. The pelleted cells were washed in 1 ml of 1x PBS for three times, two mins each time; approximately 10^7 cells were tested for each assay. Washed cells were blocked with 1ml blocking buffer for 30 mins before incubation with 100 µl of primary antibodies for another hour at RT. Cells were then washed with PBS containing 0.05%Tween 20 three times, five mins each time. Washed cells were incubated with 100 µl of the secondary antibody - Texas red conjugated goat anti-mouse antibody (1/100 dilution in blocking buffer) for 1 hour in the dark at RT. Cells were then washed with PBS containing 0.05%Tween 20 three times and PBS once, five mins each time. Cells were finally suspended in 50 µl PBS and 3 µl was applied for under a coverslip. Sampled microscope slides were sealed and placed in a microscope slide box for protection from light before observation under the Nikon_Ti fluorescence microscope.

2.2.7 Scanning Electron Microscopy

Cells were grown on YCB-GlcNAc agar plates for 72 hours at 25 °C, and then fixed with 2.5% (w/v) glutaraldehyde in 0.1 M sodium cacodylate buffer at 4°C overnight. Cells were then post-fixed with 1% aqueous osmium tetroxide for 90 minutes at room temperature. Following fixation, cells were dehydrated gradually using a 15% gradient ethanol series and subsequently dried using a critical point dryer. The samples were then coated with 20 nm of gold palladium (60:40) in an Emitech K550 sputter coater. Cells were imaged with a Hitachi S-2700 scanning electronic microscopy and collected with Quartz PCI software.

2.2.8 Mating assays

Cells were streaked on YCB-GlcNAc agar medium (with phloxine B) for 5 days at RT to select opaque colonies. Opaque cells of strains 3315 α and 3745 \mathbf{a} were used as the tester strains for mating. Opaque colonies of the *MTLa*/ α *ofr1* strain were restreaked as straight lines on separate YPD and YCB-GlcNAc agar plates as the experimental strain. Opaque cells of tester strains were streaked as straight lines on YPD plates. The two sets of tester and experimental streaks were patched onto the same YPD and YCB-GlcNAc agar plates separately after 48 hours of incubation at room temperature (RT). After 24 hours of incubation on YPD plates and 48 hours incubation on YCB-GlcNAc plates at RT, cells were replicated onto YCB-Glucose

selection medium lacking leucine, uridine, tryptophan and lysine for prototrophic selection. All the plates were incubated at 30°C for 3 days before scanning and restreaking on the selection medium for further confirmation of stable prototrophic colonies [57].

Quantitative mating assays were done in liquid YCB-GlcNAc medium. Opaque cells of strains 3315 α and 3745 \mathbf{a} were used as the tester strains for mating; SN148 \mathbf{a}/α cells and SN148 \mathbf{a} opaque cells were used as negative and positive controls. Opaque cells of 3315 α , 3745 \mathbf{a} , SN148 \mathbf{a} and *ofr1* \mathbf{a}/α were selected from YCB-GlcNAc agar medium (with phloxine B) after 5 days culture at RT. Cells were pre-cultured separately in liquid YCB-GlcNAc medium at RT with shaking at 220rpm for 24 hours. Then cells were counted with a hemocytometer at 400x magnification using an optical microscope. Cells were then centrifuged and tester and experimental strains were mixed in 5 ml fresh YCB-GlcNAc liquid medium in 50 ml Falcon tubes at a final concentration of each strain of 1×10^7 cells/ml. Cells were incubated at RT with shaking at 220 rpm for 48 hours before plating onto YCB-Glucose medium for prototrophic selection; selection plates were incubated at 30°C for 3 days before counting the colonies [35]. The mating frequency is calculated based on the number of prototrophic mating product colonies (on the trp^- , lys^- , arg^- plates) divided by the limiting value for the input of tester cells (detected on the arg^- plates) or the experimental strain cells (detected on the trp^- , lys^- plates). The latter two values were always similar.

2.2.9 Pheromone response assays

Approximately 5×10^6 opaque cells of *cpp1* Δ/Δ *MTLa/a* were evenly streaked onto YCB-GlcNAc agar medium. SN148 (*MTLa/a*) was used as the negative control. Single colonies of SN148 and *ofr1* \mathbf{a}/α opaque cells from agar plates were selected and mixed well with 20 μl milliQ sterile water separately and 5 μl was used to spot onto the hyper-responsive cell streaks. The plate was incubated at 25°C for 48 hours before scanning [58].

2.3 Results

2.3.1 Screen for genes involved in white-opaque switching

In the fungal pathogen *C. albicans*, the white-opaque transition is typically restricted to cells homozygous for the *MTL* locus, as the $\alpha 1$ - $\alpha 2$ repressor prevents expression of the transcription factor *WOR1* required for formation of the opaque state [14, 49, 50]. We screened for additional genes involved in white-opaque switching using a mutant library GRACE version 1.0 (unpublished data) containing approximately 900 *MTL* heterozygous strains disrupted for non-essential genes to identify mutants that were capable of undergoing white-opaque switching when cells were cultured on GlcNAc medium at room temperature (RT). The entire library collection was suspended in 20% glycerol-supplemented YPD medium and stocked in 96-well microtiter plates. Stock plates were mixed on a microplate mixer and then robotically pinned to GlcNAc agar medium containing phloxine B to identify dark-staining opaque cell sectors. After a week's incubation at room temperature, those colonies that formed pink (potentially opaque) sectors were restreaked and reincubated on fresh GlcNAc agar medium with phloxine B. Pink colonies were checked by optical microscopy to identify opaque-cell-like mutants, and heterozygosity at *MTL* was confirmed through colony PCR amplification of the *MTL α 1* and *$\alpha 2$* genes.

Further confirmation of a role in white-opaque switching was accomplished by testing the phenotype of the equivalent mutant from the original GRACE library. Because the GRACE library is a collection of mutant strains with one allele deleted and the other allele under Tet control [42], we examined the strains for white-opaque switching on 100 μ g/ml tetracycline supplemented YCB-GlcNAc+Phloxine B agar medium. For candidate genes we then examined the phenotype of null mutants that were constructed in the SC5314 background. One of the strains identified, *orf19.5078*, consistently showed enhanced white-opaque switching in the *MTL α* background (Figure 2.1). We designated this mutant as *OFRI*, based on its phenotype as an opaque formation regulator. *OFRI* has no clear ortholog in *Saccharomyces cerevisiae* and the function of the encoded protein is currently undefined.

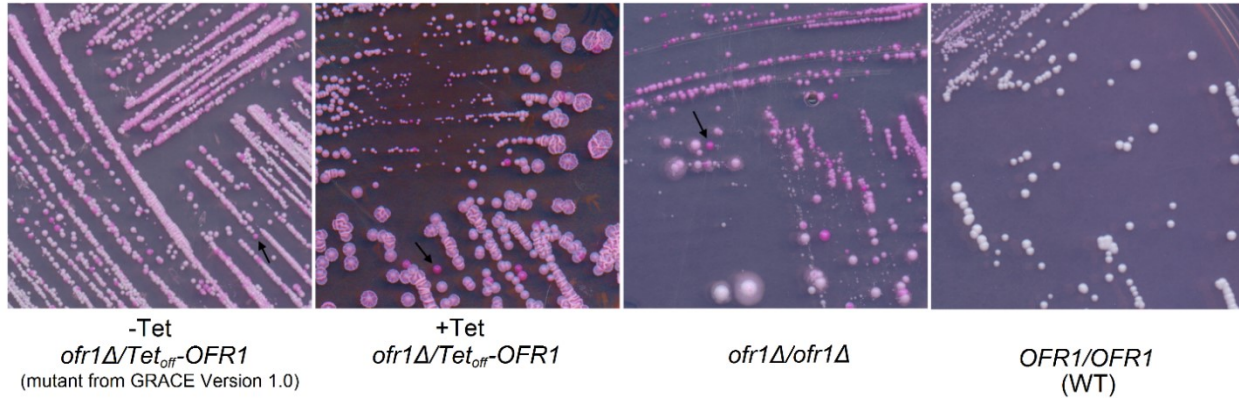


Figure 2.1 *ofr1* mutants undergo white-opaque switching on YCB-GlcNAc. Cells were streaked on YCB-GlcNAc agar plates containing phloxine B; under these conditions, opaque colonies are stained pink (representative colonies are noted by arrows). The mating types of all the strains are heterozygous *MTL a/a*. The *ofr1Δ/Tet_{off}-OFR1* (*MTL a/a*) strain is from the GRACE library, and was streaked on YCB-GlcNAc agar plate with 100 μg ml⁻¹ tetracycline (*OFR1* expression is repressed by tetracycline). The *ofr1Δ/ ofr1Δ* null mutant is derived from the wild-type strain *SN148*. *OFR1/OFR1* is *SN148* as the control. These strains were all incubated at room temperature (RT) for 7 days before being scanned.

2.3.2 Ofr1 has a conserved YciI related domain

We examined the phylogenetic distribution of *OFR1* (*ORF19.5078*) orthologs within the ascomycetes. There are orthologs in most of the CTG clade of *Candida* species (Fig. 2.2A). There is also an ortholog in *Candida glabrata*, but none in *S. cerevisiae* and the close relatives of the budding yeast. Some species, such as *Sheffersomyces stipitis* and *Candida lusitanae*, have two or three paralogs due to gene duplication.

We also investigated the domain architecture of Ofr1. The Ofr1 protein consists of 135 amino acids, and contains a single YciI-related domain located from amino acids R₄₁ to P₁₁₄. YciI-related domains belong to a dimeric alpha-beta barrel protein family. This domain is widespread in eukaryota, archaea, and a large group of both gram positive and negative bacteria, and the structure of a family member from *H. influenza* has been determined from protein crystals [59]. The YciI domain has been proposed to have enzymatic function (one member of the family was identified as a dechlorinase [60]) with putative active site residues His and Asp;

relatives, all three orthologous genes are missing or not syntenic in the genome. “ Δ ” represents that the gene is absent from the genome and “--” represents that the gene is elsewhere. (B) **T-COFFEE protein analysis among several YciI domain proteins.** The symbol * is used to label identical residues in the consensus sequence. The YciI domain has been proposed to have enzymatic function with putative active site residues Asp and His; the positions of these candidate active site residues are conserved in *Ofr1* as D7 and H22 in the consensus (noted by arrows).

2.3.3 *Ofr1p* plays a carbon-source dependent role in white-opaque switching

An *ofr1* null mutant strain constructed from the parent strain SN148 generated frequent pink (opaque) colonies when streaked on YCB-GlcNAc agar medium after a few days’ cultivation at RT. Microscopic examination of the white colonies showed white phase cells similar to the parent wild-type cells, while pink colonies showed elongated yeast cells with large vacuoles similar to opaque phase cells. We performed a further analysis of the opaque-like phenotype by immunofluorescence microscopy, using two monoclonal antibodies that can differentiate white and opaque cells. When assayed using fluorescence microscopy, the opaque-like cells from the *MTLa/a ofr1 Δ/Δ* null mutant gave staining patterns similar to the classic opaque cells of the *MTLa/a* wild-type (Fig. 2.3A). The white cells from both the null mutant *MTLa/a* and wild-type *MTLa/a* strains, showed no signal, as did the cells only treated with the secondary antibody.

Additionally, scanning electronic microscope (SEM) was used for analyzing the cell surface of the *ofr1* mutant. Gut cells were discovered from passage through the murine gut and they expressed an optimized transcriptome for the digestive tract. They have opaque-like cell shapes but fail to respond to pheromone and showed no pimples under scanning electronic microscope [55]. On the cell surface of the opaque-like cell formed by the mutant, there are the characteristic opaque pimples (Fig. 2.3B); this further supports the opaque status of the mutant cells.

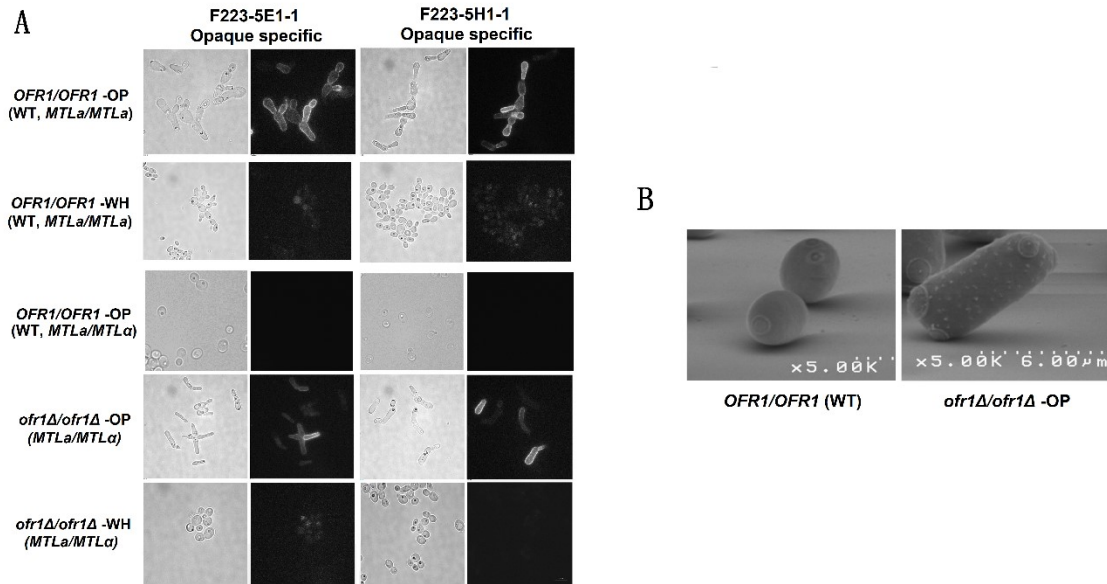


Figure 2.3 Microscopy. A. Immunofluorescence microscopy of *ofr1*. Cells were fixed with formaldehyde and washed with 1x PBS. Fixed cells were stored in 1x PBS at 4° C before immunofluorescence microscopy. F223-5E1-1 and F223-5H1-1 are two different monoclonal antibodies used in this study as primary antibodies to identify opaque cells (Fig. S1). Texas red conjugated goat anti-mouse antibody was used as the secondary antibody. OP represents opaque cells and WH represents white cells. Samples were observed and photographed under the Nikon Eclipse TiE fluorescence microscope at 400X magnification. Scale bar, 10 μ m. **B. Scanning electron microscopy.** Cells were fixed in glutaraldehyde as described after growth on YCB-GlcNAc agar plates at 25 °C for 72 hours. The samples were coated with 20 nm of gold palladium in an Emitech K550 sputter coater. Cells were photographed under scanning electron microscope at 5000x magnification. OFR1/OFR1 (WT) is the wild-type SN148 MTL α / α as the control. *ofr1* Δ /*ofr1* Δ -op represents the opaque cell of the *ofr1* null mutant.

Purified white and opaque colonies were selected to further test the overall white-opaque switching patterns. When individual cells from purified white colonies of the null mutant were incubated on YCB-GlcNAc agar medium at RT, the frequency of the opaque-like form, phloxine-staining colonies was around 2%, while no switching of wild-type strain SN148 was observed under the same conditions (Table 2.3 Row 1 and 2). Purified opaque-like colonies

treated in the same manner generated about 68% white/32% phloxine staining opaque colonies (Table 2.3 Row 11). Intriguingly, the switching rates of the *ofr1* mutant strains were carbon-source dependent. Opaque *ofr1* cells from a GlcNAc plate would switch back quantitatively to white cell colonies when plated on YCB-glucose agar medium (Table 2.3 Row 14), while white *ofr1* cells were unable to switch to opaque-form cells when cultured at room temperature on YCB-glucose agar medium (Table 2.3 Row 6). Opaque-like cells formed by the *ofr1 MTL* homozygous strain were also quite unstable compared with WT *MTL* homozygous opaque cells under glucose growth conditions (Table 2.3 Row 16 and 17).

Another condition for inducing white-to-opaque switching in *C. albicans* is to incubate cells in 5% CO₂. We tested 5% CO₂ incubation, but found that on YCB-glucose agar medium, white cells of the null mutant did not switch to opaque even after several days of incubation (Table 2.3 Row 7), and opaque cells of the null mutant would all revert back to white cells after three days incubation (Table 2.3 Row 15). *ofr1 MTL* heterozygous mutant could even form opaque colonies at the body temperature 37° C. At this temperature, in GlcNAc medium, the frequency of white-to-opaque switching was around 0.5% and the switching frequency of opaque-to-white was close to 90%.

2.3.4 Opaque phase stability of *ofr1* null mutants is carbon source dependent

We tested the null mutant on other carbon sources to observe white-opaque switching. Galactose, mannitol, fructose, and xylose were all tested, together with glucose and GlcNAc as carbon source controls. Only GlcNAc could efficiently trigger the null mutant to switch to the opaque state. All *ofr1* mutant opaque cells were unstable and could revert to the white state, but this reversion was also carbon source dependent. Opaque cells transferred to glucose medium would switch efficiently to the white state, generating 100% white colonies, while re-culturing to GlcNAc medium resulted in only ~70% white colonies (Table 2.3 Row 14 and 11, respectively).

Table 2.3 Ratio of white-opaque switching. (A) White-to-opaque switching. (B) Opaque-to-white switching. Carbon sources used were GlcNAc and glucose. Strains were either WH, white or OP, opaque. The ratios are based on at least 2 separate experiments; colony types were calculated from among 200 to 1000 colonies in total after 7 days incubation at room temperature.

Row	Strain		Initial Cell type	Carbon source		Switch Ratio %
	Relevant Genotype			Starter Colony	Scored Cells	
1	WT	<i>MTLa/α</i>	WH	GlcNAc	GlcNAc	<.05
2	<i>ofr1Δ/Δ</i>	<i>MTLa/α</i>	WH	GlcNAc	GlcNAc	1.92
3	WT	<i>MTLa/a</i>	WH	GlcNAc	GlcNAc	90.91
4	<i>ofr1Δ/Δ</i>	<i>MTLa/a</i>	WH	GlcNAc	GlcNAc	94.78
5	WT	<i>MTLa/α</i>	WH	GlcNAc	Glucose	<.01
6	<i>ofr1Δ/Δ</i>	<i>MTLa/α</i>	WH	GlcNAc	Glucose	<.05
7	<i>ofr1Δ/Δ</i>	<i>MTLa/α</i>	WH	GlcNAc	Glucose +CO2	<.02
8	WT	<i>MTLa/a</i>	WH	GlcNAc	Glucose	4.91
9	<i>ofr1Δ/Δ</i>	<i>MTLa/a</i>	WH	GlcNAc	Glucose	3.93
11	<i>ofr1Δ/Δ</i>	<i>MTLa/α</i>	OP	GlcNAc	GlcNAc	68.21
12	WT	<i>MTLa/a</i>	OP	GlcNAc	GlcNAc	0.14
13	<i>ofr1Δ/Δ</i>	<i>MTLa/a</i>	OP	GlcNAc	GlcNAc	<.1
14	<i>ofr1Δ/Δ</i>	<i>MTLa/α</i>	OP	GlcNAc	Glucose	99.6
15	<i>ofr1Δ/Δ</i>	<i>MTLa/α</i>	OP	GlcNAc	Glucose +CO2	99.5
16	WT	<i>MTLa/a</i>	OP	GlcNAc	Glucose	0.17
17	<i>ofr1Δ/Δ</i>	<i>MTLa/a</i>	OP	GlcNAc	Glucose	98.05

2.3.5 Mating ability of *ofr1* mutant

We used wild-type tester strains 3315 α (*MTL* α/α) and 3745 \mathbf{a} (*MTL* \mathbf{a}/\mathbf{a}) to investigate the mating properties of the *MTL* \mathbf{a}/α *ofr1* mutant strain switched to the presumptive opaque state. We observed prototrophic colonies arising from auxotrophic marker complementation of both testers within 3 days incubation on YCB-Glucose selection medium after initial culturing on YCB-GlcNAc medium: the prototrophs were stable and represented true mating products. The mating assay thus suggested the *MTL* \mathbf{a}/α *ofr1* mutant could undergo mating with both *MTL* α/α wild-type cells and *MTL* \mathbf{a}/\mathbf{a} wild-type cells when the *ofr1* opaque state was stabilized on YCB-GlcNAc medium (Fig. 2.4A and Table 2.4).

This mating is not the result of rare *MTL* homozygosity arising within the *MTL* \mathbf{a}/α *ofr1* population. We confirmed the presence of the $\mathbf{a}1$ and $\alpha2$ genes by colony PCR before performing the mating assays. As well, the mating frequency of the *MTL* \mathbf{a}/α *ofr1* mutant is around 4×10^{-4} with *MTL* \mathbf{a} cells and 1×10^{-6} with *MTL* α cells (Table 2.4); these values are close to the frequencies seen for mating of a control *MTL* homozygous strain (9×10^{-4} with the *MTL* α tester), and much higher than the undetected (less than 1×10^{-10}) frequency of a wild-type *MTL* heterozygote with *MTL* homozygotes. We further investigated whether the frequency of *MTL* homozygosity was elevated in *ofr1* mutant cells. We continuously restreaked the null mutant onto GlcNAc agar medium and retested opaque colonies for the *MTL* loci by colony PCR. The heterozygosity of the *MTL* loci was stable during weeks of culturing. A direct assay for potential loss of heterozygosity at the *MTL* loci involves growth on sorbose medium; homozygosis of chromosome 5, which contains the *MTL* locus, allows growth on sorbose medium [10]. We found the frequency of colonies identified after sorbose selection in the *ofr1* mutants to be low, in fact lower than the rate characteristic of wild-type \mathbf{a}/α cells under sorbose selection (data not shown). Further, when we characterized the sorbose resistant colonies from the *ofr1* mutant strain, we observed a high frequency of colonies that survived the sorbose selection without loss of heterozygosity (LOH) at the *MTL* locus. *ofr1* null mutant cells thus appear unusually stable for heterozygosity at the *MTL* locus. The somewhat lower than wild-type mating efficiency even on GlcNAc medium may result from the switching of the *ofr1* mutant from the opaque to white form, since *ofr1* opaque cells are quite unstable and we observed a 68% switching ratio on YCB-GlcNAc medium. This observation importantly suggests that *ofr1* *MTL* \mathbf{a}/α mutants fully

resemble *MTL* homozygous wild-type cells in that they also need to first switch to the opaque state to become mating competent.

Table 2.4 Quantitative mating assays. *Tester strains and experimental strains were pre-cultured in YCB-GlcNAc liquid medium for 24 hours and then mixed in fresh YCB-GlcNAc liquid medium at a concentration of 1×10^7 cells/ml for both strains. Mixed cells were incubated at RT for 48 hours and then plated onto selection media to detect auxotrophic mating products. The mating frequency is calculated as described in the materials and methods session. Exp. Strain, experimental strain.*

Tester				OFR1		Mating Frequency
Strain	Type	OFR1 Genotype	Exp. Strain	Type	Genotype	
3315 α	OP	WT	SN148 a/ α	WH	WT	$<1.22 \times 10^{-10}$
3315 α	OP	WT	SN148 a/a	OP	WT	$9.31 \pm 5.69 \times 10^{-4}$
3315 α	OP	WT	<i>ofr1</i> a/ α	OP	<i>ofr1</i> Δ / <i>ofr1</i> Δ	$1.15 \pm 0.03 \times 10^{-6}$
3315 α	OP	WT	<i>ofr1</i> α	OP	<i>ofr1</i> Δ / <i>ofr1</i> Δ	$<1.02 \times 10^{-10}$
3745 a	OP	WT	SN148 a/ α	WH	WT	$<5.78 \times 10^{-10}$
3745 a	OP	WT	<i>ofr1</i> a/ α	OP	<i>ofr1</i> Δ / <i>ofr1</i> Δ	$4.06 \pm 0.53 \times 10^{-4}$
3745 a	OP	WT	<i>ofr1</i> α	OP	<i>ofr1</i> Δ / <i>ofr1</i> Δ	$1.21 \pm 0.18 \times 10^{-2}$
3745 a	OP	WT	<i>ofr1</i> a	OP	<i>ofr1</i> Δ / <i>ofr1</i> Δ	$<1.44 \times 10^{-9}$
<i>ofr1</i> a/ α 1.0	OP	<i>ofr1</i> Δ /TetoffOFR1	<i>ofr1</i> a/ α	OP	<i>ofr1</i> Δ / <i>ofr1</i> Δ	$9.80 \pm 3.76 \times 10^{-7}$
<i>ofr1</i> α 1.0	OP	<i>ofr1</i> Δ /TetoffOFR1	<i>ofr1</i> a	OP	<i>ofr1</i> Δ / <i>ofr1</i> Δ	$1.27 \pm 0.09 \times 10^{-2}$

We performed pheromone response assays to check if *MTLa/a* *ofr1* can produce the α -factor pheromone. These assays showed *MTLa/a* *ofr1* opaque cells can cause sensitive *MTLa* opaque cells to arrest similarly to the *MTLa* opaque cells (Fig. 2.4B) [62]. *MTLa/a* wild-type cells failed to cause *MTLa* opaque cells to arrest. The cells in the zone of inhibition form shmoo tubes (data not shown). Pheromone response assays were also performed to confirm that *MTLa/a* *ofr1* mutants can respond to α pheromone, and we detected shmoo tubes after 24 hours pheromone treatment in liquid medium (data not shown).

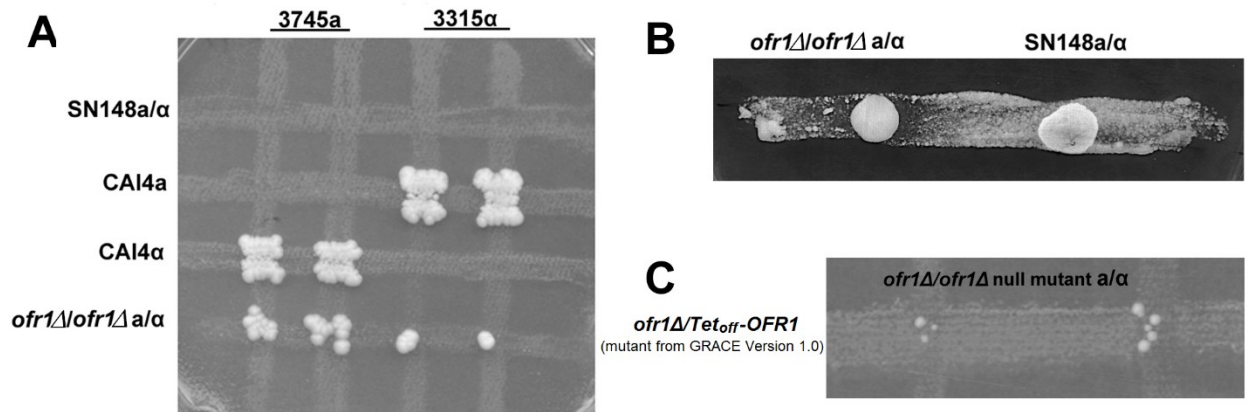


Figure 2.4 Mating ability of *ofr1* mutant. (A) An *ofr1* Δ/Δ strain undergoes mating with both wild-type *MTL* homozygous strains. Strains 3745a and 3315a, in the opaque state, were used as mating type testers. They had the auxotrophic markers *trp1/trp1*; *lys2/lys2*. These testers were crossed with WT strains SN148a/a (*arg4/arg4*; *leu2/leu2*; *his1/his1*; *ura3::imm434/ura3::imm434*); CAI4a (*ura3::imm434/ura3::imm434*); CAI4a (*ura3::imm434/ura3::imm434*) and the null mutant *ofr1a/a* (*arg4/arg4*; *leu2/leu2*) on GlcNAc medium at RT for two days and then replicated on selection medium YCB-glucose (*trp*⁻, *lys*⁻, *arg*⁻, *ura*⁻) at 30°C for 3 days to detect auxotrophic mating products. (B) **Pheromone response assays.** Approximately 5×10^6 opaque cells of the highly pheromone sensitive strain *cpp1* Δ/Δ *MTLa/a* were evenly streaked onto YCB-GlcNAc agar medium. Spots of strains SN148a/a, (wild-type, white cells) and *ofr1 a/a*, (opaque cells, *MTLa/a*) were assessed for pheromone production. SN148 a/a, represents the negative control. Single colonies of *ofr1 a/a* and SN148 a/a from GlcNAc agar medium were separately suspended in 20 μ l milliQ sterile water. 5 μ l was used to spot onto the hyper-responsive cell streaks and the plate was incubated at 25°C for 48 hours prior to scanning. (C) **Homothallic mating of *ofr1* Δ/Δ .**

*Opaque cell colonies of the *ofr1 a/a* null mutant (*arg4/arg4; leu2/leu2*) and the *ofr1 a/a* GRACE1.0 (*ura3/ura3*) strains were mixed on GlcNAc medium for 2 days and then replicated on selection medium (*arg⁻, ura⁻*) to detect auxotrophic mating products.*

Since *MTLa/a* *ofr1* opaque cells can undergo mating with both *MTL* homozygous wild-type opaque cells, we assessed if deletion of *OFRI* could allow *MTLa/a* opaque cells to mate among themselves. We performed a mating assay between the *MTLa/a* *ofr1* null mutant and the *MTLa/a* *ofr1* mutant from the GRACE 1.0 library; these strains had complementing auxotrophies. We observed prototrophic colonies arising from auxotrophic marker complementation within three days incubation on YCB-Glucose selection medium after initial culturing on YCB-GlcNAc medium (Fig. 2.4C). We assayed the prototrophic mating products arising through mating among these *ofr1* *MTLa/a* mutants for DNA content, and found them to be the expected tetraploids with twice the content of the diploid parents (data not shown). As well, strains with *MTLa1* polymorphisms were used for mating and sequencing the prototrophic mating products showed a combination of both allelic polymorphisms (data not shown). The quantitative mating assay showed a mating frequency of around 1×10^{-6} between the *MTLa/a* *ofr1* null mutant and the *MTLa/a* *ofr1* mutant from the GRACE 1.0 library (Table 2.4).

2.3.6 Comparison of transcription profiles between *ofr1* mutant and wild-type white cells on glucose-containing medium

OFRI expression is neither regulated by white-opaque switching nor pheromones according to compilations of transcription data provided by the CGD database. We used transcription profiling to examine the differences in gene expression levels between the *ofr1* null mutant and wild-type in normal glucose growth conditions. Since the *MTLa/a* wild-type cannot form opaque cells, we used microarrays to compare the *ofr1 a/a* white cells with wild-type *a/a* white cells for gene expression under glucose incubation conditions at room temperature after 12 hours. In the glucose conditions, hundreds of genes were significantly up-regulated and a few genes were significantly down-regulated in the *ofr1* null strains (data not shown). Among these modified genes were *WOR1* (up-regulated) and *WH11* (down-regulated) in *ofr1 a/a* white cells (Table 2.5). As well, mating pheromone precursor genes *MFA1* and *MFA 1* were both up-

regulated in *ofr1* \mathbf{a}/α cells, as were both \mathbf{a} and α pheromone receptor genes *STE3* and *STE2*. The G protein subunit genes *CAG1* and *STE18* were up-regulated along with other genes involved in mating and pheromone response such as *HST6*, *IFA4*, *AKL1*, *PRM1*, *FUS1* and *CTF5*. Genes involved in carbohydrate transport and utilization were also up-regulated in the null mutant background (Table 2.5). In these growth conditions, eight out of 19 glucose transporter family members (*HGT1*, *HGT12*, *HGT13*, *HGT17*, *HGT2*, *HGT6*, *HGT9* and *HXK2*) were up-regulated in the mutant relative to the wild-type; chitin synthesis genes *CHS1*, *CHS2* and *CHT3* as well as other genes involved in carbohydrate metabolism including *CIT1*, *CRH11*, *PGM2*, *PHR3*, *SCW11* are also more highly expressed in the mutant. Similarly, SAPs and LIPs genes which affect the maturation of pheromones and phenotype switching were also up-regulated, including *SAP1*, *SAP30*, *SAP8*, *SAP2*, *SAP5*, *SAP7*, *LIP4*, *LIP2* and *LIP1*. Overall, these expression characteristics highly resembled the gene expression profiles of white type *MTL* homozygous cells treated with pheromone [63].

Table 2.5 Highlighted significant genes in white cells of the *ofr1* null mutant compared with white cells of the wild-type reference strain. Highlighted significant genes changed in expression for the α/α *ofr1* null mutant in the white state compared with the wild-type α/α SN148 strain under both GlcNAc and glucose conditions. Microarrays, based on at least two replicates with dye-swaps. $\text{Log}_2 > 1$ or < -1 , p -value < 0.1 . Down-regulated genes are noted by *. For details, see Table S1 and Fig.S2.

Category	Significant genes on GlcNAc	Significant genes on Glucose
White-opaque Switching	--	WOR1, WHI1*
Involved in Mating and Pheromone response	PCL1, FAV3 EMC9, MET28	MNN4-4, orf19.5896, RBT4, SLF1, STE2, STE3, HST6, IFA14, orf19.104 MFALPHA, AKLI, PRM1, FUS1, MFA1, CTF5, CAG1, STE18, SAP30
Other significant groups		
Histone genes	HHF1, HHF22, HHT1, HHT2, HHT21, HTA1, HTA2, HTA3, HTB1, HTB2	--
Chitin synthesis genes	CHS1, CHT3	CHS1, CHS2, CHT3
Alcohol dehydrogenase	ADH1, ADH2, FDH3	ADH3
SAPs and LIPs	--	SAP1, SAP30, SAP8, SAP2, SAP5, SAP7, LIP4, LIP2, LIP1
Glucose transport	HGT6, HGT13, HGT17	HGT1, HGT2, HGT6, HGT9, , HGT12, HGT13, HGT17, HXK2
Carbohydrate metabolism	ADH1, ADH2, ALG8, AMS1, ARA1, BMH1, CDC19, CHS1, DAK2, GLK4, IPP1, KAR2, MDH1, MNT1, PDA1, PFK2, PGM2, RHO1, SCW11, SRB1, UGPI, ZWF1	CIT1, CRH11, PGM2, PHR3, SCW11, GAL1, GUP1, MAL31

2.3.7 Comparison of transcription profiles between *ofr1* mutant and wild-type white cells on GlcNAc medium

Since *ofr1* white cells switch to the opaque form opaque specifically on GlcNAc medium, we also investigated white mutant and wild-type cells using transcription profiling on this carbon source. We compared the transcriptional profile of the **a/α** *ofr1* white cells (which have the potential to switch to the opaque state) with the **a/α** wild-type white cells (which have no potential to switch to opaque) to see if *WOR1* expression was misregulated in the *ofr1* mutant cells grown on GlcNAc. This analysis revealed that *WOR1* gene expression, as well as that of other white-opaque switching-related transcriptional factors and genes, was not dramatically changed in the null mutant *ofr1* white cells in GlcNAc when compared with wild-type **a/α** SN148 white cells after 12 hours incubation at RT. The *ofr1* strain exhibited general differences in genes implicated in processes such as carbohydrate metabolism, oxidation/reduction, ATP metabolism, nucleosome organization and RNA processing (data not shown). Under GlcNAc growth conditions, the *ofr1* mutant did not significantly modulate transcripts related to the Wor1 circuit but did up-regulate transcripts for genes involved in glycolysis such as *PFK2*, *TP11*, *TDH3* and *CDC19*, genes involved in fermentation such as *ADH1*, *ADH2*, *ADH5* and *ORF19.3045*, and genes involved in UDP-glucose conversion such as *PGM2*, *IPPI1* and *UGPI1*. Intriguingly, histone genes are dramatically up-regulated in the mutant when grown on GlcNAc. All 10 histone genes (*HTA1*, *HTA2*, *HTA3*, *HTB1*, *HTB2*, *HHT1*, *HHT2*, *HHT21*, *HHF1* and *HHF22*) were among the top up-regulated genes (7 out of 10 showed >2-fold of the log₂ ratio (top 30) between the mutant and the wild-type) (Table 2.5). Together, these histone genes encode a histone octamer composed of two histone H2A-H2B dimers and one histone tetramer (H3-H4)₂. It has been reported that post-translational modifications of histones or chromatin can influence the white-opaque transition [64]. Based on this microarray data, it is possible that the potential of the white, **a/α** *ofr1* mutant strains to switch to the opaque state is a consequence of this improper histone gene expression.

2.3.8 Comparison of transcription profiles between the *ofr1* **a/α** opaque and white states

We wanted to establish if the transcription profile difference between the *ofr1* **a/α** opaque and white cells was similar to that of the wild-type **a/a** opaque cells compared with white cells. Because *ofr1* opaque cells were relatively stable when incubated in liquid YCB-glucose medium

at RT for 12 hours, and the published white/opaque data sets were derived from glucose grown cells, we transferred both white and opaque cells from YCB-GlcNAc medium and grew them separately in liquid YCB-glucose medium for 12 hours before collecting the cells for RNA extraction. We investigated the *ofr1 a/a* opaque cells compared with white cells for gene expression under the glucose incubation conditions, and we compared these microarray data with that of the *MTLa/a* wild-type opaque/white comparison from the literature [65, 66]. The genes significantly up and down regulated suggest that the *ofr1* opaque cells follow the expression patterns of classic opaque cells for key functions (data not shown). The *MTLa/a ofr1* opaque cells cultured on glucose turn up the *Wor1* circuit up-regulated genes (*WOR1*, *WOR2*, *CZF1*), they turn down typically down-regulated genes (*EFG1* and *WH11*) (Table 2.6). They also upregulate Krebs cycle genes (*PYC2*, *PDC11*, *IDP2*, *SDH1*, *SDH2*, *FAA4*, *CIT1*), as previously noted for standard opaque cells (Table 2.6) [66]. In addition, the *MTLa/a ofr1* opaque cells upregulate genes involved in carbohydrate transport (*ORF19.4923*, *ORF19.1867*, *ORF19.3782*, *MNT4*, *MNN11*) and utilization (*ORF19.3325*, *HGT8*, *GAL10*, *GAL1*, *ORF19.1340*, *UTR2*, *FBP1*, *ORF19.2308*, *GCA2*, *GUT2*) relative to the white cells. The GlcNAc metabolism genes (*HXK1*, *NGT1*, *GFA1*, *DAC1*, *NAG1*) are also dramatically upregulated which is potentially a residual from the transition from the initial GlcNAc growth conditions. Interestingly, we have histone genes (*HHF1*, *HHF22*, *HHT21*, *HTA2*, *HTB1*) and chitin synthesis genes (*CHS1*, *CHS8*, *CHS5*, *CHS7*) highly expressed in the *ofr1 a/a* opaque cells relative to the white cells; these genes were not upregulated in the classic opaque cells.

2.3.9 Comparison of transcription profiles between the *ofr1 a/a* opaque and white states on GlcNAc medium

Finally, we also compared the gene expression between *ofr1 a/a* opaque and white cells in the GlcNAc growth condition that allows the mutant cells to mate. Under these conditions *WOR1* is up-regulated in the opaque cells, and there were some significantly expressed genes that also showed up during glucose growth of the mutant (Table 2.6). Other up-regulated genes in GlcNAc included genes involved in secretion such as *SAP30*, *SAP4*, *SAP98* and *LIP7*, in adhesion such as *ALS2*, *ALS4* and *ALS9* as well in glucose transport such as *HGT1*, *HGT6*, *HGT7* and *HGT19* (Table 2.6). Histone gene expression was not significantly changed here

because all the histone genes were highly expressed in both white and opaque states on GlcNAc, but the expression levels were marginally higher in white cells.

Table 2.6 Highlighted significant genes in opaque cells compared with white cells of the *ofr1* null mutant. Highlighted significant genes changed in the gene expressions of the *ofr1* null mutant in opaque states compared with in white states under both GlcNAc and glucose conditions. Microarray, based on at least two replicates with dye-swaps. $\text{Log}_2 > 1$ or < -1 , p -value < 0.1 . Down-regulated genes are noted by *. For details, see Table S2 and Fig. S4.

Category	Significant genes on GlcNAc	Significant genes on Glucose
White-opaque Switching	WOR1	WOR1, WOR2, CZF1, EFG1*, WHI1*
Kreb cycle genes	--	PYC2, PDC11, IDP2, SDH1, SDH2, FAA4, CIT1
Involved in Mating and Pheromone response	CEK2, RMS1, RSN1, PRM1, SAP30	CEK2
Other significant groups		
Histone genes	--	HHF1, HTB2, HHF22, HTA2, HTB1, HHT21
Chitin synthase	--	CHS1, CHS8, CHS5, CHS7, GFA1
SAPs and LIPs	SAP30, SAP4, SAP98, LIP7	SAP10
ALS family protein	ALS2, ALS4, ALS9	ALS3
Glucose transport	HGT1, HGT6, HGT7, HGT19	HGT8
Carbohydrate metabolism	ORF19.4923, AMS1, ATC1, BMT4, GAC1, GCA1, GPD2, GPM1, HSP104, INO1, KTR2, MAL2, MNN22, PFK26	ORF19.4923, ORF19.1867, ORF19.3782, MNT4, MNN11, ORF19.3325, GAL10, GAL1, ORF19.1340, UTR2, FBP1, ORF19.2308, GCA2, GUT2
GlcNAc utilization	--	DAC1, NAG1, HXK1, NGT1, GFA1

2.4 Discussion

Candida albicans has a complex signalling pathway to regulate mating, involving receptor proteins, a heterotrimeric G protein, a scaffolded MAP kinase cascade and a transcriptional control module [67]. However, the ability of this circuitry to trigger mating is maintained behind several layers of regulation. Most *C. albicans* cells are diploid and heterozygous at the mating-type locus, and thus blocked in mating because they cannot enter the opaque stage necessary for conjugation [68]. Even mating type homozygous strains have to undergo an infrequent epigenetic switch to attain this mating competent opaque state, a switch that is inherently

difficult at 37°C, the temperature of the mammalian host [69]. This situation is in contrast to many other ascomycetes with similarly structured mating regulation pathways, such as *S. cerevisiae* and *S. pombe*; these yeasts lack the epigenetic circuit, although they can link environmental signals to the mating decision.

We have identified that the *OFR1* gene, encoding a YciI domain protein, plays a key role in keeping the mating capacity of *C. albicans* cells cryptic. When this gene is deleted, it is possible for mating type heterozygous *C. albicans* cells to enter the opaque state and mate. This process is environmentally controlled, occurring when cells are grown on GlcNAc but not on other carbon sources such as glucose or galactose. This is consistent with the role of GlcNAc as an efficient inducer of opaque cell formation [70]. This mating ability of *ofr1 MTL α* cells is intriguing, because normally mating is precluded in cells heterozygous at the *MTL* locus. The *ofr1 MTL α* cells are able to mate with *MTL α* and *MTL a* cells, and, to a lesser extent, with *ofr1 MTL α* cells. The latter situation represents homothallic mating of *MTL α* cells. Pheromone response arrest assays show that the *ofr1 MTL α* cells can produce abundant α -factor, and pheromone response experiments show that the *ofr1 MTL α* cells can also respond to α -factor and shmoo.

We used transcriptional profiling to probe gene expression in *ofr1* mutant strains. *MFA1* (*ORF19.2164.1*) the gene encoding the **a**-factor mating pheromone precursor and *MFA α 1* (*ORF19.4481*) the gene encoding the α -factor mating pheromone precursor are somewhat up-regulated in the *ofr1 MTL α* background when compared with the wild-type. Unisexual mating can happen in *C. albicans* through inhibition of Bar1 protease, which promotes autocrine signalling, or through the presence of α cells, which provide α pheromone [15]. Addition of synthetic α pheromone or presence of α white cells is also sufficient to drive unisexual **a-a** mating in *C. albicans* [71]. Both **a** and α pheromone receptor genes *STE3* and *STE2* are up-regulated in the *ofr1* mutant, potentially allowing these cells to activate the mating response in the presence of either pheromone. By producing both the pheromones and the pheromone receptors, *ofr1 MTL α* cells can undergo mating with either mating type. The previous reported *MTL α* opaque cells are nonmating probably because they cannot produce pheromones to induce mating. It appears that once these *C. albicans* cells enter the mating

competent opaque state, whether the mating type is *MTLa*, *MTL α* , or *MTLa/ α* , cells can undergo mating if presented with either **a** or α pheromones.

The overall transcriptional consequences of deletion of *OFRI* are influenced by the carbon source of the cell, and are not limited to modulating genes involved in mating. Genes involved in carbohydrate metabolism, chitin synthesis and histone production are all changed in the absence of *OFRI*, but these influences are also affected by whether the cells are grown on GlcNAc or glucose; in general the transcriptional effects are greater for the cells grown on GlcNAc. These consequences in transcriptional regulation are intriguing given that *OFRI* is a member of the Yci1 family of proteins that have primarily been implicated in simple chemical reactions such as dechlorination [60]. A family member was crystalized in *Haemophilus influenzae*; the protein formed an α/β ferredoxin-like fold, and was complexed with $ZnCl_3$ [59]. This structure predicts a conserved His(H)-Asp(D) catalytic dyad, with Arg and Ser residues forming an oxyanion hole stabilized by a conserved Asp [59, 60]. However, links to transcriptional control have been noted with several family members; in *Streptomyces coelicolor* a Yci1 domain is fused to a sigma factor involved in global gene regulation [61], while in other bacterial species operons containing Yci1 family members are implicated in gene expression control and regulation of morphogenesis [60].

In *C. albicans* it is possible that Ofr1 could serve directly or indirectly to strengthen the **a1- α 2** repression of *MTL* homozygous-specific gene expression. Without Ofr1p, the **a1- α 2** repressor complex could allow a low level expression of *MTL* repressed genes such as white-opaque switching specific genes and pheromone response genes. If the threshold of switching to opaque on glucose is higher than that on GlcNAc, and deleting *OFRI* allows genes that are repressed by **a1- α 2** to be expressed at a relatively higher level than within the wild-type, this could allow the mutant to pass the threshold of switching to opaque when grown on GlcNAc but not on glucose. As well, switching to opaque on GlcNAc might not be only under control of the Wor1 circuit; there may be other potential regulators when the cells are grown on GlcNAc. This explanation is also suggested by the fact that the opaque cells formed by *ofr1* null mutant on GlcNAc would all switch back to white cells on glucose. If GlcNAc turns on the Wor1 circuit, the effects should keep going on glucose conditions. This instability of the **a/ α** opaques formed on GlcNAc suggests other possible routes present on GlcNAc conditions to regulate the white-

opaque switching. Histone gene dosage can affect histone modifications as well as gene transcription [72, 73]. The highly expressed histone genes of the *ofr1* mutant may influence white-to-opaque switching on GlcNAc medium, and affect white-opaque switching in both directions. It is also possible that Ofr1 involvement in the white-opaque switching process results from a role in chromatin assembly or structures that control the switch. Some opaque-specific genes were not upregulated in the *ofr1* opaque cells compared with control white cells. This might be caused by the instability of the opaque cells and the presence of α pheromone. It has been reported that α -pheromone down-regulates expression of some opaque phase specific genes (such as *OP4*) [74].

It has been noted that only 3-9% of clinical *C. albicans* isolates in nature are *MTL* homozygous [29, 75]. If mating of *C. albicans* is limited to *MTL* homozygous cells, it should be a rare event in nature, particularly when coupled to a requirement for switching to the mating competent opaque state. GlcNAc and other environmental factors may trigger white to opaque switching in *MTLa*/ α cells by up-regulating the Wor1 circuit or modulating chromatin assembly. In certain niches in the host, Ofr1 activity could be repressed which could allow *MTL* heterozygous cells to switch to opaque, produce pheromones and undergo mating. Also, in the presence of *MTL* homozygous cells that are producing either **a** or α pheromone, *MTL* heterozygous opaque cells can become as mating competent as *MTL* homozygous opaque cells.

Overall our study describes a single gene, *OFRI*, which influences the control of the barriers to mating in *Candida albicans*. The Ofr1 protein is needed to ensure that white-opaque switching, pheromone production and mating, is blocked in *MTL* heterozygotes, and it also regulates the expression of all histone genes in a carbon-source dependent manner. This suggests a critical role of the conserved YciI domain, which up to now has been identified with simple chemical reactions but implicated in more complex regulatory roles [59]. As more than 90% of *C. albicans* clinical isolates are *MTL* heterozygous, the presence of a complex, but apparently restricted, mating pathway is intriguing. The evidence that single gene mutations can allow carbon-source-dependent mating behaviour of *MTL* heterozygous strains suggests the possibility that *in vivo*, *C. albicans* may exploit alternate routes to mating, and that the apparently cryptic pathway may not be as hidden as it appears.

Chapter 3: Ofr2 regulates white opaque switching and lipid droplets

3.1 Introduction

Candida albicans is a human commensal fungal pathogen that is the major cause of yeast infections in humans [76]. When compared to the well-studied model organism *Saccharomyces cerevisiae*, *C. albicans* has a more complex morphology and a unique mating behaviour, perhaps due to coevolution with its human host. In *Saccharomyces cerevisiae*, the mating type is determined by the mating type locus (*MAT*). In natural settings, *S. cerevisiae* can be either haploid or diploid. As a haploid, it has either mating type **a** expressing *MATa1* or mating type α expressing *MATa1* and *MATa2* [77]. *MATa1* activates the expression of alpha-specific genes. However, there is no specific inducer for **a**-specific gene expression, and **a**-specific genes express as default. During mating, *MATa* cells can fuse with *MAT α* cells to generate diploid yeast cells of mating type *MATa/ α* . In the diploid cells, **a1- α 2** forms a homeodomain corepressor for haploid-specific gene expression and coactivator for the expression of diploid-specific genes [30]. As well, *S. cerevisiae* has a mating type switching system to ensure the population contains equal numbers of both **a** and α type of cells [78].

In *C. albicans*, however, the mating type switching system does not exist. Most of the clinical isolates are naturally diploid with the mating type *MTLa/ α* . These diploids have **a1** and **a2** encoded at *MTLa* and $\alpha1$, $\alpha2$ encoded at *MTL α* . As in *S. cerevisiae*, $\alpha1$ positively regulates α -specific gene expression and **a1- α 2** represses the homozygous *MTL* induced gene expression. However, distinct from *S. cerevisiae*, **a2** at *MTLa* is required to activate the expression of **a**-specific genes. As well there are other, non-mating-control-related genes, located at the mating type locus of *C. albicans* [30]. There are *PAPa*, *OBPa*, and *PIKa* at the *MTLa* and *PAP α* , *OBP α* and *PIK α* at the *MTL α* locus. Both *PAP* and *PIK* are essential genes, and all of these genes have distinct alleles at the two loci. The Pap protein is a poly(A) polymerase, with 89% protein identity and 66% DNA sequence identity between the two alleles [79]. The Pik protein is a phosphatidylinositol kinase, with 81% protein identity and 58% DNA sequence identity between the two alleles. OBP is the only nonessential gene among these non-sex-determining genes at the *MTL* locus; it encodes an oxysterol binding protein, with 91% protein identity and 66% DNA sequence identity between two alleles [79]. Until quite recently, *C. albicans* had been thought to be incapable of mating. Like *S. cerevisiae*, *C. albicans* can form mating type **a/a** and α/α cells

from loss of heterozygosity at the mating type locus from \mathbf{a}/α [20]. The competence of mating in *C. albicans* not only relies on such rare cases of loss of heterozygosity at the *MTL* locus but also requires that the cells undergo a specific phenotype switching from the typical white cells to the opaque state. The master regulator of white-to-opaque switching, *WOR1*, is blocked by the $\mathbf{a}1-\alpha2$ repressor [13, 14]. In *C. albicans*, *MTL* \mathbf{a}/\mathbf{a} cells can mate efficiently with *MTL* α/α only when both cells are in the opaque state [29].

In *S. cerevisiae*, *Pik* has roles in both membrane transport and mating pheromone response. It acts to catalyze phosphorylation of the 4'-OH position of a myo-inositol lipid to produce inositol-1,4,5-trisphosphate that can act as a secondary messenger in response to cell surface stimuli. It can participate in intracellular signal transduction cascades such as the pheromone response [80, 81]. Overexpression of *PIKI* cloned in a multicopy plasmid can increase the response to mating pheromone [81]. The protein shows localization to the nucleus but is also a cytoplasmic protein in the Golgi [82].

In *C. albicans*, it has been proposed that opaque cells are more lipidic in metabolism than white cells [66]. Lipid metabolism and energy homeostasis are also controlled by lipid droplets which are monolayer organelles with inert deposits of lipid biogenesis at the endoplasmic reticulum (ER) [83]. *OFR2* (opaque formation regulator 2) is another gene involved in white opaque switching identified from library screening that is predicted to encode a lipid raft associated protein. Through staining with the dye BODIPY, we have confirmed that the *ofr2* null mutant controls not only white-opaque switching, but also the size of lipid droplets of *C. albicans*.

3.2 Materials and Methods

3.2.1 Strains, media and culture conditions

The GRACE version 1.0 library with a collection of 887 mutants was used to identify colonies that could undergo white to opaque switching on GlcNAc agar medium containing phloxine B. Subsequently, the *ofr2* Δ/Δ null mutant strain was constructed by using *C. albicans* strain SN76 as the parent (see Table 3.1).

Table 3.1 Strains used in this study.

Strain	Parent	Mating type	Description	Source
SN76	RM1000	<i>a/α</i>	<i>arg4/arg4; his1/his1; ura3 imm434/ura3 imm434</i>	Noble/ Johnson
SN148a	SN148	<i>a/a</i>	<i>arg4/arg4; leu2/leu2; his1/his1; ura3 imm434/ura3 imm434; iro1 imm434/iro1 imm434</i>	Renjie Tang
GRACE version 1.0 library	GRACE library	<i>a/α</i>		Whiteway
GRACE library	CASS1	<i>a/α</i>		Merck
3315	A505	<i>α/α</i>	<i>trp1/trp1; lys2/lys2</i>	Magee
3745	A505	<i>a/a</i>	<i>trp1/trp1; lys2/lys2</i>	Magee
CAI4 MTLα	CAI-4	<i>a/a</i>	<i>ura3 ::imm434/ ura3 ::imm434</i>	Doreen Harcus
CAI4 MTLα	CAI-4	<i>α/α</i>	<i>ura3 ::imm434/ ura3 ::imm434</i>	Doreen Harcus
<i>ofr2</i>	SN76	<i>a/α</i>	<i>ofr2::HIS1/ofr2::ARG4; ura3 ::imm434/ ura3 ::imm434</i>	This study

For cultivation, SC-medium with glucose (2%) or GlcNAc (1.25%) was used. Plate cultures were grown at a density of 40-120 colonies per 90 mm plate. For opaque colony identification, Phloxine B (5 μ g ml⁻¹) was added to the agar media. For routine liquid cultivation, YPD (1% yeast extract, 2% peptone, and 2% glucose) medium was used.

3.2.2 Strain construction

OFR2 was replaced by standard one-step disruptions using PCR products [35]. The markers *HIS1* and *ARG4* were amplified by PCR from plasmids pFA-CaHIS1 and pFA-CaARG4 using primers that provided flanking regions of *OFR2*. The *HIS1* and *ARG4* markers were sequentially transformed to the parent strain SN76, and the transformants were selected on SD-his and SD-arg agar plates. Successful transformants were further confirmed by PCR. One pair

of long oligonucleotides for deletion and three pairs of short oligonucleotides for confirmation were used for the PCR reactions (see Table 3.2).

Table 3.2 Primers used in this study.

Name	Description	Sequence (5' to 3')	Source
OFR2 _F	<i>OFR2</i> deletion PCR cassette forward primer	TCCTTTATTTTCAAGTTTTCAGTTTTCCTTCTATTTTTTCT GTTCTAACAATAATTTAATCAACTATTAATTGGATTTTCATTT CATCTATACCCAACgaagcttcgtacgctgcaggtc	This study
OFR2 _R	<i>OFR2</i> deletion PCR cassette reverse primer	TGGAAAGAAGTCGAGAATGCATTGCAAAATCGTGTATCAA AACAGATTTGACAAAGACGCAAGAAATCTTGGATTTGAT TACGTTCCAGTGGAGAAGtctgatcatcgatgaattcgag	This study
OFR2 _ex_F	<i>OFR2</i> external forward primer	TCCAGTAACCTGTCCGTAC	This study
OFR2 _ex_R	<i>OFR2</i> external reverse primer	AGAGATGTTGCTAAAGCTC	This study
OFR2 _in_F	<i>OFR2</i> internal forward primer	TCACTGATGATGGGACATTC	This study
OFR2 _in_R	<i>OFR2</i> internal reverse primer	ACAATAGTATGATAAGTTCC	This study
HIS1 F	<i>HIS1</i> forward primer	TTTAGTCAATCATTTACCAGACCG	<i>OFRI</i> study
HIS1R	<i>HIS1</i> reverse primer	TCTATGGCCTTTAACCCAGCTG	<i>OFRI</i> study
ARG4 -F	<i>ARG4</i> forward primer	TATGAGAATTTTCGTTCTCGTG	This study
ARG4 -R	<i>ARG4</i> reverse primer	AGCACCAGATCCTAATGGAG	This study
MTLa F	<i>MTLa1</i> forward primer	TTGAAGCGTGAGAGGCAGGAG	Magee
MTLa R	<i>MTLa1</i> reverse primer	GTTTGGGTTCCCTTCTTCTCATTC	Magee
MTLa F	<i>MTLa2</i> forward primer	TTCGAGTACATTCTGGTCCG	Magee
MTLa R	<i>MTLa2</i> reverse primer	TGTAAACATCCTCAATTGTACCCG	Magee

3.2.3 Phenotype switching

White and opaque cells were all from single colonies on SC-GlcNAc medium after 5 days at 25°C. Cells were suspended in water, the cell concentration was adjusted, and the suspensions plated onto agar media containing 5 µg ml⁻¹ phloxine B with either 2% glucose or 1.25% GlcNAc as the carbon source. Plates were incubated at 25°C. Data were collected, and plates were scanned on the 7th day and the frequency of sectored colonies calculated by standard statistical methods.

3.2.4 Microarrays

The wild-type SN76 and the *ofr2Δ/Δ* null mutant were selected from single colonies and grown in either SC-glucose or SC-GlcNAc liquid medium overnight at RT and then were diluted to OD₆₀₀=0.1 in fresh SC-glucose or SC-GlcNAc liquid medium. Cells were grown at RT until the culture reached an OD₆₀₀ between 0.8 and 1.2, harvested, and stored at -80°C until RNA extraction. Total RNA was isolated by the hot phenol method as described elsewhere [35]. Subsequently, mRNA was purified using the New England Biolabs polyA Spin mRNA isolation kit, then reverse transcription for cDNA production was followed by direct cDNA labeling with either Cy3 or Cy5. Arrays were purchased and designed by Agilent; hybridization chamber was used to hybridize for 16 hours before scanning [35].

3.2.5 Microscopy and imaging

Optical microscopic images of cells were captured using a Nikon Eclipse TS100. Immunofluorescence microscopic images were visualized and photographed using a Leica DS6000 with 630x magnification with settings: Objective: 63x Oil, Filter: TxRed-560/40, Dichroic beam splitter: bs585, Emission: 630/75, Ex wavelength: 555 nm using Multi-laser Heliophor and Camera: Photometrics Evolve. Images of plates and colonies were scanned at 800dpi by an Epson Perfection v500 photo scanner.

3.2.6 Immunofluorescence

Cells from single colonies cultured for 5 days on SD agar medium at RT were pre-grown in SD liquid medium overnight at RT, 220 rpm shaking and then diluted in fresh SD liquid medium for another 12 h incubation at RT, 220 rpm. The cells were pelleted and washed in 1 ml

of 1xPBS for three times, 2 min each time. Approximately 10^7 cells were tested for each assay. Washed cells were blocked with 1ml blocking buffer for 30 min before incubation with 100 μ l of primary antibodies for one hour at RT. Cells were then washed with PBS containing 0.05% Tween 20 for three times, 5 min each time. Washed cells were incubated with 100 μ l of the secondary antibody - Texas red conjugated goat anti-mouse antibody (1/100 dilution in blocking buffer) for 1 hour in the dark at RT. Cells were then washed with PBS containing 0.05% Tween 20 three times and PBS once, five min each time. Cells were finally suspended in 50 μ l PBS, and 3 μ l was applied under a coverslip. Microscope slides were sealed and placed in a microscope slide box for protection from light before observation under the Leica DM6000 fluorescence microscope.

3.2.7 Observation of lipid droplets

BODIPY 490/503 (Life Technologies) was diluted in the reagent PBS containing 0.5 mg/ml BSA, 0.1 mg/ml Saponin. Then 1 μ l of diluted BODIPY was added to a 1 ml overnight cell culture and stored in the dark for 10 min before being washed by 1xPBS twice. After washing, the samples were ready for observation under the Leica DM6000 fluorescence microscope.

3.2.8 Scanning Electron Microscope

Cells were grown on SC-GlcNAc agar plates for 72 hours at 25 °C and then fixed with 2.5% (w/v) glutaraldehyde in 0.1 M sodium cacodylate buffer at 4°C overnight. Cells were then post-fixed with 1% aqueous osmium tetroxide for 90 minutes at room temperature. Following fixation, cells were dehydrated gradually using a 15% gradient ethanol series and subsequently dried using a critical point dryer. The samples were then coated with 20 nm of gold palladium (60:40) in an Emitech K550 sputter coater. Cells were imaged with a Hitachi S-2700 scanning electronic microscopy and collected with Quartz PCI software.

3.2.9 Mating assays

Cells were streaked on SC-GlcNAc agar medium (with phloxine B) for 5 days at RT to select opaque colonies. Opaque cells of strains 3315 α and 3745 \mathbf{a} were used as the tester strains for mating. Opaque colonies of the *MTLa/ α ofr2* strain were restreaked as straight lines on separate YPD and SC-GlcNAc agar plates then the experimental strain. Opaque cells of the tester

strains were streaked as straight lines on YPD plates. The two sets of the tester and experimental streaks were patched onto the same YPD and SC-GlcNAc agar plates separately after 48 hours of incubation at room temperature (RT). After 24 hours of incubation on YPD plates and 48 hours incubation on SC-GlcNAc plates at RT, cells were replicated onto SC-Glucose selection medium lacking leucine, uridine, tryptophan and lysine for prototrophic selection. [57].

3.3 Results

3.3.1 *OFR2* (*ORF19.6869*) mutants can undergo white-opaque switching in a *MTL a/α* background

The *ofr2* mutant was a second strain with enhanced white-opaque switching in the *MTL a/α* background identified from the screen of the GRACE 1.0 library that also found *OFR1* (see Chapter 3). Further testing of the phenotype of the equivalent mutant from both the original GRACE library and a newly constructed null mutant in the SC5324 wild-type background identified the same phenotype as the original mutant. All *ofr2* null mutant strains can form phloxine B stained pink colonies on GlcNAc medium although they retain the heterozygous *MTL* locus (Figure 3.1A).

Microscopic examination of the white colonies showed white phase cells similar to the wild-type *MTL a/α* yeast cells, while the pink colonies showed elongated yeast cells similar to the wild-type *MTL* homozygous opaque phase cells. We conducted a further analysis of the opaque-like phenotype by immunofluorescence microscopy, using a monoclonal antibody that can distinguish white and opaque cells. When tested using fluorescence microscopy, the cells from the phloxine B staining pink colonies of the *MTL a/α ofr2Δ/Δ* null mutant yielded staining patterns similar to the typical opaque cells of the *MTL a/a* wild-type (Figure 3.1C Right). The white cells from the null mutant *MTL a/α* showed no signal (Figure 3.1C Left), as did the cells only treated with the secondary antibody.

Additionally, scanning electronic microscope (SEM) was used to analyze the cell surface of the *ofr2* null mutant. This identified the characteristic opaque pimples on the cell surface of the opaque-like cell formed by the mutant (Fig. 3.1B Right); this further supports the opaque status of the mutant cells.

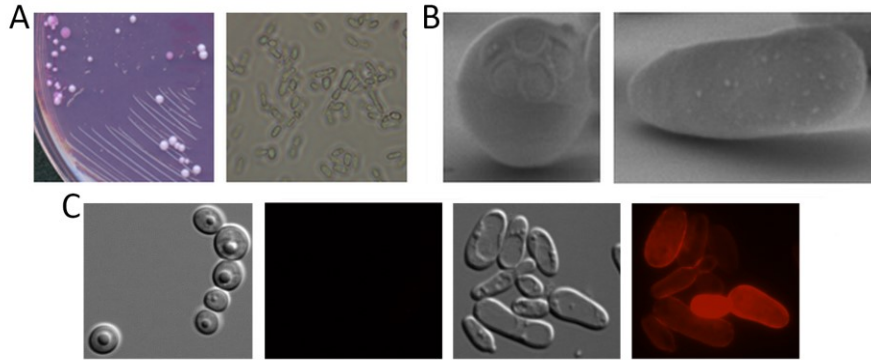


Figure 3.1 White opaque switching of *ofr2* null mutant. *A. White opaque switching of *ofr2* null mutant.* Left, streaking of *ofr2* null mutant (SN76 background) on SC-GlcNAc (plus phloxine B) agar medium at 25 °C for 3 days; right, opaque cells from a pink staining colony selected from left plate, visualized by optical microscope 400X. *B. Scanning electron microscopy.* Cells were fixed in glutaraldehyde as described after growth on SC-GlcNAc agar plates at 25 °C for 72 hours. The samples were coated with 20nm of gold palladium in an Emitech K550 sputter coater. Both white (left) and opaque (right) cells of the *ofr2* null mutant are shown at 5000x magnification. *C. A. Immunofluorescence microscopy of *ofr2*.* F223-5E1-1 is the monoclonal antibody used in this study as the primary antibody to identify opaque cells. Texas red conjugated goat anti-mouse antibody was used as the secondary antibody. White cells of *ofr2* without signal and opaque cells of *ofr2* with signal are shown here. Samples were observed and photographed under the Leica DM6000 fluorescence microscope at 630X magnification.

3.3.2 The stability of white- opaque switching in strains deleted for *OFR2*

Isolated white and opaque colonies were tested further for their overall white-opaque switching patterns. When individual cells from purified *MTL* heterozygous white colonies of the null mutant were incubated on GlcNAc agar medium at RT, the frequency of the opaque-like form, phloxine-staining colonies was around 1.5%, while no switching of the *MTL* heterozygous wild-type strain SN76 was observed under the same conditions (Table 3.3). Purified opaque-like colonies treated in the same manner undergo unstable cell divisions with about an 8.8% ratio of

switching back to white colonies on GlcNAc medium and about 15% switching back on glucose medium (Table 3.4).

Table 3.3 Ratio of white to opaque switching of *ofr2* null mutant. Carbon sources used were GlcNAc (GLC) and glucose (GLU). Strains were all initiated from white (WH) cells. The ratios are based on at least three separate experiments; colony types were calculated from among 500 to 1000 colonies in total after 7 days incubation at room temperature. *ofr2* Δ/Δ , *ofr2* null mutant, *MTLa/a*. WT, wild-type, *MTLa/a*. WTa, wild-type, *MTLa/a*.

GLC-WH to OP		GLU-WH to OP	
Genotype	Switch Ratio (%)	Genotype	Switch Ratio (%)
<i>ofr2</i> Δ/Δ	1.5 \pm 0.10	<i>ofr2</i> Δ/Δ	<0.3
WT	<0.05	WT	<0.05
WTa	91 \pm 7.5	WTa	5 \pm 1

Table 3.4 Ratio of opaque to white switching of *ofr2* null mutant. Carbon sources used were GlcNAc (GLC) and glucose (GLU). Strains were all initiated from opaque (OP) cells. The ratios are based on at least three separate experiments; colony types were calculated from among 400 to 1000 colonies in total after 7 days incubation at room temperature. *ofr2* Δ/Δ , *ofr2* null mutant, *MTLa/a*. WT, wild-type, *MTLa/a*. WTa, wild-type, *MTLa/a*.

GLC-OP to WH		GLU-OP to WH	
Genotype	Switch Ratio (%)	Genotype	Switch Ratio (%)
<i>ofr2</i> Δ/Δ	8.8 \pm 0.15	<i>ofr2</i> Δ/Δ	16 \pm 0.5
WTa	0.2 \pm 0.2	WTa	0.2 \pm 0.2

3.3.3 *ofr2* mutants can mate as *MTLa* cells

We used wild-type tester strains 3745a (*MTLa/a*) and 3315 α (*MTLa/a*) to examine the mating properties of the *MTLa/a ofr2* mutant strain switched to the presumptive opaque state. We observed prototrophic colonies arising from auxotrophic marker complementation of 3315 α (*MTLa/a*) tester (Figure 3.2) but not 3745a (*MTLa/a*) (data not shown) within three days incubation on SD-Glucose selection medium after initial culturing on SD-GlcNAc medium: the prototrophs were stable and represented real mating products. The *ofr2* null mutant failed to mate detectably on YPD medium perhaps due to the instability of the opaque state on glucose and its inherent low mating efficiency. The mating assay thus suggested the opaque *MTLa/a ofr2* mutant could undergo mating with *MTLa/a* wild-type cells as *MTLa*.

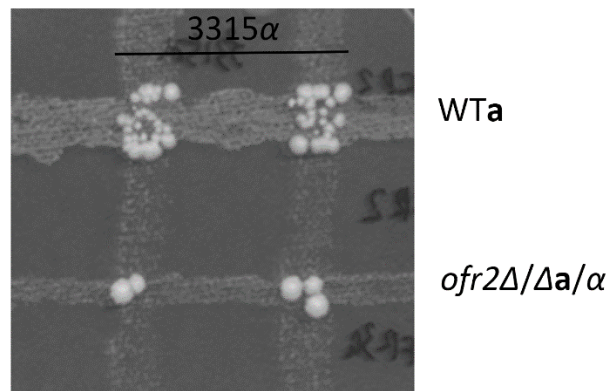
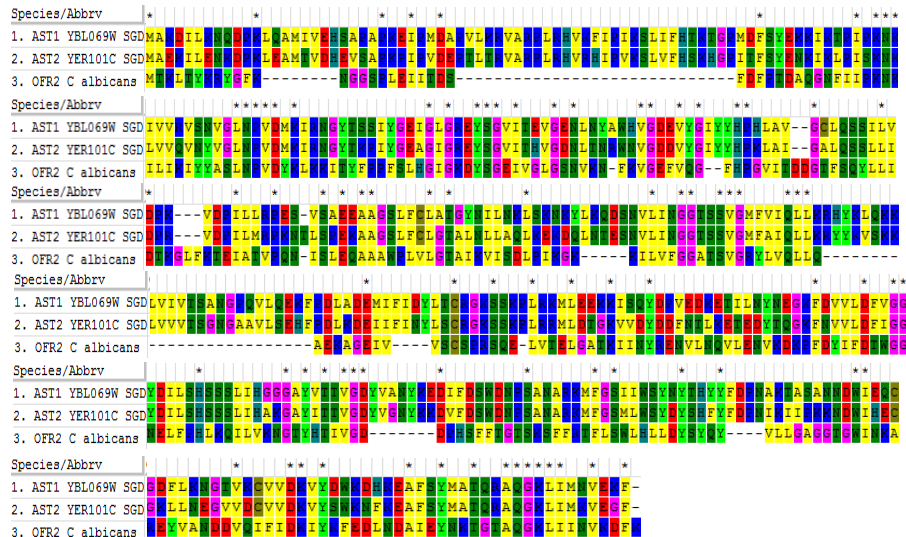


Figure 3.2 Mating ability of *ofr2* mutant. Strain 3315 α , in the opaque state, was used as the mating type tester. It had the auxotrophic markers *trp1/trp1*; *lys2/lys2*. The tester was crossed with *WTa* strain SN148a (*arg4/arg4*; *leu2/leu2*; *his1/his1*; *ura3::imm434/ura3::imm434*) and the null mutant *ofr2a/a* (*ura3::imm434/ura3::imm434*) on GlcNAc medium at RT for two days, and then replicated on selection medium SD-glucose (*trp*⁻, *lys*⁻, *arg*⁻, *ura*⁻) at 30°C for 3 days to detect prototrophic mating products.

3.3.4 The domain architecture of Ofr2

We examined the phylogenetic distribution of *ORF2/ORF19.6869* orthologs within the ascomycetes. There are no orthologs in most of the CTG clade of *Candida* species, but there are orthologs in the very close relatives *Candida dubliniensis* and *Candida tropicalis*. There is also an ortholog, *AST2*, in *Saccharomyces cerevisiae*. As well, in *S. cerevisiae* *AST2* has a paralog *AST1* that appeared due to the genome duplication. We have done a Blast search to confirm that *AST1* and *AST2* are the best hits identified for *OFR2* in *S. cerevisiae*. The predicted Ofr2 protein contains several NAD(P) binding sites and an *AST1*-like domain. This group contains members identified in the targeting of yeast membrane protein ATPase. ScAst1p is a lipid raft associated cytoplasmic protein; the *AST1*-like domain belongs to the medium chain dehydrogenase/reductase (MDR)/zinc-dependent alcohol dehydrogenase-like family, which also contains the zinc-dependent alcohol dehydrogenases (ADH-Zn). These medium chain dehydrogenase/reductase proteins have two domains: a C-terminal NAD(P) binding-Rossmann fold domain and an N-terminal catalytic domain. Therefore, based on its orthology, *OFR2* is potentially a lipid raft associated medium chain dehydrogenase/reductase.

Figure 3.3 Protein sequence alignments among Ofr2, Ast1 and Ast2. Protein sequence alignment was performed by the software MEGA6 using MUSCLE. Different colors show different amino acids groups. * is used to represent the identity of some amino acid.



We have also searched the best hit of Ofr2p within *C. albicans*; this identified a protein named Yim1 sharing a similar domain architecture to Ofr2. The orthologous protein Yim1 in *S. cerevisiae* has a localization to lipid droplets, suggesting a possible role in lipid metabolism [84].

3.3.5 Lipid droplets in *ofr2* mutants

As Ofr2p is predicted to be a lipid raft associated protein based on its orthology with Ast1 and shares a similar domain architecture with the potential lipid droplet-localized protein Yim1, we asked if this protein was implicated in lipid metabolism. Lipid droplets are involved in lipid homeostasis and metabolism through the storage of lipids within the cells, so we tested the pattern of lipid droplets by staining them using BODIPY. Compared to wild-type, the *ofr2* null mutant forms bigger lipid droplets inside the cell (Figure 3.4). Further lipid content analysis is currently underway.

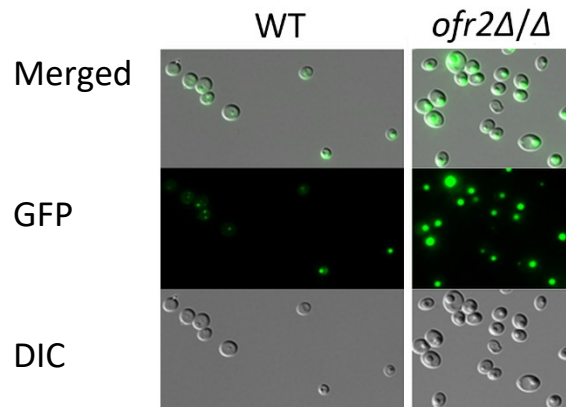


Figure 3.4. Fluorescence microscopy of lipid droplets. Overnight liquid cell cultures were treated with BODIPY for 10 min and then washed by 1xPBS twice before observation under a Leica DM6000B fluorescence microscope. WT, SN76, *MTLa/α*. *ofr2* Δ/Δ is the *ofr2* null mutant with *MTLa/α*. Filter cube system for lipid droplets signal is GFP ET (excitation filter 450-490nm). Merged channel, GFP channel and DIC channel are shown in order. Magnification is 400X.

3.4 Discussion

The absence of Ofr2 in the *MTLa/α* background in *Candida albicans* can result in formation of opaque cells when cells are grown on GlcNAc as the carbon source. Furthermore,

such *ofr2* opaque cells can mate as **a** type cells. Like the previously discovered *ofr1* null mutant, *ofr2* null mutant only switch to opaque under GlcNAc conditions, but unlike the *ofr1* mutant, the opaque cells of *ofr2* are not completely unstable under glucose growth conditions. *ofr2* opaque cells can maintain the opaque states when grown on glucose as the carbon source and are thus relatively stable under both GlcNAc and glucose conditions. However, *ofr2* opaque cells are still less stable when compared with *MTL* homozygous opaque cells under both conditions. Unlike *ofr1* mutants, which can mate with both **a** and α cells, the loss of Ofr2 permits the opaque form cells to mate in only one direction - with α type cells.

There are nine possible *MTL* variants that could permit some form of mating [30]. If either **a1** or $\alpha2$ (or both) are disrupted, cells can switch to the opaque form and undergo mating with both **a** and α types of cells. This fits the phenotype of the *ofr1* mutant. If **a1** and **a2**; or **a2** and $\alpha2$; or **a2**, $\alpha2$ and $\alpha1$ are missing, the cells can undergo white opaque switching and can mate with **a** type cells. To mate only with α type cells, there are three possibilities: both $\alpha1$ and $\alpha2$ are disrupted; **a1** and $\alpha1$ are both deleted; or **a1**, $\alpha1$ and $\alpha2$ are all inactivated [30]. As all the *MTL* cassettes are physically present, a potential explanation of the mating behavior of the *ofr2* null mutant is that the expression of $\alpha1$ is suppressed, and at the same time, either/both $\alpha2$ or/and **a1** is/are repressed somehow due to the absence of Ofr2 function.

The Ofr2 is a predicted lipid raft associated protein, and we have shown that the absence of Ofr2 can result in the appearance of bigger- sized lipid droplets in the cells. Lipid rafts are commonly found in the plasma membrane as well as in Golgi and lysosomal membranes [85]. As a possible lipid raft associated protein, Ofr2 potentially has a membrane localization. However, it is not immediately obvious why the loss of a gene implicated in lipid raft association and influencing lipid droplet formation should have any impact on mating. A possible link between lipid metabolism and the mating type locus is that the non-mating-related gene *PIK* is localized within the *MTL* locus. As both Ofr2 and *Pik* are potentially lipid metabolism related, it is possible that the absence of Ofr2 modifies the expression of *PIK* by influencing lipid metabolism levels, and this, as a result, impacts the expression of the adjacent *MTLa* and *MTL α* genes. If the expression of genes within the *MTL* locus is directly influenced, the phenotypic switching of white to opaque and subsequent mating could be straightforward to explain. We note that based on a previous study, *OFR2* is typically highly expressed only in white cells [30].

It is thought that opaque cells have a more lipidic metabolism than white cells in *C. albicans* [66]. Lipid metabolism and energy homeostasis are also influenced by lipid droplets, which are monolayer organelles with inert deposits of lipid that form at the endoplasmic reticulum (ER). The Ofr2 protein is potentially a lipid raft associated protein. The link to the size of lipid droplets may be due to a role in lipid trafficking and lipid metabolism. As Ofr2 has two orthologs Ast1 and Ast2 in *S. cerevisiae*, it will be interesting to see if *ast1ast2* double mutants in *S. cerevisiae* could also form larger lipid droplets.

Through screening a mutant library, we found a gene we named *OFR2* that has a predicted function of encoding a lipid raft associated protein; *ofr2* mutants can undergo white opaque switching and mating with α type cells. When cells lack this putative lipid-raft-associated protein, which is usually highly expressed in white cells, it appears lipid metabolism of the cell is affected and then cells accumulate more lipids by forming bigger lipid droplets in the cells. Intriguingly, these cells are also able to form opaque cells in a *MTLa*/ α background.

Chapter 4: Transcripts of *ORF19.7060* modulate white opaque switching

4.1 Introduction

As a pathogen, the success of *C. albicans* stems not only from its ability to generate an opportunistic infection when there are changes in the host physiological environment and habitat niche, but also from its capacity to grow and transition to different morphological forms including unicellular yeast, pseudohyphae and elongated hyphae [86]. When growing in the yeast form, *C. albicans* has both white and opaque states that transition through a specific cell type switch termed white-opaque switching [19]. This transition is very important for its sexual reproduction [12]. Typically, *C. albicans* is diploid with a heterozygous *MTLa/a* mating type locus [10]. To allow for gametogenesis, *C. albicans* needs to first lose heterozygosity at the *MTL* locus to become *MTLa/a* or *MTLa/a*, then switch from the typical white yeast cells to opaque yeast cells. *MTLa/a* cells can only mate efficiently with *MTLa/a* cells when both are in the opaque state [12, 29]. Both white-opaque switching and mating are blocked by the homeodomain **a1- α 2** heterodimer encoded from the *MTL* locus. Transcription factor **a2**, which activates **a** type specific gene expression, is, together with **a1**, localized at *MTLa*, while α 1, which positively regulates the expression of α specific genes, is, together with α 2, localized at *MTLa* [12]. In an *MTLa/a* cell, the heterodimeric **a1- α 2** repressor blocks *MTL* homozygous specific gene expression, including the white-opaque switching master regulator *WOR1* as well as genes related to pheromone response and mating [13, 14, 30].

Classic transformation allows us to manipulate the genes of *Candida albicans* by replacing any gene with a convenient selective marker. However, as the default state is diploid, each disruption requires the replacement of two alleles, and thus two consecutive transformations. Sometimes, it can be technically challenging and time-consuming to have the target gene knocked out successfully. Recently, a CRISPR system for *Candida* has been created by Vyas *et al.* [87]. This allows a single transformation to generate homozygous mutations of a target gene.

In this study, we first created a classic knock-out of *ORF19.7061* (*OFR3*) by replacing both alleles with selective markers. This classic *ofr3* mutant could undergo white opaque switching and mating in the *MTLa/a* background, similarly to the Grace version 1 mutant. However, later we found out that the transcript of the adjacent gene *ORF19.7060* was also

disrupted by the transformation due to overlapping regions. Intriguingly, *ORF19.7060* has both a long transcript and a short transcript; the long transcript present in white cells, the short transcript present in opaque cells. Using the CRISPR system, we inserted a stop codon into *ORF19.7061* without disrupting the overlapping long transcript of *ORF19.7060*. The new mutant did not switch to opaque, so it appears the phenotype of the white opaque switching was caused by disrupting the long transcript of *ORF19.7060* in the white state, rather than disrupting the function of *OFR3*.

4.2 Materials and Methods

4.2.1 Strains, media and culture conditions

The GRACE version 1.0 library with a collection of 887 mutants was used to identify colonies that could undergo white to opaque switching on GlcNAc agar medium containing phloxine B. Subsequently, an *ofr3* Δ/Δ null mutant strain was constructed by using *C. albicans* strain SN76 as the parent strain (See Table 4.1). Both alleles of *OFR3* were also disrupted in a specific area by using the CRISPR-CAS9 system with SN148 as the parent strain.

Table 4.1 Strains used in this study.

Strain	Parent	Mating type	Description	Source
SN76	RM1000	a/ α	<i>arg4/arg4; his1/his1; ura3 imm434/ura3 imm434</i>	Noble/ Johnson
SN148	SN76	a/ α	<i>arg4/arg4; leu2/leu2; his1/his1; ura3 imm434/ura3 imm434; iro1 imm434/iro1 imm434</i>	Noble/ Johnson
GRACE version 1.0 library	GRACE library	a/ α		Whiteway
GRACE library	CASS1	a/ α		Merck
3315	A505	α / α	<i>trp1/trp1; lys2/lys2</i>	Magee
3745	A505	a/a	<i>trp1/trp1; lys2/lys2</i>	Magee
CAI4 <i>MTLa</i>	CAI-4	a/a	<i>ura3 ::imm434/ ura3 ::imm434</i>	Doreen Harcus
CAI4 <i>MTLa</i>	CAI-4	α / α	<i>ura3 ::imm434/ ura3 ::imm434</i>	Doreen Harcus
<i>ofr3</i>	SN76	a/ α	<i>ofr3::HIS1/ofr3::ARG4; ura3 ::imm434/ ura3 ::imm434</i>	This study
<i>ofr3_crispr</i>	SN148	a/ α	<i>arg4/arg4; leu2/leu2; his1/his1; ura3 imm434/ura3 imm434; iro1 imm434/iro1 imm434; NAT⁺</i>	This study
<i>Orf19.7060_crispr</i>	SN148	a/ α	<i>arg4/arg4; leu2/leu2; his1/his1; ura3 imm434/ura3 imm434; iro1 imm434/iro1 imm434; NAT⁺</i>	This study

For cultivation, SC-medium with glucose (2%) or GlcNAc (1.25%) was used. Plate cultures were grown to a density of 40-120 colonies per 90 mm plate. For opaque colony identification, Phloxine B (5 $\mu\text{g ml}^{-1}$) was added to the agar medium. For routine liquid cultivation, YPD (1% yeast extract, 2% peptone, and 2% glucose) medium was used for *C. albicans*; LB medium (1% Tryptone, 1% NaCl, 0.5% Yeast extract) was used for *E. coli*. YPD plus Nourseothricin (200 $\mu\text{g l}^{-1}$) was used for selection of CRISPR mutants.

4.2.2 Strain construction

OFR3 was replaced by standard one-step disruptions using PCR products [35]. The markers *HIS1* and *ARG4* were amplified by PCR from plasmids pFA-CaHIS1 and pFA-CaARG4 using primers that provided flanking regions of *OFR3*. The *HIS1* and *ARG4* markers were sequentially transformed to the parent strain SN76, and the transformants were selected on SD-his and SD-arg agar plates. Successful transformants were further confirmed by PCR. CRISPR mutants were selected on YPD plus Nourseothricin (200 µg/l). Successful transformants were further confirmed by sequencing. Primers used in this study are listed below (See Table 4.2).

Table 4.2 Primers used in this study.

Name	Description	Sequence (5' to 3')	Source
<i>OFR3</i> _F	<i>OFR3</i> deletion PCR cassette forward primer	TTATGGTACTTGGTCGTTTGCAACTCCAGCATAATTTTCTTT TTTCTTGTTTTGTCGCTCCAGCATCTGACAAGTTTGATCTGA TTCCAATTTTCGAAGCTTCGTACGCTGCAGGTC	This study
<i>OFR3</i> _R	<i>OFR3</i> deletion PCR cassette reverse primer	CGATACCACAACTGTGGCAATACCTTTTGTATTGAAATATT TGGATAGTGAGTTGTCGGCAATGGGTATAAAGATGCGTTA TAATGTTGAACCAATCTGATATCATCGATGAATTCGAG	This study
<i>OFR3</i> _ex_F	<i>OFR3</i> external forward primer	AGAGATGAACAATATGAGAG	This study
<i>OFR3</i> _ex_R	<i>OFR3</i> external reverse primer	ATGTAGAAGATGTGCAGTC	This study
<i>OFR3</i> _in_F	<i>OFR3</i> internal forward primer	TACTTCTAATGAAATTCCTC	This study
<i>OFR3</i> _in_R	<i>OFR3</i> internal reverse primer	TATTCGGATAGAATTAGAAC	This study
HIS1 F	<i>HIS1</i> forward primer	TTTAGTCAATCATTTACCAGACCG	<i>OFR1</i> study
HIS1R	<i>HIS1</i> reverse primer	TCTATGGCCTTTAACCCAGCTG	<i>OFR1</i> study
ARG4 -F	<i>ARG4</i> forward primer	TATGAGAATTTTCGTTTCGTG	<i>OFR2</i> study
ARG4 -R	<i>ARG4</i> reverse primer	AGCACCAGATCCTAATGGAG	<i>OFR2</i> study
<i>MTLa</i> F	<i>MTLa1</i> forward primer	TTGAAGCGTGAGAGGCAGGAG	Magee
<i>MTLa</i> R	<i>MTLa1</i> reverse primer	GTTTGGGTTCCCTTCTTTCTCATTC	Magee
<i>MTLa</i> F	<i>MTLa2</i> forward primer	TTCGAGTACATTCTGGTTCGC	Magee
<i>MTLa</i> R	<i>MTLa2</i> reverse primer	TGTAAACATCCTCAATTGTACCCG	Magee
<i>OFR3</i> repair F	<i>OFR3</i> repair DNA forward	ACGGTAATGTAGACATTATAATAATCGAAGGAAATTATGT ATAACTTCGAGACTAGTACT	This study
<i>OFR3</i> repair F	<i>OFR3</i> repair DNA reverse	TTTATAAACCAAGTGTCGTCAACAAAATTTTCAATTT CATCGCAGTACTAGTCTCGAAGTTAT	This study
<i>OFR3</i> sgF	<i>OFR3</i> guide DNA forward	ATTTGATCACTTCGAGACAAATACTG	This study
<i>OFR3</i> sgR	<i>OFR3</i> guide DNA reverse	AAAACAGTATTTGTCTCGAAGTGATC	This study

4.2.3 CRISPR-CAS9

The “solo system” strategy was used for *Candida albicans* CRISPR-Cas9 following the detailed protocol described by Vyas *et al* [87]. To design CRISPR guide sequences, the online database Benchling was used to select the sgRNA sequences with guide parameters as follows. Design type: single guide; Guide length: 20; Genome: CA22(*CANDIDA ALBICANS* SC5314(DIPLOID)); PAM: NGG [88]. To avoid disrupting the long transcript part of *ORF19.7060*, the target region was selected after 2/3 of the full-length sequence. A guide sequence was chosen based on the position nearer to the start codon and higher on-target and off-target scores. Also, it was checked in the file named (Targ.NoTs.subs12nt.HitsGenesOnly.Hits1Gene2Alle.3letterName) from the supplemental material of Vyas *et al* [87]. This file shows sequences that match any given gene in both alleles. The plasmid for the solo system with both Amp⁺ and Nat⁺ markers as well as CAS9 is called pV1093. There were three sets of primers designed for CRISPR mutant construction: sgRNA, Repair DNA, and Screening primers. For the sgRNA design, a 20 nt guide with an attached sequence encoding restriction enzyme digestion sites on both the 5' and 3' ends to allow cloning into plasmid PV1093, so this set of primers had this form: Forward – 5'-atttgX₂₀g-3' and Reverse – 5'-aaaacX₂₀c-3'. The repair DNA was derived from sequences flanking the sgRNA target sequence. It was co-transformed with the plasmid that contains the sgRNA. Repair DNA was modified with four different changes including two in frame stop codons (TGA used in this mutant), a disrupted PAM region (NGG) and introduction of a restriction enzyme site for confirmation of transformants. A CviQ1 digestion site was introduced into this pair of repair DNAs. The repair DNA was also designed using Benchling. The screening primers were designed to amplify around 1kb as well as for sequencing. Detailed PCR, cloning, transformation and confirmation were as described elsewhere [87].

4.2.4 Phenotype switching

White and opaque cells were picked from single colonies on SC-GlcNAc medium after 5 days at 25°C. Cells then were suspended in water, the cell concentration was adjusted, and the suspensions plated onto agar medium containing 5 µg ml⁻¹ phloxine B with either 2% glucose or 1.25% GlcNAc as the carbon source. Plates were incubated at 25°C. Data were collected, and

plates were scanned on the 7th day and the frequency of sectored colonies calculated by standard statistical methods.

4.2.5 Microscopy and imaging

Optical microscopic images of cells were captured using a Nikon Eclipse TS100. Immunofluorescence microscopic images were visualized and photographed using Leica DS6000 with 630x magnification with settings: Objective: 63x Oil, Filter: TxRed-560/40. Images of plates and colonies were scanned at 800 pi by an Epson Perfection v500 photo scanner.

4.2.6 Immunofluorescence

Cells from single colonies cultured for 5 days on SD agar medium at RT were pre-grown in SD liquid medium overnight at RT, 220 rpm shaking and then diluted in fresh SD liquid medium for another 12 h incubation at RT, 220 rpm. The cells were pelleted and washed in 1 mL of 1xPBS for three times, 2 min each time; approximately 10^7 cells were tested for each assay. Washed cells were blocked with 1ml blocking buffer for 30 min before incubation with 100 μ l of the primary antibody for one hour at RT. Then cells were washed with PBS containing 0.05% Tween 20 for three times, 5 min each time. Washed cells were incubated with 100 μ l of the secondary antibody - Texas red conjugated goat anti-mouse antibody (1/100 dilution in blocking buffer) for 1 hour in the dark at RT. Then cells were washed with PBS containing 0.05% Tween 20 three times and PBS once, 5 min each time. Cells were finally suspended in 50 μ l PBS, and 3 μ l was applied under a coverslip. Sampled microscope slides were sealed and placed in a microscope slide box for protection from light before observation under the Leica DM6000 fluorescence microscope.

4.2.7 Scanning Electron Microscope

Cells were grown on SC-GlcNAc agar plates for 72 hours at 25 °C and then fixed with 2.5% (w/v) glutaraldehyde in 0.1 M sodium cacodylate buffer at 4°C overnight. Then cells were post-fixed with 1% aqueous osmium tetroxide for 90 minutes at room temperature. Following fixation, cells were dehydrated gradually using a 15% gradient ethanol series and subsequently dried using a critical point dryer. The samples were then coated with 20 nm of gold palladium

(60:40) in an Emitech K550 sputter coater. Cells were imaged with a Hitachi S-2700 scanning electronic microscopy and collected with Quartz PCI software.

4.2.8 Mating assays

Cells were streaked on SC-GlcNAc agar medium (with phloxine B) for five days at RT to select opaque colonies. Opaque cells of strains 3315 α and 3745 α were used as the tester strains for mating. Opaque colonies of the *MTL* α /*ofr3* strain were restreaked as straight lines on separate YPD and SC-GlcNAc agar plates as the experimental strain. Opaque cells of tester strains were streaked as straight lines on YPD plates. The two sets of tester and experimental streaks were patched onto the same YPD plate and were incubated at room temperature (RT). After 24 hours of incubation on YPD plates and 48 hours incubation on SC-GlcNAc plates at RT, cells were replicated onto SC-Glucose selection medium lacking uridine, tryptophan and lysine for prototrophic selection [57].

4.3 Results

4.3.1 *OFR3* can undergo white opaque switching in a *MTL* α / α background.

ofr3 was the third strain identified with enhanced white-opaque switching in the *MTL* α / α background through screening the GRACE1.0 library. The 5-FOA selection process can result in a simultaneous loss of the *URA3* marker and loss of heterozygosity (LOH) elsewhere in the genome [44], and we have identified that this mutant has become a homozygous knockout due to LOH of *OFR3*. Intriguingly, attempts at confirmation by testing the phenotype of the equivalent mutant from the original GRACE library failed, but a null mutant of *OFR3* constructed in the SC5324 wild-type background provided the same phenotype as the mutant from the GRACE 1.0 library. The *ofr3* null mutant strain can form phloxine B stained pink colonies on GlcNAc medium (Figure 4.1A).

Microscopic examination of the white colonies showed white phase cells similar to the wild-type *MTL* α / α yeast cells, while pink colonies showed elongated yeast cells similar to the wild-type *MTL* homozygous opaque phase cells (Figure 4.1B). We performed a further analysis of the opaque-like phenotype by immunofluorescence microscopy, using a monoclonal antibody

that can differentiate between white and opaque cells. When assayed using fluorescence microscopy, the opaque-like cells from the *MTLa/a ofr3Δ/Δ* null mutant gave staining patterns similar to the classic opaque cells of the *MTLa/a* wild-type (Fig 4.1C). The white cells from both the null mutant *MTLa/a* and wild-type *MTLa/a* strains, showed no signal, as did the cells only treated with the secondary antibody (data not shown).

Additionally, scanning electron microscope (SEM) was used for analyzing the cell surface of the *ofr3* mutant. On the cell surface of the opaque-like cell formed by the mutant, there are the characteristic opaque pimples (Figure 4.1D); this further supports the opaque status of the mutant cells.

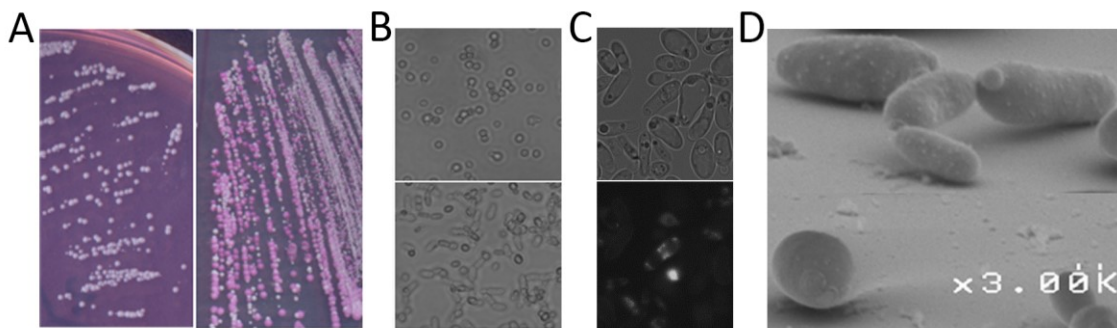


Figure 4.1. White-opaque switching with mutated *OFR3*. *A. *OFR3* can undergo white opaque switching in the *MTL a/a* background with *GlcNAc* as the carbon source. Cells were streaked on *SC-GlcNAc* agar plates containing *phloxine B*; under these conditions, opaque colonies are stained pink. The mating types of both the wild-type (left) and *ofr3* null mutant (right) are heterozygous *MTL a/a*. These strains were all incubated at room temperature (RT) for 7 days before being scanned. B. White and opaque cells of *ofr3* null mutant under the optical microscope. Top panel, white cells; bottom panel, opaque cells, 400X. C. Immunofluorescence microscopy of *ofr3* opaque cells. Cells were fixed with formaldehyde and washed with 1x PBS. Fixed cells were stored in 1x PBS at 4° C before immunofluorescence microscopy. F223-5E1-1 is the monoclonal antibodies used in this study as the primary antibodies to identify opaque cells. Texas red conjugated goat anti-mouse antibody was used as the secondary antibody. Samples were observed and photographed under the Nikon Eclipse TiE fluorescence microscope at 400X magnification. D. Scanning electron microscopy. Cells were fixed in glutaraldehyde as*

described after growth on SC-GlcNAc agar plates at 25 °C for 72 hours. The samples were coated with 20nm of gold palladium in an Emitech K550 sputter coater. Cells were photographed under scanning electron microscope at 5000x magnification. Both opaque (top panel) and white (bottom panel) cells of the *ofr3* null mutant are shown.

4.3.2 The stability of white-opaque switching in the absence of *OFR3*

Purified white and opaque colonies were selected to test the overall white-opaque switching patterns further. When individual cells from purified white colonies of the null mutant were incubated on GlcNAc agar medium at RT, the frequency of the opaque-like form, phloxine-staining colonies was around 4.2%, while no switching of wild-type strain SN76 was observed under the same conditions (Table 4.3). Purified opaque-like colonies treated in the same manner undergo very stable cell divisions with a less than 0.1% ratio of switching back to white colonies (Table 4.4).

Table 4.3 Ratio of white to opaque switching of *ofr3* null mutant. Carbon sources used were GlcNAc (GLC) and glucose (GLU). Cultures were all initiated from white (WH) cells. The ratios are based on at least three separate experiments; colony types were calculated from among 300 to 1000 colonies in total after seven days incubation at room temperature. *Ofr3*Δ/Δ, *ofr3* null mutant, *MTLa/a*. *WTa*, wild-type, *MTLa/a*.

GLC-WH to OP		GLU-WH to OP	
Genotype	Switch Ratio (%)	Genotype	Switch Ratio (%)
<i>ofr3</i> Δ/Δ	4 ±1.5	<i>ofr3</i> Δ/Δ	<0.3
WT	<0.05	WT	<0.05
WTa	91±7.5	WTa	5 ±1

Table 4.4 Ratio of opaque to white switching of *ofr3* null mutant. Carbon sources used were GlcNAc (GLC) and glucose (GLU). Cultures were all initiated from opaque (OP) cells. The ratios are based on at least three separate experiments; colony types were calculated from among 200 to 1000 colonies in total after seven days' incubation at room temperature. (*ofr3* Δ/Δ , *ofr3* null mutant, *MTLa*/ α . *WTa*, wild-type, *MTLa*/ α .)

GLC-OP to WH		GLU-OP to WH	
Genotype	Switch Ratio (%)	Genotype	Switch Ratio (%)
<i>ofr3</i> Δ/Δ	<0.10	<i>ofr3</i> Δ/Δ	<0.10
<i>ofr3</i> Δ/Δ a	<0.10	<i>ofr3</i> Δ/Δ a	<0.10
WTa	0.2 \pm 0.2	WTa	0.2 \pm 0.2

4.3.3 *ofr3* mutants can mate as *MTLa* cells

We used wild-type tester strains 3315 α (*MTLa*/ α) and 3745**a** (*MTLa*/**a**) to investigate the mating properties of the *MTLa*/ α *ofr3* mutant strain switched to the presumptive opaque state. We observed prototrophic colonies arising from auxotrophic marker complementation of the 3315 α (*MTLa*/ α) tester (Figure 4.2) but not the 3745**a** (*MTLa*/**a**) tester (data not shown) within three days incubation on SD-Glucose selection medium after initial culturing on YPD medium: the prototrophs were stable and represented real mating products. The mating assay thus suggested the *MTLa*/ α *ofr3* mutant could undergo mating with *MTLa*/ α wild-type cells as *MTLa* cells.

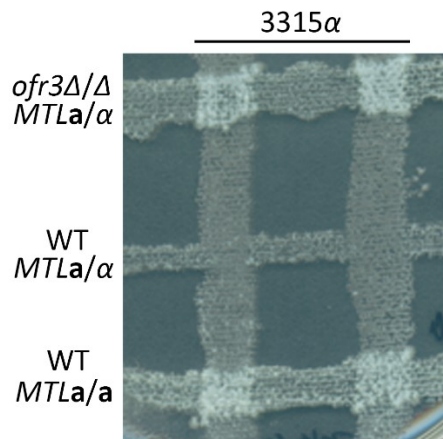


Figure 4.2. Mating ability of *ofr3* mutant. Strain 3315 α , in the opaque state, was used as mating type tester. It had the auxotrophic markers *trp1/trp1*; *lys2/lys2*. The tester was crossed with WT *MTL α / α* strain SN148 (*arg4/arg4*; *leu2/leu2*; *his1/his1*; *ura3::imm434/ura3::imm434*), WT *MTL α /a* strain CAI4a (*ura3::imm434/ura3::imm434*) and the null mutant *ofr3 α / α* (*ura3::imm434/ura3::imm434*) on YPD medium at RT for 24 hours and then replicated on selection medium SD-glucose (*trp*⁻, *lys*⁻, *ura*⁻) at 30°C for 3 days to detect prototrophic mating products.

4.3.4 The architecture of Ofr3

We have examined the architecture of the *Ofr3* locus. Intriguingly, the adjacent gene to *OFR3*, *ORF19.7060*, had different transcripts in white and opaque cells [89]. The short transcript in the opaque cell begins at genomic position ~96790. The long transcript found in white cell starts at genomic position 96250-96300, which means the long transcript of *ORF19.7060* overlaps significantly (about 2/3) with the open reading frame of *OFR3* [89]. Thus disruption of the *OFR3* gene also disrupts the long transcript found in white state cells. In these disruptants, white cells would only express the short transcript normally expressed only in the opaque state, or no transcript at all. To establish whether the opaque cell formation phenotype is caused by disruption of the long form transcript of *ORF19.7060* or results from the disruption of the *OFR3* gene itself, we designed a CRISPR-cas9 disrupted *OFR3* mutant. We inserted stop codons in the *OFR3* gene instead of replacing it by a selective marker to avoid disruption of the long transcript of the adjacent gene. Then we tested several successful CRISPR mutant isolates for white-

opaque switching on GlcNAc medium with phloxine B. There was no appearance of pink colonies on the plate or elongated opaque-like cells under the optical microscope. Thus we believe that the phenotype of *OFR3* was caused by the disruption of the long transcript of *ORF19.7060* in the white state, and not through the disruption of *ORF19.7061*. Both the long and short transcripts of *ORF19.7060* produce the same protein; one transcript initiates approximately 100 nucleotides before the start of translation, the other transcript begins about 650 nucleotides before the start of translation. We constructed a null mutant of *orf19.7060* to investigate its impact on white-opaque switching, but this disruption did not affect the switching in either a *MTL* heterozygous or *MTL* homozygous background.

According to a previous study, only *EFG1*, *ORF19.7060*, and *ORF19.2049* have distinct transcripts in white and opaque phases [89]. They all produce a longer transcript in white phase cells and a shorter transcript in opaque state cells. *EFG1* is so far the most well-studied of these genes. For cells that undergo white-opaque switching, *EFG1* is transcribed as a 3.2-kb mRNA in the white state and a less-abundant 2.2-kb mRNA in the opaque state [90]. The two transcripts have different transcription start sites, but both encode the same protein. Based on the previous study, the complete *EFG1* promoter was integrated into the (*Renila reniformis* luciferase) RLUC reporter system [34]. It turned out that *EFG1* expressed about 38-fold higher RLUC activity in the white phase than in the opaque phase. To express the more abundant white-phase-specific transcript of *EFG1*, sequences upstream of the 5'- untranslated region of the white-phase *EFG1* transcript are essential [90]. Deletion of the full length of upstream region *EFG1* results in a decreased white phase expression to the low level expressed in the opaque state [91].

Analysis of *Orf19.2049* shows that it has seven transmembrane domains, but the function of the protein remains to be characterized [92]. A search for the domain structure of *Orf19.7060* revealed an XLF domain and a C-terminal EBP50 domain. XLF is Xrcc4-like-factor, which interacts with the XRCC4-DNA ligase IV complex to promote DNA nonhomologous end-joining. The C-terminal EBP50 domain can interact with FERM domains of Ezrin-radixin-moesin (ERM) to regulate cytoskeletal modulation and cellular growth control. This domain contains two well-conserved hydrophobic regions with a disordered section in between [93].

We examined the phylogenetic distribution of *ORF19.7060* orthologs within the ascomycetes. Although there are orthologs in most of the CTG clade of *Candida* species, only

very close relatives *Candida dubliniensis* and *Candida tropicalis* share both the XLF and EBP50-C domains identified in the *C. albicans* protein. There is no ortholog in either *Candida glabrata* or *Saccharomyces cerevisiae* [94]. However, in *S. cerevisiae*, Nej1, involved in non-homologous end-joining, also contains an XLF domain. This protein interacts with DNA ligase IV complex as a ligase interacting factor to promote DNA nonhomologous end-joining, and the expression is repressed in *MAT* heterozygous cells.

4.4 Discussion

In this study, we have found a mutant that could undergo white opaque switching through screening a *MTLa/α* mutant library. Construction of the null mutant of this *ORF19.7061* repeated the phenotypes as the white to opaque switching and the mating with *MTLa/a* cells at the *MTLa/α* background. However, according to a previous study, the adjacent gene *ORF19.7060* provides two different transcripts in white and opaque cell states. So we used the CRISPR system to insert stop codons into *ORF19.7061(ORF3)* without disrupting the overlapping long transcript of *ORF19.7060*. It turned out that the new CRISPR mutant could not switch to opaque, so the phenotype of the white opaque switching may actually be caused by the disruption of the long transcript of *ORF19.7060* in the white state. *ORF19.7060* generates the long transcript when cells are in the white state and provides the short transcript when cells are in the opaque state. When the long transcript is disrupted, even in the white state, the cells can produce only the short form of the transcript of *ORF19.7060*, which is normally opaque specific. The *MTL* heterozygous cells are able to produce only the opaque state's transcript of *ORF19.7060* and this may promote white opaque switching. However, deletion of *ORF19.7060* did not affect the white opaque switch in either the *MTL* heterozygous or the *MTL* homozygous strains. This suggests that it may be the amount or location of the protein or the transcript that influences the white opaque switching, not the specific presence of the protein.

Chapter 5: ATPase chaperone Atp12 is involved in white opaque switching of *Candida albicans*

5.1 Introduction

White opaque switching is a specific phenotype switching in *Candida albicans* [19]. The switch is controlled the master regulator Wor1, itself repressed by the $\alpha 1$ - $\alpha 2$ homeodomain co-repressor [14]. White-opaque switching is regulated through a series of environmental cues including carbon sources, CO₂, oxidative pressure, temperature and genotoxic stress [27]. Oxidative stress can enhance the switching from the white state to the opaque state [95].

ATP12 deletion can induce white opaque switching potentially due to the creation of oxidative stress. Atp12p is the chaperone for biogenesis of F1-ATPase in the mitochondria [96]. The F1F0-ATPase functions in ATP biogenesis through oxidative phosphorylation [97]. The F1-ATPase is a multimer composed of $\alpha 3\beta 3\gamma\delta\epsilon$ subunits [98]. The α and β subunits are assembled by a pair of chaperones, Atp11p and Atp12p [96]. Atp11p helps in the assembly of β subunits while Atp12p serves the role in assembling α subunits as part of the F1-ATPase. Atp12p can select and bring the mature α subunits to the F1 machinery. Dysfunction of Atp12 will lead both mature and unprocessed α subunits to assemble to the F1-ATPase, which causes a growth deficiency in *S. cerevisiae* and a fatal disease in humans called mitochondrial biosynthesis disorder [98]. The effect on *C. albicans* is not yet clear. In this study, we identified the *atp12* mutant from our screening for white opaque switching, and further characterized *ATP12* as well as with γ subunit gene *ATP16* as to their roles in *C. albicans* metabolism.

5.2 Materials and Methods

5.2.1 Strains, media and culture conditions

The GRACE version 1.0 library containing a collection of 887 mutants was used to identify colonies that could undergo white to opaque switching on GlcNAc agar medium containing phloxine B. Subsequently an *atp12* CRISPR mutant was constructed from the parent strain SN148 by inserting two stop codons within the *ATP12* coding sequence (See Table 6.1).

Table 5.1 Strains used in this study.

Strain	Parent	Mating type	Description	Source
SN148	SN76	a/α	<i>arg4/arg4; leu2/leu2; his1/his1; ura3 imm434/ura3 imm434; iro1 imm434/iro1 imm434</i>	Noble/ Johnson
GRACE version 1.0 library	GRACE library	a/α		Whiteway
GRACE library	CASS1	a/α		Merck
3315	A505	<i>α /α</i>	<i>trp1/trp1; lys2/lys2</i>	Magee
3745	A505	a/a	<i>trp1/trp1; lys2/lys2</i>	Magee
CAI4 MTLα	CAI-4	a/a	<i>ura3 ::imm434/ ura3 ::imm434</i>	Doreen Harcus
CAI4 MTLα	CAI-4	<i>α /α</i>	<i>ura3 ::imm434/ ura3 ::imm434</i>	Doreen Harcus
<i>atp12_crispr</i>	SN148	a/α	<i>arg4/arg4; leu2/leu2; his1/his1; ura3 imm434/ura3 imm434; iro1 imm434/iro1 imm434; NAT⁺</i>	This study

For cultivation, SC (synthetic complete)-medium with glucose (2%) or GlcNAc (1.25%) was used. Plate cultures were grown at a density of 40-120 colonies per 90 mm plate. For opaque colony identification, Phloxine B (5 µg ml⁻¹) was added to the agar medium. For routine liquid cultivation, YPD (1% yeast extract, 2% peptone, and 2% glucose) medium was used. LB medium (1% Tryptone, 1% NaCl, 0.5% Yeast extract) was used for *E. coli* cultivation. YPD plus Nourseothricin (200 µg l⁻¹) was used for selection of CRISPR mutants.

5.2.2 Strain construction

To design CRISPR guide sequences, the file Targ.NoTs.subs12nt.HitsGenesOnly.Hits1Gene2Alle.3letterName from the supplemental material of Vyas *et al* was used [87]. This file only shows sequences that hit one gene in both alleles. The plasmid for the solo system with both Amp⁺ and Nat⁺ markers as well as CAS9 is pV1093. There were three sets of primers designed for CRISPR mutant construction: sgRNA, Repair DNA, and Screening primers. For the sgRNA design, a 20 nt guide with attached restriction enzyme digestion sites at both 5' and 3' ends to allow cloning into the plasmid PV1093 was designed: this set of primers had the form: Forward – 5'-atttgX₂₀g-3' and Reverse – 5'-aaaacX₂₀c-3'. The repair DNA includes the sequence flanking the sgRNA target sequence, and is co-transformed with the plasmid that contains the sgRNA. Repair DNA was modified with three different changes including two in-frame stop codons (TAA used in this mutant), a disrupted PAM region (NGG) and a restriction enzyme site for confirmation of transformants. A *Bam*HI digestion site was introduced into this pair of repair DNAs. The screening primers were designed to amplify around 1kb suitable for sequencing. Detailed PCR, cloning, transformation and confirmation were done as described elsewhere [95]. CRISPR mutants were selected from YPD plus Nourseothricin (200 µg l⁻¹). Successful transformants were further confirmed by sequencing. Primers used in this study are listed in Table 5.2.

Table 5.2 Primers used in this study.

Name	Description	Sequence (5' to 3')	Source
<i>MTLa</i> F	<i>MTLa</i> 1 forward primer	TTGAAGCGTGAGAGGCAGGAG	Magee
<i>MTLa</i> R	<i>MTLa</i> 1 reverse primer	GTTTGGGTTTCCTTCTTTCTCATTC	Magee
<i>MTLa</i> F	<i>MTLa</i> 2 forward primer	TTCGAGTACATTCTGGTCGC	Magee
<i>MTLa</i> R	<i>MTLa</i> 2 reverse primer	TGTA AACATCCTCAATTGTACCCG	Magee
ATP12 repair F	<i>ATP12</i> repair DNA forward	AAAAAAGGTGAAGTTAAATTCAATAAAGAA ACTCAAAAATATGTAATAGAATTGGATCCG	This study
ATP12 repair R	<i>ATP12</i> repair DNA reverse	ATTCTAATGGGAATCCAAGTGGTGTGCGTAG AGTTTTTCGGATCcAATTGAATTCATATT	This study
ATP12 sgF	<i>ATP12</i> guide DNA forward	ATTTGAATATGAAATTCAATTAGATG	This study
ATP12 sgR	<i>ATP12</i> guide DNA reverse	AAAACATCTAATTGAATTCATATTC	This study
ATP12 scF	<i>ATP12</i> screening primer forward	GTTCAGTTTTGGAATGGAAGG	This study
ATP12 scR	<i>ATP12</i> screening primer forward	GAGTATCTTCTACTTCACCC	This study

5.2.3 Phenotype switching

White and opaque cells were from single colonies on SC-GlcNAc medium after five days at 25°C. Cells were suspended in water, the cell concentration was adjusted, and the suspensions

plated onto agar medium containing 5 $\mu\text{g ml}^{-1}$ phloxine B with either 2% glucose or 1.25% GlcNAc as the carbon source. Plates were incubated at 25°C. Data were collected, and plates were scanned on the 7th day and the frequency of sectorized colonies calculated by standard statistical methods.

5.2.4 Microscopy and imaging

Optical microscopic images of cells were captured using a Nikon Eclipse TS100. Immunofluorescence microscopic images were visualized and photographed using a Leica DS6000 with 630x magnification with settings: Objective: 63x Oil, Filter: TxRed-560/40. Images of plates and colonies were scanned at 800 dpi by an Epson Perfection v500 photo scanner.

6.2.5 Immunofluorescence

Cells from single colonies cultured for five days on SD agar medium at RT were pre-grown in SD liquid medium overnight at RT, 220 rpm shaking and then diluted in fresh SD liquid medium for another 12 h incubation at RT, 220 rpm. The cells were pelleted and washed in 1 mL of 1xPBS for three times, 2 mins each time; approximately 10^7 cells were tested for each assay. Washed cells were blocked with 1ml blocking buffer for 30 mins before incubation with 100 μl of primary antibodies for one hour at RT. Cells were then washed with PBS containing 0.05% Tween 20 for three times, five mins each time. Washed cells were incubated with 100 μl of the secondary antibody - Texas red conjugated goat anti-mouse antibody (1/100 dilution in blocking buffer) for 1 hour in the dark at RT. Cells were then washed with PBS containing 0.05% Tween 20 three times and PBS once, five mins each time. Cells were finally suspended in 50 μl PBS, and 3 μl was applied for under a coverslip. Sampled microscope slides were sealed and placed in a microscope slide box for protection from light before observation under the Leica DM6000 fluorescence microscope.

5.2.6 Mating assays

Cells were streaked on SC-GlcNAc agar medium (with phloxine B) for five days at RT to select opaque colonies. Opaque cells of strains 3315 α and 3745 \mathbf{a} were used as the tester strains for mating. Opaque colonies of the *MTLa/α atp12* strain were restreaked as straight lines on separate YPD and SC-GlcNAc agar plates as the experimental strain. Opaque cells of tester

strains were streaked as straight lines on YPD plates. The two sets of tester and experimental streaks were patched onto the same YPD and SC-GlcNAc agar plates separately after 48 hours of incubation at room temperature (RT). After 24 hours of incubation on YPD plates and 48 hours incubation on SC-GlcNAc plates at RT, cells were replicated onto SC-Glucose selection medium lacking leucine, uridine, tryptophan and lysine for prototrophic selection [57].

5.3 Results

5.3.1 *ATP12* can undergo white-opaque switching at the *MTL a/alpha* background

ATP12 is an ATPase subunit assembler. Mutations in this gene were identified with enhanced white-opaque switching through screening the *MTLa/α* GRACE1.0 library. Further confirmation by testing the phenotype of the equivalent mutant from the original GRACE library and newly constructed null mutant in the SC5324 wild-type background by using CRISPR-Cas9 system reconstructed the white-to-opaque switching phenotype. The *atp12* null mutant strain can form phloxine B stained pink colonies on both SD-glucose and GlcNAc (Figure 5.1A) media.

Microscopic examination of the white colonies showed white phase cells similar to the wild-type *MTLa/α* yeast cells, while pink colonies showed elongated yeast cells similar to the wild-type *MTL* homozygous opaque phase cells (Figure 5.1B). We performed a further analysis of the opaque-like phenotype by immunofluorescence microscopy, using a monoclonal antibody that can differentiate white and opaque cells. When assayed using fluorescence microscopy, the opaque-like cells from the *MTLa/α atp12* null mutant gave staining patterns similar to the classic opaque cells of the *MTLa/a* wild-type (Figure 5.1C). The white cells from both the null mutant *MTLa/α* and wild-type *MTLa/a* strains, showed no signal, as did the cells only treated with the secondary antibody. However, the opaque cells of the *atp12* null mutant at the *MTLa/α* background cannot undergo mating, unlike previously identified white-opaque switchers such as *ofr1* (See Chapter 3).

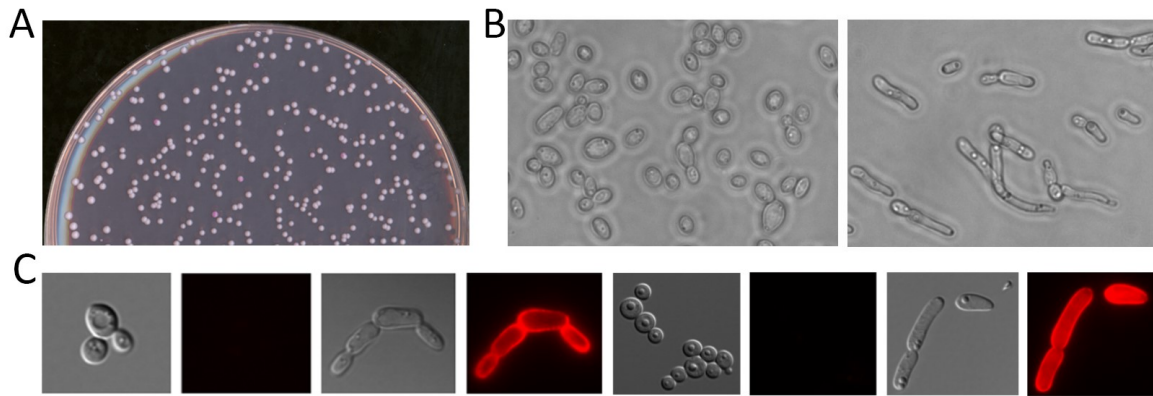


Figure 5.1 White opaque switching of *atp12* null mutant. *A. White opaque switching of *atp12* null mutant on agar plate.* Colonies formed from plating of *atp12* null mutant (SN148 background) on SC-GlcNAc (plus phloxine B) agar medium at 25 °C for 7 days; *B. White and opaque cells of *atp12* null mutant under optical microscope.* Left, white cells of *atp12* null mutant from white colony of the left plate under optical microscope; right, opaque cells of *atp12* null mutant from pink-staining colony of the left plate under optical microscope, 400X. *C. Immunofluorescence microscopy of *atp12*.* F223-5H1-1 is the monoclonal antibody used in this study as the primary antibody to identify opaque cells. Texas red conjugated goat anti-mouse antibody was used as the secondary antibody. From left to right, white cells of wild-type SN148a show no signal, opaque cells of wild-type SN148a show the signal, white cells of *atp12* null mutant show no signal, and opaque cells of *atp12* null mutant show the signal. Samples were observed and photographed under the Leica DM6000 fluorescence microscope at 630X magnification.

5.3.2 The stability of white-opaque switching in the absence of *ATP12*

Purified white and opaque colonies were selected to test the overall white-opaque switching patterns further. When individual cells from purified white colonies of the null mutant were incubated on SD-glucose and GlcNAc agar media at RT, the frequency of the opaque-like form, phloxine B-staining colonies were around 0.2% on glucose and 1.7% on GlcNAc, while no switching of the wild-type strain SN148 was observed under the same conditions (Table 5.3). Purified opaque-like colonies treated in the same manner undergo relatively stable cell division

with about a 2.6% ratio of switching back to white colonies on GlcNAc medium but were unstable on glucose medium with an average of 37% switching rate (Table 5.4).

Table 5.3 Ratio of white to opaque switching of *atp12* null mutant. Carbon sources used were GlcNAc (GLC) and glucose (GLU). Strains were all started from white (WH) cells. The ratios are based on at least 3 separate experiments; colony types were calculated from among 500 to 2000 colonies in total after 7 days incubation at room temperature. *atp12Δ/Δ*, *atp12* null mutant, *MTLa/a*. *WTa*, wild-type, *MTLa/a*.

GLC-WH to OP		GLU-WH to OP	
Genotype	Switch Ratio (%)	Genotype	Switch Ratio (%)
<i>atp12Δ/Δ</i>	1.7±0.02	<i>atp12Δ/Δ</i>	0.20±0.02
WT	<0.05	WT	<0.05
<i>WTa</i>	91±7.5	<i>WTa</i>	5 ±1

Table 5.4 Ratio of opaque to white switching of *atp12* null mutant. Carbon sources used were GlcNAc (GLC) and glucose (GLU). Strains were all initiated from opaque (OP) cells. The ratios are based on at least three separate experiments; colony types were calculated from among 400 to 1000 colonies in total after 7 days incubation at room temperature. *Atp12Δ/Δ*, *atp12* null mutant, *MTLa/a*. *WTa*, wild-type, *MTLa/a*.

GLC-OP to WH		GLU-OP to WH	
Genotype	Switch Ratio (%)	Genotype	Switch Ratio (%)
<i>atp12Δ/Δ</i>	2.56±0.00	<i>atp12Δ/Δ</i>	37±2.5
<i>WTa</i>	0.2 ±0.2	<i>WTa</i>	0.2 ±0.2

5.3.3 Metabolism of *ATP12*

We tested the role of Atp12p as a chaperone in its effect on the growth of *C. albicans*. Also, we wanted to investigate a link between the growth properties and the white-opaque switching of this *atp12* mutant. Different carbon sources were tested for growth metabolism for both white and opaque cells of the *atp12* null mutant with both the wild-type SN148 cells and SN148a opaque cells as the controls. The observations lasted for 45 hours, and the OD₆₀₀ was tested every three hours. The growth curves are shown in Figure 5.2. Surprisingly, instead of having a deficiency for growing in some of the sugar sources, the *atp12* mutant actually grew better than the wild-type on most of the carbon sources, especially on galactose and mannitol. Even the opaque cells of *atp12* grew better than the wild-type opaque cells on most of the carbon sources.

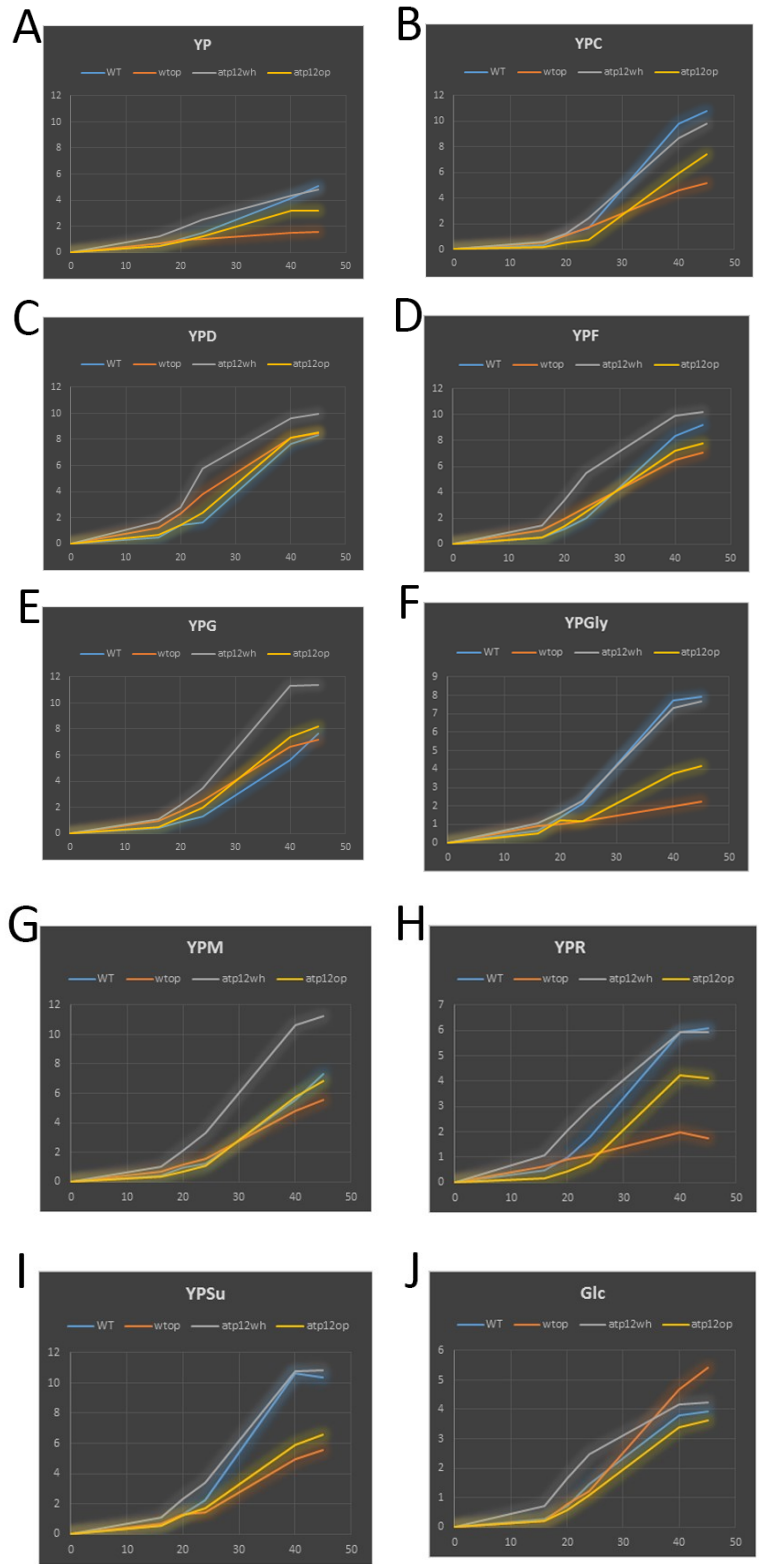


Figure 5.2. Growth curve of *atp12* compared with WT. Overnight cell cultures were diluted to a start $OD_{600}=0.01$. RT, 220 rpm, 45 hours. OD_{600} was measured every three hours. A. YP (1% yeast extract, 2% peptone), no carbon source; B. YPC, YP plus 2% citric acid; C. YPD; D. YPF, YP plus 2% fructose; E. YPG, YP plus 2% galactose; F. YPGly, YP plus 2% glycerol; G. YPM, YP plus 2% mannitol; H. YPR, YP plus 2% rhamnose; I. YPSu, YP plus 2% sucrose; J. Glc, SC-GlcNAc.

5.3.4 Metabolism of *ATP16*

We wondered if the white-opaque switching is related to ATPase function, or to some other potential function of the chaperone. So we also assayed the γ subunit Atp16 of the ATPase. To our surprise, the *atp16* null mutant could not survive on GlcNAc, and so different carbon sources were tested. The *atp16* strain can grow properly with glucose or fructose as the carbon source, and it can survive but grow slowly on galactose. It cannot survive on other carbon sources we tested including mannitol, YP with no carbon, lactose, citric acid, a low carbon source such as spider's medium, sucrose, sorbitol and glycerol (data not shown).

5.4 Discussion

To test directly whether the ability to express the ATPase affects growth on different carbon sources, we examined the phenotype of a strain lacking the F1-ATPase subunit gamma. However, the deletion mutant of *ATP16*, the F1-ATPase subunit γ , cannot survive on most carbon sources. It grows well only on rich media like YPD (dextrose) and YP plus fructose. By contrast, the *atp12* null mutant not only survives but also grows faster than the wild-type on most carbon sources.

The fast and relatively rapid growth and adaption in different carbon sources of the *atp12* mutant may cause significant damage to the cells themselves. With the stress of making proper ATPase, the cells may accumulate genotoxic ROS within the cells. Both oxidative stress and genotoxicity are stimuli for the white-to-opaque switching. The mutants may have stress on both glucose and GlcNAc media, so on both carbon sources, the *atp12* mutant can undergo the white opaque switching even in the *MTLa/a* background.

In *S. cerevisiae*, *atp12* shows a growth deficiency on non-fermentable carbon sources. For example, in the absence of *ATP12* in *S. cerevisiae*, the cells cannot survive with Glycerol as the

sole carbon source. However, in *C. albicans* *ATP12* mutants could survive on all of the carbon sources assayed. Moreover, the *atp12* mutant grew better than the wild-type in most of the carbon sources, especially in galactose and mannitol. Even the opaque cells of *atp12* grew better than the wild-type opaque cells in most of the carbon sources. This may be due to the only homozygous genes expressed in the wild-type opaque cells compared with the gene expression of an *MTLa/α* strain. The metabolism of an *MTLa/α* strain is stronger than an *MTL* homozygous strain even when they are both in the opaque states. However, rapid growth caused the earlier death due to the nutrient limitation and oxidative stress as well as the assembling of partial dysfunctional ATPases. These outcomes may further cause oxidative stress and genotoxicity within the cells. Oxidative stress and genotoxicity can increase white opaque switching [95]. In this way, accumulated genotoxic stimuli and oxidative stress may cause the white opaque switching even to happen in the *MTLa/α* background.

Another explanation of these observations is that Atp12p is the chaperone not only for the assembly of ATPase but also affects the expression of *MTL* locus. We can mimic a similar phenotype as the *atp12* mutant by deleting *a1*, *a2*, *α1* and *α2* genes at the *MTL* locus. When all four genes are deleted, cells can switch from white to opaque but are unable to mate. So in the absence of *ATP12*, the *MTL* locus is less functional; then white opaque switching can happen in the *MTLa/α* background but the cells still cannot undergo mating.

Chapter 6: Ste18p is a positive control element in the mating process of *Candida albicans*

This Chapter was published as a manuscript in journal Eukaryotic Cell (Lu H, Sun Y, Jiang YY, Whiteway M. Ste18p is a positive control element in the mating process of *Candida albicans*. Eukaryotic Cell. 2014 Apr;13(4):461-9. doi: 10.1128/EC.00320-13.). I am responsible for Figure 6.3 and Table 6.3 in this Chapter.

6.1 Introduction

Heterotrimeric G protein-mediated signal transduction is ubiquitous and regulates many critical processes in eukaryotic cells (for review, see [99]). The general paradigm for the function of these heterotrimeric G proteins is that the $G\alpha$ and $G\beta\gamma$ elements are activated through dissociation or conformational changes triggered by GTP binding to the $G\alpha$ subunit in response to ligand binding to a G-protein-linked 7-transmembrane spanning receptor protein [100]. The signal is ultimately inactivated by re-association after GTP hydrolysis to GDP [101], often through the aid of a regulator of G protein signaling (RGS) protein that serves as a GTPase activating protein (GAP) for the process [102].

The involvement of a heterotrimeric G protein in a fungal mating signaling pathway was first noted for the baker's yeast *Saccharomyces cerevisiae* [103-105]; for review, see [106]. Detailed genetic analysis in *S. cerevisiae* suggested the functioning of this module fit well to the paradigm established through biochemical analysis of mammalian G protein systems, in that the α and $\beta\gamma$ subunits played distinct (and opposing) roles in the signaling process. Although many of the well-studied mammalian pathways used the α subunit as the effector activator, the yeast system was an initially identified member of the now extensive class of pathways where the $\beta\gamma$ subunit served to activate the downstream components of the pathway, in this case by directing the membrane association and activation of members of a Ste5p-scaffolded MAP kinase module [107]. The *S. cerevisiae* $G\alpha$ (ScG α) subunit serves a role primarily in down-regulating the pheromone signaling pathway [108], while the activated MAP kinase triggers the activity of the transcription factor Ste12p, which induces the transcription of pheromone-responsive genes [109], and also phosphorylates and stabilizes Far1p to initiate cell cycle arrest [110].

Recently, the number of fungal mating pathways known to involve a heterotrimeric G protein has been increased. The fungal pathogen *Candida albicans* has been demonstrated to show mating between *MTL α* and *MTL α* strains *in vivo* [111] and *in vitro* [112], and to have a pheromone response pathway similar to that of *S. cerevisiae* [113]. As is the case in *S. cerevisiae*, *C. albicans* also has a unique G α subunit implicated in regulation of cAMP signaling [114], while the classic heterotrimeric G protein is implicated in the mating process. However, in the *C. albicans* system, loss of either CaG α 1 or CaG β results in full sterility [115], unlike *S. cerevisiae* where loss of G α leads to constitutive signaling. In *Schizosaccharomyces pombe*, the pheromone signaling pathway is regulated only by the SpG α 1 subunit; it appears that neither the SpG β subunit nor the SpG γ subunit are involved in this process [116]. In *Cryptococcus neoformans*, there are three G α subunits, one G β subunit and two G γ subunits; CnG α 2 up-regulates the pheromone response pathway while CnG α 3 inhibits the signaling pathway [117]. In *Kluyveromyces lactis* the signal transduction pathway that mediates mating is positively regulated by both the KlG α [118] and KlG β [119] subunits of the heterotrimeric G protein, while loss of the KlG γ subunit produces only a minor mating defect [120]. Thus while a heterotrimeric G protein is a common element in many fungal mating response pathways, the specific roles of the subunits appear to differ significantly from one system to another.

In the present study, we have focused on the function of the heterotrimeric G protein G γ subunit of the fungal pathogen *C. albicans*. Mating in *C. albicans* is a somewhat more complex process than that in *S. cerevisiae* or *K. lactis*, in that the typical *C. albicans* strain is a nonmating **a/a** diploid. Mating type homozygosis must occur prior to mating: a low percentage of clinical isolates have become homozygous at the *MTL* locus, forming either **a/a** or **α/α** cells [121], and this homozygosis can be selected for in the lab by growth of **a/a** strains on sorbose medium [10]. However, homozygosis of the mating type locus *MTL* is not sufficient for mating in *C. albicans*; it simply eliminates the **a1- α 2** repressor that blocks potential activation of the mating-competent opaque state [50]. In the absence of the **a1- α 2** repressor, cells can establish this mating-competent epigenetic state, which is characterized by high-level expression of the *WOR1* gene and by unique cell and colony morphologies [13]. However, once the mating-competent opaque state is achieved, *C. albicans* mating proceeds in a manner similar to that of *S. cerevisiae* and *K. lactis*.

In *S. cerevisiae*, G γ is critical for normal mating and loss of G γ blocks mating in strains with pathways activated either normally, by overproduction of Ste4p (G β) [122], or by deletion of *GPA1*(G α) [105]. In contrast, in *K. lactis* cells, the G γ subunit is essentially dispensable for mating, as loss of G γ compromises mating only moderately and then only when both partners lack the subunit [120]. As the *K. lactis* and *S. cerevisiae* lineages diverged from the *C. albicans* lineage before the split between *K. lactis* and *S. cerevisiae*, it is of interest to establish what role the G γ of the pathogen plays in mating signal transduction. We found that, as in *S. cerevisiae*, the *C. albicans* G γ is required for mating. However, in contrast to the situation in *S. cerevisiae*, this requirement can be eliminated by ectopic expression of either the G α or G β subunit of the G protein.

6.2 Materials and Methods

6.2.1 Strains and culture conditions

The *C. albicans* strains and oligonucleotides used in this work are listed in Table 6.1 and Table 6.2. For general growth and maintenance of the strains in the white phase, the cells were cultured in fresh YPD medium (1% yeast extract, 2% Bacto peptone, 2% dextrose, 2% agar for solid medium, PH 6.5) at 30°C. Strains were switched from the white phase to the opaque phase in two rounds of screening on plates with synthetic N-acetylglucosamine (GlcNAc) (0.67% yeast nitrogen base, 0.15% amino acid mix with uridine at 100 μ g/ml, 2% GlcNAc, and 2% agar for solid medium) [123] and synthetic dextrose medium (SD; 0.67% yeast nitrogen base, 0.15% amino acid mix with uridine at 100 μ g/ml, 2% dextrose, and 2% agar for solid medium). Phloxine B was added to nutrient agar for opaque colony staining [115]. Cultures in SD medium at room temperature were used to maintain the cells in the opaque phase, and the typical oblong cell morphology phenotype of the cells in the opaque phase was confirmed by microscopy.

Table 6.1 *C. albicans* strains used in this study.

Strain	Mating		Description	Source
	Parent	type		
3294	CNC43	a/a	<i>his1/his1 ura3/ura3 arg5,6/arg5,6</i>	P. T. Magee
3315	CNC43	α/α	<i>trp1/trp1 lys2/lys2</i>	P. T. Magee
LH001	3294	a/a	<i>STE18/ste18::HIS1 ura3/ura3 arg5,6/arg5,6</i>	This study
LH002	LH001	a/a	<i>ste18::HIS1/ste18::URA3 arg5,6/arg5,6</i>	This study
LH003	LH002	a/a	<i>ste18::HIS1/ste18::HIS1 ura3/ura3 arg5,6/arg5,6</i>	This study
LH006	LH003	a/a	<i>ste18::HIS1/ste18::HIS1 ura3/ura3 arg5,6/arg5,6 (CIP10)</i>	This study
LH011	3294	a/a	<i>STE18-carboxy-terminal MTD/ste18-carboxy-terminal MTD::HIS1 ura3/ura3 arg5,6/arg5,6</i>	This study
LH012	LH011	a/a	<i>ste18-carboxy-terminal MTD::HIS1/ste18-carboxy-terminal MTD::URA3 arg5,6/arg5,6</i>	This study
LH004	LH003	a/a	<i>ste18::HIS1/ste18::HIS1 RPS1/rps1::STE18-URA3 arg5,6/arg5,6</i>	This study
LH005	LH003	a/a	<i>ste18::HIS1/ste18::HIS1 RPS1/rps1::STE18ΔC-URA3 arg5,6/arg5,6</i>	This study
LH021	LH003	a/a	<i>ste18::HIS1/ste18::HIS1 RPS1/rps1::act-STE4-URA3 arg5,6/arg5,6</i>	This study
LH022	LH003	a/a	<i>ste18::HIS1/ste18::HIS1 RPS1/rps1::act-CAG1-URA3 arg5,6/arg5,6</i>	This study

Table 6.2 Oligonucleotides used in this work

Name	Description	Sequence (5' to 3')
STE18-TB-F	<i>STE18</i> deletion PCR cassette	TTTTGATGTAAAAATTAACATGAAAGATTGTGTTTCAGA
	forward primer	ATTTTCTCCACCTACAACAACAACGACGACAATAACTA
STE18-TB-R	<i>STE18</i> and <i>STE18ΔC</i> deletion PCR cassette reverse primer	ATGTATATATATATATATAAATACATATGTGTGTGATTT
STE18ΔC-T	<i>STE18ΔC</i> deletion PCR cassette	CATTCTTGTGGGTTGATTAATTGGAGA ACTATTTCTGTC
R-F	forward primer	TGGAGTTTACCTCCAGATCAGAATAGATTTGCCAATAT
STE18-F-ex	<i>STE18</i> forward external primer	AAACAGTTGAGAAATGCACGCAATTCATCTCAAGCTACA GATTATTACAAGGTGCATTTGC
STE18-R-ex	<i>STE18</i> reverse external primer	AACATTGAAAGCTCAATTAGGC
STE18-F-in	<i>STE18</i> forward internal primer	GAATTCAAGAGTTGACTAATCG
HIS1-F	<i>HIS1</i> forward primer	TTTAGTCAATCATTTACCAGACCG
HIS1-R	<i>HIS1</i> reverse primer	TCTATGGCCTTTAACCAGCTG
URA3-F	<i>URA3</i> forward primer	TTGAAGGATTAACAGGGAGC
URA3-R	<i>URA3</i> forward primer	ATACCTTTTACCTTCAATATCTGG
STE18-SalI	<i>STE18</i> and <i>STE18ΔC</i> forward primer for reintegration	CTGATGGTCGACGATTATTACAAGGTGCATTTGC
STE18-Hind III	<i>STE18</i> reverse primer for reintegration	CCCAAGCTTGGAACATTGAAAGCTCAATTAGGC
STE18ΔC-H indIII	<i>STE18ΔC</i> reverse primer for reintegration	CCCAAGCTTGGGTTAAACTGTAGCTTGAGATGAATTGCG
RPS1-R-in	<i>RPS1</i> reverse internal primer	TTTCTGGTGAATGGGTCAACGAC
ACT-F	Actin promoter internal primer	TTTTCTAATTTTCACTCCTGG
<i>CAG1</i> -F-in	<i>CAG1</i> forward internal primer	ATTGAACAAAGTTTACAATTGCGTC
<i>CAG1</i> -R-in	<i>CAG1</i> reverse internal primer	TCATTAGTATCGTCTGGTTTGCC
<i>STE4</i> -F-in	<i>STE4</i> forward internal primer	ACTATACAACACCTTGCGAGGA
<i>STE4</i> -R-in	<i>STE4</i> reverse internal primer	CAGTTGCCAAAGCTACACCATC

6.2.2 Disruption of the *STE18* gene and deletion of the C terminus of the *STE18* gene

The *C. albicans* sequence (assembly 19) from the *Candida* Genome Database (<http://www.candidagenome.org/>) was used as the reference for the genomic sequence. The two alleles of the *STE18* gene (*ORF19.6551.1*) were deleted from the *MTLa* strain 3294. All the disruptions were done with the two-step PCR method as described previously [124], with the replacement of the first allele with *HIS1* and of the second allele with *URA3*. Oligonucleotides STE18-TB-F and STE18-TB-R were used to prepare the cassettes for the deletion of the *STE18* gene. The strain produced by replacing the first copy of the *STE18* gene by *HIS1* in the *MTLa* strain 3294 was named LH001. The correct insertion of the *HIS1* cassette at the *STE18* locus was confirmed by PCR analysis of genomic DNA from strain LH001 with oligonucleotides STE18-F-ex plus HIS1-R, STE18-R-ex plus HIS1-F and STE18-F-ex plus STE18-R-ex. Oligonucleotides STE18-F-ex and STE18-R-ex flank, and are external relative to the recombination sites of the PCR cassettes. Oligonucleotides HIS1-F and HIS1-R are internal relative to the *HIS1* gene of the PCR cassettes. The second copy of the *STE18* gene was deleted from strain LH001 by replacement with the *URA3* cassette to generate the *ste18* null strains LH002. The correct insertion of the *URA3* cassette at the *STE18* locus was confirmed by PCR with oligonucleotides STE18-F-ex plus *URA3*-R and STE18-R-ex plus *URA3*-F. The carboxy-terminus of the *STE18* gene was deleted using a similar strategy. Oligonucleotides STE18 Δ C-TB-F and STE18-TB-R were used to prepare the PCR cassettes. The strain produced by deleting one allele from the parent strain 3294 was named LH011. The correct insertion of the *HIS1* cassette at the carboxy-terminus of the *STE18* gene was confirmed by PCR with oligonucleotides STE18-F-in plus HIS1-R and STE18-R-ex plus HIS1-F. Strain LH011 was then transformed with the *URA3* cassette to remove the CAAX box of the second allele to *STE18* gene to generate the carboxy-terminal CAAX-box deleted strain LH012. The correct insertion site of the *URA3* cassette was confirmed by PCR with oligonucleotides STE18-F-in plus STE18-R-ex.

6.2.3 Reintegration

A copy of the wild-type gene for complementation experiments was reintegrated at the *RPS1* locus in the *ste18* Δ strain as described previously [115]. The recipient strain LH002 was treated with 5-fluoroorotic acid (5-FOA) to recover the *URA3* marker. A resulting uridine-negative strain

was named LH003. For the *STE18* gene, a 1320 bp DNA fragment from genomic DNA was amplified by PCR using oligonucleotides STE18-SalI and STE18-HindIII. Oligonucleotide STE18-SalI contains an exogenous *SalI* restriction site, absent in the *STE18* gene sequence, near its 5' tail, and STE18-HindIII contains an exogenous *HindIII* restriction site in the 3'-end noncoding sequence of the *STE18* gene. The PCR fragment was digested with *SalI* and *HindIII*, the resulting 1.3-kb fragment was ligated with vector CIP10 [125] also cut with *SalI* and *HindIII*, and *E. coli* strain DH5 α was transformed with the construct. The integrity of the clone with respect to the *STE18* wild-type sequence was confirmed by DNA sequencing. The selected clone for the wild-type *STE18* gene was named plasmid pCIP-STE18 and was digested with the enzyme *StuI* for transformation of the strain LH003. The new *STE18* strain was named LH004. A similar strategy and protocol was used for the reintegration of the *STE18 Δ C* gene. An 820 bp fragment was amplified with oligonucleotides STE18-SalI and STE18 Δ C-HindIII. Oligonucleotide STE18 Δ C-HindIII was designed with an exogenous *HindIII* restriction site, absent in the *STE18* gene sequence, and is positioned in the 3'-end of *STE18* gene ORF that did not include the last 21bp (GGTTGTTGTACAATTGTTTAA). This PCR fragment was digested with *SalI* and *HindIII* enzymes, and the 820bp fragment was ligated to the CIP10 vector cleaved with the same two enzymes. The integrity of the clone was confirmed by DNA sequencing, and the selected clone with the *STE18 Δ C* gene sequence was named plasmid pCIP-STE18 Δ C. This plasmid was digested with *StuI*, and strain LH003 was transformed with the construct. These new *STE18* strain was named LH005. The integration of pCIP-STE18 and pCIP-STE18 Δ C at the correct site in the *RPS1* locus was confirmed by PCR. A strain carrying an insertion of the original vector CIP10 with no insert was also constructed and designated LH006.

6.2.4 Overproduction of either the *STE4* gene or the *CAG1* gene in *ste18* null mutant strains

To overexpress the *STE4* gene or the *CAG1* gene in *ste18 Δ* strains, we used plasmids p1390 (wild-type *STE4* gene under *ACT1* promoter) or p1391 (wild-type *CAG1* gene under *ACT1* promoter) [115] for transformation. Plasmids p1390 and p1391 were digested with *StuI* and then transformed into *ste18 Δ* strains. The *ste18 Δ* strain transformed with plasmid p1390 was named LH021, while that with plasmid p1391 was named LH022. The correct integration of the plasmids was confirmed by PCR.

6.2.5 Microarray analysis

The transcriptional response to pheromone treatment was measured in the wild-type strain, in a strain (LH003) deleted for *STE18*, and in *STE18*-deleted strains overexpressing either the *STE4* gene (LH021) or the *CAG1* gene (LH022). Standard protocols were performed as follows: we collected cells from SD-complete cultures in log phase with and without pheromone induction, and we used the hot-phenol method for RNA extraction [57], the polyA Spin mRNA isolation kit for mRNA isolation [57], and reverse transcription for cDNA production, followed by indirect chemical labeling for dye addition. Arrays obtained from NRC-BRI [57] were hybridized in a hybridization chamber at 42°C for overnight incubation and then washed and scanned. The scanning was done using a GenePix4000B microarray scanner, and the images were analyzed in GenePix Pro 4.1; the output data were processed with Microsoft Excel 2013 and MultiExperiment Viewer (MeV). Microarray data have been deposited in the GEO database under accession number GSE54031.

6.2.6 Mating assay

Patch mating experiments, using auxotrophic marker complementation with strain 3315 as the *MTLα* tester strain, were done as described previously [126]. Briefly, all the assayed strains were maintained in the opaque phase at room temperature. Experimental and tester strains were streaked as straight lines on separate YPD plates. After 24 h of incubation at room temperature, the two sets of streaks were crossed onto a single fresh YPD plate and incubated for 24h at room temperature. After 24 h of incubation, cells were replicated to dropout plates containing SD medium minus five amino acids (uridine, histidine, arginine, tryptophan, and lysine) for selection of mating products, and to YPD plates as a control. All the plates were incubated at room temperature for 5 days prior to scoring.

Quantitative mating assays were done as follows: opaque cells of the tester strain 3315 and experimental strains were cultured overnight in SD-complete liquid media in the shaker at room temperature. Each of the experimental strains was mixed with the tester strain in fresh SD-complete liquid medium (10^7 cells \times 10^7 cells /ml), then incubated in the shaker for 48 h at room temperature. Cells were quantified with counting chamber under microscope, collected by

centrifuge, washed and resuspended with water before plating onto SD-Trp⁻ Lys⁻ Arg⁻, SD-Uri⁻ His⁻ or SD- Trp⁻ Lys⁻ Arg⁻ Uri⁻ His⁻ medium for prototrophic selection.

6.2.7 Pheromone response assay

Strains were examined microscopically for shmoo formation after treatment with synthetic α -factor. Strains in opaque phase were incubated for 24 hours at room temperature, diluted for a final OD₆₀₀=0.05 and treated with pheromone (1mg/ml) for 12 hours before being photographed. Strains were visualized using a Nikon eclipse TS100 microscope with 400X magnification using DIC optics.

6.2.8 Alignment of G protein γ subunit sequences in ascomycete yeasts

Multiple protein sequence alignments were performed with the MAFFT web application (<http://mafft.cbrc.jp/alignment>) and visualized with Jalviewer (Version 2). The protein sequences of the different ascomycete yeast species were downloaded from the Fungal Orthogroups Repository (<http://www.broadinstitute.org/cgi-bin/regev/orthogroups>) hosted by the Broad Institute, MIT. Pairwise protein alignments and identity percentages were established with BLASTP, which is from BLAST (<http://blast.ncbi.nlm.nih.gov/Blast.cgi>).

6.3 Results

6.3.1 *ORF19.6551.1 (CaSTE18)* encodes a typical G γ subunit of heterotrimeric G protein in *C. albicans*

The *C. albicans* genome contains a single copy of a (*STE18* or *ORF 19.6551.1*) gene that has the structural and expression characteristics of a typical γ subunit of heterotrimeric G proteins involved in mating. Expression of this gene is repressed by the $\alpha 1/\alpha 2$ repressor, and is thus limited to *MTL* homozygous cells, either in the white or opaque state [127]. This expression pattern is found for other genes such as *FAR1* and *STE4*, which have been shown to be part of the mating pheromone response pathway in this organism [115, 128]. Analysis of the deduced primary structure of the protein showed a high degree of identity with the ScG γ subunit of *S. cerevisiae* (40% identity and 58% similarity) and the KlG γ subunit of *K. lactis* (38% identity and 56%

We then identified opaque derivatives of the *ste18* null mutant strain on phloxine B plates and tested them for mating capacity. When the opaque *ste18* null mutant strain was tested in a cross-patch mating assay, no prototrophic products derived from mating were detected, showing that the *ste18* null strain was totally sterile (Figure 6.2). In addition, the strain was totally defective in pheromone-induced gene expression, as treatment of opaque *ste18* strains with synthetic α -factor failed to induce expression of any of a set of classic pheromone-responsive genes (Figure 6.3). The cells were also defective in shmoo formation in the presence of α -factor (see the supplemental material). This sterile, nonresponsive phenotype was a result of the loss of Ste18p function in the mutant strain, as the reintroduction of a single copy of the *STE18* gene at the *RPS1* locus reestablished mating competence (Figure 6.2). Thus, Ste18p, along with both the G β subunit Ste4p and the G α subunit Cag1p, is a positive component in the pheromone response pathway of *C. albicans*.

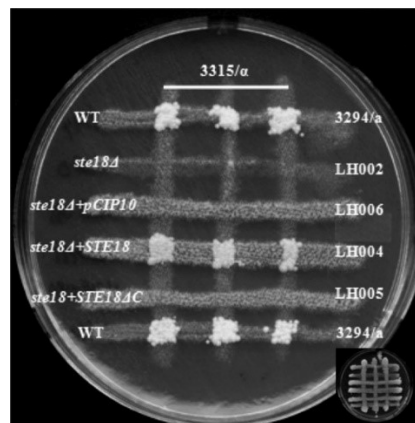


Figure 6.2 Ste18 null mutant strains are sterile. Mating was assayed by auxotrophic marker complementation between strains of opposite mating types as described in Materials and Methods. The mating assay for MTL+ *ste18*Δ strains, strains with *STE18* reintegrated (*ste18*Δ + *STE18*), and strains with *STE18*ΔC reintegrated (*ste18*Δ + *STE18*ΔC) is shown. No colonies were formed by complementation of the *ste18*Δ strains (LH002 and LH006) and the strain with *STE18*ΔC reintegrated (LH005), while the strain with *STE18* reintegrated (LH004) reverted the sterile phenotype. WT, wild-type. The original mating cross is shown at the bottom corner.

		WT	$\Delta ste18$	$\Delta ste18+STE4$	$\Delta ste18+CAG1$	
		3294	LH003	LH021	LH022	
<i>n</i> =		3	3	3	3	
ID	Gene					Bargraph
orf19.696	<i>STE2</i>	10.30	2.55	19.65	22.19	
orf19.6667	<i>SAP30</i>	11.44	1.64	17.14	12.98	
orf19.1616	<i>FGR23</i>	10.91	2.08	14.32	26.84	
orf19.460	<i>CEK2</i>	8.94	2.36	13.99	17.30	
orf19.5046	<i>RAM1</i>	9.47	2.33	14.32	11.75	
orf19.138	<i>FIG1</i>	6.38	1.46	44.29	30.46	
orf19.5557	<i>MNN4-4</i>	5.03	1.51	3.18	1.67	
orf19.3801	<i>FAV1</i>	6.09	2.36	14.19	16.04	
orf19.7440	<i>HST6</i>	8.19	1.79	20.90	30.26	
orf19.3736	<i>KAR4</i>	5.02	1.82	3.98	21.20	
orf19.5520	<i>ASG7</i>	4.45	2.52	6.71	5.64	
orf19.1120	<i>FAV2</i>	4.13	1.26	5.86	2.27	
orf19.5896	orf19.5896	5.22	1.39	23.64	29.49	
orf19.1827	orf19.1827	3.80	2.28	30.67	31.64	
orf19.669	<i>PRM1</i>	3.39	1.52	15.29	36.29	
orf19.4222	<i>SST2</i>	2.66	2.49	11.79	4.50	
orf19.2886	<i>CEK1</i>	2.37	1.97	8.07	5.26	

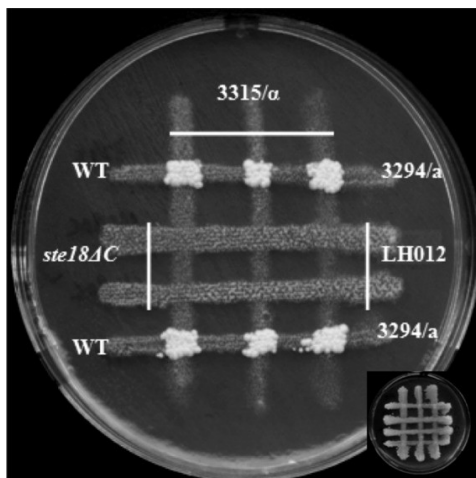
Figure 6.3 Transcriptional response to pheromone treatment. *The values shown represent the averages from three independent biological samples for 17 pheromone-inducible genes from C. albicans. The stronger signals have the deeper red color. The final column presents a graphical summary of the data. Deletion of the STE18 gene eliminates the pheromone induction of the genes, while ectopic expression of either STE4 or CAG1 enhances the responsiveness to induction by pheromone treatment. The complete data files are accessible at GEO through accession no. GSE54031.*

6.3.3 The CAAX box of CaGγ subunit is critical for mating in *C. albicans*

The C terminus of the Gγ subunits is subjected to a complex post-translational processing that generates a hydrophobic region of the protein through the addition of a methyl group and lipid moieties (for review, see [130]). As an initial means of investigating whether this modified domain is required for mating in *C. albicans*, we deleted the CAAX (cysteine, aliphatic, aliphatic, X) box (CCTIV) of both copies of the *CaSTE18* gene. Opaque versions of doubly modified strains were identified on phloxine B plates to assess the role of the CaGγ subunit carboxy terminus in the mating process. Like the *ste18* null mutant strain, the *ste18ΔC* mutant strain was unable to mate (Figure 6.4). We also reintroduced a single copy of the *STE18ΔC* gene

(without the last 21 bp) at the *RPS1* locus in the *ste18* null mutant strain, and this *STE18ΔC* strain was also unable to mate (Figure 6.2). These results demonstrated that the carboxyl terminus of CaSte18p is critical for mating in *C. albicans*; reverse transcription-PCR (RT-PCR) analysis showed that the CAAX-deleted gene was expressed at normal levels (data not shown), so the mating defect could not be attributed to reduced expression of the mutant allele.

Figure 6.4 Strains with C termini of CaG γ subunits (CCTIV) deleted are sterile. *The mating assay was done as described in Materials and Methods. No prototrophic colonies from the ste18ΔC strain LH012 were detected after 5 days of incubation at room temperature. WT, wild-type.*



6.3.4 Overproduction of either the G α 1 subunit or the G β subunit of the heterotrimeric G protein permits mating in the absence of the G γ subunit in *C. albicans*

In *S. cerevisiae*, over-expression of the *STE4* gene product led to cell cycle arrest of haploid cells, and suppressed the sterility of cells defective in the mating pheromone receptors encoded by the *STE2* and *STE3* genes [122]. The G β subunit of the heterotrimeric G protein triggered the pheromone response pathway in the absence of the G γ subunit in *K. lactis*. Over-expression of the *CAG1* gene and the *STE4* gene product in wild-type strains of *C. albicans* did not result in any constitutive expression of pheromone responsive genes, or lead to increased shmoo formation or cell cycle arrest in the presence of the pheromone. In addition to this, overproduction of the *STE4* gene did not suppress the sterility caused by deletion of the *CAG1* gene, while the over-expression of the *CAG1* gene was similarly unable to suppress the sterility

caused by deletion of the *STE4* gene [115]. We assessed the role of overproduction of the *CAG1* and *STE4* genes in the absence of the *STE18* gene in *C. albicans*. We over-expressed either the *CAG1* gene or the *STE4* gene (under the control of the strong *ACT1* promoter found in the plasmid pACT1) in the *ste18* null mutant strain. Intriguingly, overproduction of either the *CAG1* gene or the *STE4* gene is able to partially suppress the mating defect caused by deletion of the Gy subunit (Figure 6.5 and Figure 6.6).

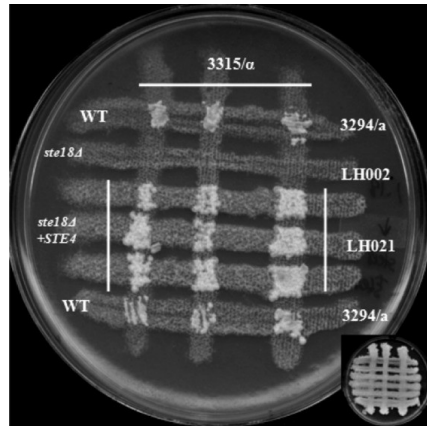


Figure 6.5 Ectopic expression the *STE4* gene in a *ste18Δ* strain reverts the sterile phenotype. The mating assay was done as described in Materials and Methods. Prototrophic colonies from the *ste18Δ* strain with the *STE4* gene overexpressed were detected after 5 days of incubation at room temperature. WT, wild-type.

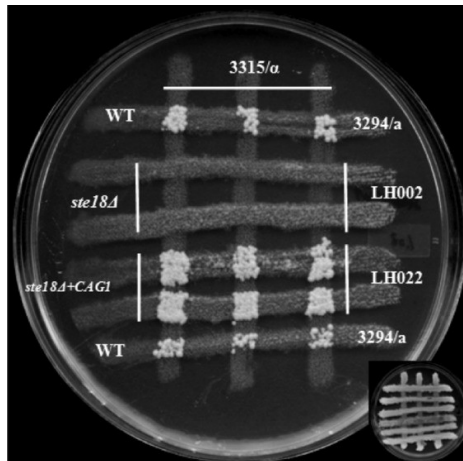


Figure 6.6 Ectopic expression of the *CAG1* gene in a *ste18Δ* strain reverts the sterile phenotype. The mating assay was done as described in Materials and Methods. Prototrophic colonies from the *ste18Δ* strain with the *CAG1* gene overexpressed (LH022) were detected after 5 days of incubation at room temperature. WT, wild-type.

We further assessed the consequences of the ectopic expression of the G α or G β subunit on pheromone-induced gene expression in cells lacking *STE18*. The strains containing G α or G β expressed under *ACT1* control showed a higher level of gene induction in the presence of α -factor than did the wild-type cells (Figure 6.3). This enhancement in response was associated with an increase in quantitative mating over wild-type levels as well (Table 6.3). Intriguingly, although all the responsive strains showed shmoo formation (see the supplemental material), they showed no evidence for a clear cell cycle arrest leading to the formation of halos in a classic halo assay (data not shown).

Table 6.3 Quantitative mating of wild-type strain 3294 and mutant strains.

Relevant genotype (strain)	Mating frequency (10^4 , mean \pm SD)
Wild-type (3294)	2.63 \pm 0.21
$\Delta ste18$ (LH003)	0
$\Delta ste18 + STE18$ (LH004)	6.84 \pm 0.45
$\Delta ste18 + STE18\Delta C$ (LH005)	0
$\Delta ste18 + CIP10$ (LH006)	0
<i>STE18</i> ΔC (LH012)	0
$\Delta ste18 + STE4$ (LH021)	12.0 \pm 0.6
$\Delta ste18 + CAG1$ (LH022)	4.83 \pm 0.87

6.4 Discussion

The γ subunits of heterotrimeric G proteins play key roles in the function of these important signaling molecules. Structural studies have shown that γ subunits form a very stable coiled-coil interaction with the N-terminus of a G β subunit; this association is almost as stable as would be generated by a covalent linkage between the proteins [131]. In addition, G γ subunits typically undergo a complex post-translational modification process of their carboxyl terminus. These proteins have a CAAX (cysteine, aliphatic, aliphatic, X) box motif at their C terminus, and the cysteine residue of this motif is a target for the addition of both a prenyl (typically a farnesyl or geranylgeranyl) and a methyl residue (for review, see [130]). These modifications, and a

further addition of a palmitoyl residue to a second cysteine often found adjacent to the CAAX box generate a highly hydrophobic G γ C terminus that helps to anchor the protein, together with the attached G β subunit, to cellular membranes (for review, see [132]).

Deletion of the G γ subunit of the *C. albicans* mating response G protein generates sterility. In the present study this test was only done in the *MTLa* background, but there is no reason to anticipate the function is in any way mating type dependent. The positive functioning of the G γ subunit is similar to the situation in *S. cerevisiae*, where the loss of the G-protein γ subunit Ste18p results in the loss of mating competence [105]. However, the role of G γ subunit in *C. albicans* contrasts with the role of G γ subunit in *K. lactis*, where the loss of the G γ subunit produces only a slight mating defect [120]. Thus, in the evolutionarily divergent species *S. cerevisiae* and *C. albicans* the G γ subunit is essential for pheromone response and mating, while in the phylogenetically intermediate species *K. lactis* the subunit is almost totally dispensable.

However, the observation that overproduction of either the G α or G β subunit of the *C. albicans* heterotrimeric G protein can suppress the mating defect caused by deletion of the G γ subunit suggests that the molecular role of the *C. albicans* G γ may be actually closer to that of the *K. lactis* protein than to the *S. cerevisiae* one. In *S. cerevisiae*, changes in the stoichiometry of the α or β subunits did not influence the need for the G γ protein. Furthermore, engineering the G β subunit with the addition of a C terminal membrane anchor was not sufficient to allow signal transduction, implying that the G γ subunit played a role beyond simply serving as a membrane attachment [107]. Because directly anchoring the Ste5p scaffold to the membrane through the addition of a membrane attachment motif activated the response pathway [107], a likely non-anchoring role of the G γ subunit in yeast was to serve as part of the Ste5p binding interface. Considering the overproduction of either the *C. albicans* G α or G β subunits can bypass the need for CaSte18p, it is likely that G γ is not an essential component in any Ste5p binding surface for this organism. The *C. albicans* Ste5p is considerably smaller than the yeast Ste5 protein, and the binding interface with the G protein, if any, is currently undefined [133, 134]. Similarly, the *K. lactis* system does not have an essential role for the G γ subunit, perhaps because the normal level of the G α or the G β protein in this organism was sufficient to permit mating in its absence. *K. lactis* has a candidate Ste5 protein, but its molecular function has not yet been assessed, and its link, if any, to the G protein has not been established.

The observation that deletion of the CAAX box of CaSte18p causes sterility, while overproduction of the G α or G β subunits can suppress even complete deletion of the G γ gene further suggests that membrane association of the G protein is a key component of function in the *C. albicans* mating pathway. It is possible that a critical role of this membrane association is to bring the G β subunit into proximity with a membrane-linked effector. This could explain the ability of overproduction of either G β itself or of G α to bypass the need for G γ ; subunit overproduction would generate more $\alpha\beta$ dimers, and with G α having its own membrane attachment capability due to myristoylation, this increases the overall amount of membrane associated G β . The *C. albicans* and *K. lactis* pathways may thus represent relatively unspecialized heterotrimeric G protein modules, with all subunits playing a positive role in the mating process, and the G γ subunit being relatively dispensable, while *S. cerevisiae* is more specialized, with the α and $\beta\gamma$ subunits having distinct functions, and the G γ subunit being critical for effector activation.

Overall the function of only a limited number of fungal mating pathway G γ subunits has been assessed, but their roles have been found to be surprisingly variable. Less functional variability has been noted for higher eukaryotes. However, the mammalian G $\beta 5$ subunit has been found to associate with Regulator of G protein Signaling (RGS) proteins with a G γ homology region, as well as with classical G γ subunits [135], showing that even in higher eukaryotes, G protein function can accept variation in the involvement of the G γ subunit. It is likely that continued genetic and biochemical analysis of the function of G protein systems in fungal mating pathways will provide important insights into the functional plasticity of this important class of signaling molecules.

Chapter 7: Conclusions and Future work

Candida albicans is a prominent opportunist fungal pathogen causing disease in humans. This organism has a recently discovered, highly cryptic, mating ability. For efficient mating in a laboratory setting, *C. albicans* has to first exhibit loss of heterozygosity at its mating type locus, transitioning from *MTL***a/a** to *MTL***a/a** or *MTL***a/a**. Then, under specific conditions, the *MTL* homozygous strains can undergo an epigenetic switch from the normal white form yeast state to an elongated yeast state, termed the opaque form, and become mating competent. This infrequent two-step process greatly reduces the potential for mating, as less than 10% of clinical isolates are *MTL* homozygous, and the opaque state is intrinsically unstable at the normal temperature of the mammalian host. Thus it appears *C. albicans* has a complex mechanism for mating that is designed to ensure mating is infrequent.

In this study, we have developed an efficient library screening method to uncover the following interesting and intriguing results. Here we have characterized four unrelated genes *OFRI*, *OFR2*, *ORF19.7060* and *ATP12* and three possible categories of influencing white opaque switching in the *MTL a/a* background. The absence of *OFRI* allows switching from white to opaque and mating in both directions in the *MTL a/a* background. The second category, the absence of *OFR2* or the white specific long transcript of *ORF19.7060* allows white opaque switching and mating in one direction in the *MTL a/a* background. Third, the disruption of *ATP12* allows only white opaque switching but not mating in the *MTL a/a* background. These results suggest that some genes can directly or indirectly regulate gene expression at the *MTL* locus, and therefore interfere with the white opaque switching and mating in the *MTL a/a* background. These three categories can also be defined based on carbon sources. In the first category, when lacking expression of *OFRI* in the *MTL a/a* background, cells can switch from white state to opaque state when GlcNAc is used as the carbon source while cells will always remain in the white form when glucose is provided as the sole carbon source. Second, in the *MTL a/a* background the absence of *OFR2* allows white to opaque switching under GlcNAc conditions and opaque cells can remain stable when switched to glucose as the carbon source. Third, deleting *ATP12* in the genome allows cells of the *MTL a/a* background to undergo white opaque switching under either GlcNAc or glucose condition.

The *ofr1* null mutant can mate efficiently with *MTL* homozygotes of either mating type, or even mate homothallically. It is possible that down-regulating *OFRI* in the host environment could allow mating in *C. albicans* by a route that does not involve *MTL* homozygosis. *OFRI* is also involved in switching from mating incompetent form to the mating competent form and the *MTLa/α* cells can mate with *MTLa/α* cells. The *MTLa/α* cells can switch to opaque and mate as **a** type cells if only the opaque specific transcripts of *ORF19.7060* can be produced. The F1-ATPase chaperone Atp12 is also involved in white opaque switching of *Candida albicans*. Mating is important for this commensal fungal pathogen to adapt and survive in the dynamically changed host niches. As more than 90% of *C. albicans* clinical isolates are *MTL* heterozygous, the presence of a complex, but apparently restricted, mating pathway is intriguing. In this study, I have identified several genes influencing the control of the barriers to mating in *C. albicans*. These proteins are needed to ensure that white-opaque switching, pheromone production and mating, is blocked in *MTL* heterozygotes. The evidence that single gene mutations can allow mating behaviour of *MTL* heterozygous strains suggests the possibility that *in vivo*, *C. albicans* may exploit alternate routes to mating, and that the apparently cryptic pathway may not be as hidden as it appears. *In vivo*, some genes like the genes identified in this study can be positively or negatively regulated in a group of *C. albicans* cells to increase the flexibility of the population undergo sexual mating or morphological switching in response to the host environment such as the carbon source.

For the MAPK mating pathway, *Gγ* is confirmed to have the positive role in the regulation of genes in response to pheromone.

Overall, this study unveils some of the hidden mystery of sexual mating of *Candida albicans*. However, the host environmental niches *in vivo* are very dynamic and complex. There are a lot of questions that remain to be studied and future work can be done in the following directions. What is the clear picture of homothallic mating in *C. albicans*? As we propose, opaque cells of *C. albicans* may undergo mating when exposed to both a factor and α factor pheromone regardless of the mating type. To address this question, we can test mating among those opaque cells incapable of mating of *MTL* heterozygous background, for example, opaque cells formed by the absence of Atp12. Both types of pheromone can be additive when mating assay is performed. If our assumption is correct, all the mutants that can undergo white to opaque switching in the *MTL*

a/α background can undergo homothallic mating when both types of pheromone are provided. Homothallic mating data can then be supplemented with mating between opaque and white cells. Animal models can be used to provide evidence of homothallic mating *in vivo*. For example, cells of same mating type but different selective markers can be injected through the tail vein or passaged via the gut in murine models. Prototrophic colonies arising from auxotrophic marker complementation of both parents could be recovered by identifying cells with both selective markers present. With more comprehensive data, statistic analysis and comparisons can be done to provide a better picture of homothallic mating *in vivo*.

Can all of these white-opaque regulating genes identified in this study bypass the master regulator *Wor1* to affect switching? To address this question, we can simply make deletion of *WOR1* in these mutant backgrounds. For example, if we delete *WOR1* in the *ofr1* null mutant strain background, we will have three possible results. In the first possibility, deletion of *WOR1* will completely block the switching from white cells to opaque cells in the *ofr1* null mutant background. This will confirm that the white opaque switching regulated by *OFRI* is completely depend on the *Wor1* circuit. A second possibility that deletion of *WOR1* will have no impact on white to opaque switching in the *ofr1* null mutant background, which means that *Ofr1* regulates white to opaque switching independently of the *Wor1* circuit. Third, deletion of *WOR1* will clearly reduce the switching from the white to opaque state, but still permit the switching in the *ofr1* null mutant background. This will also confirm the existence of an alternate route to control the white opaque switching, with *Ofr1* is involved with both circuits of controlling the white opaque switching in the *MTL* homozygous background.

Do these genes identified in this study regulate directly or indirectly white opaque switching and mating? How do they cross talk with well-studied regulators or pathways involved in mating? According to the study of *Ste18*, it reveals that all three subunits of the G protein serve as positive regulators of the MAKP mating pathway. Since $G\alpha$ and $G\beta\gamma$ do not serve opposite roles, the interaction with the scaffold protein *Cst5* and cAMP pathway may also differ. Genetic and protein studies can be done to determine the interaction and regulations. The relationship between the G protein subunits with other MAPK cascade proteins also remain to be investigated.

Is there an alternate route to control white opaque switching, especially under GlcNAc conditions? In this study, we have identified some mutants which can undergo white opaque switching by screening under GlcNAc condition. For these mutants, GlcNAc can induce them to start the switch to opaque forms, however, the stabilities of the opaque cells formed under the same condition are quite different. Since we know that GlcNAc is an inducer of white to opaque switching and some GlcNAc induced opaque cells can easily revert back to white cells if we switch the carbon source from GlcNAc to glucose while some GlcNAc induced opaque cells are relatively stable towards the changing of the carbon source. We have the reason to believe that GlcNAc can turn on the Wor1 circuit as well as a currently unknown route to control the switch from the white state to the opaque state. The possible alternate route to control white opaque switching can be conditional specific, for example GlcNAc specific. In this case, GlcNAc induced Wor1 circuit will remain working under glucose condition to allow opaque cells maintain, while GlcNAc involved unknown pathway will shut down when environmental condition is changed. The novel route to control white to opaque switching under GlcNAc condition may need the involvement of Ofr1. To address this question, gene expression between opaque states and white states under GlcNAc condition should be carefully paid attention to some novel genes especially transcription factors. Other white to opaque induced conditions such as lower pH, 5% CO₂ and oxidative stresses can also be incorporated into the study to screen more mutants affect white to opaque switching and then we will have a broader view to look for an alternate route controlling the white opaque switch.

Appendix: Construction of new strain library

Construction of GRACE version 1.0 library

Derivative library construction

The GRACE 1.0 library for phenotype screening, mating ability identification and drug target discovery was derived from the initial GRACE library, by selecting against the *URA3* marker that was used to direct the integration of the tet transactivator cassette [136]. The GRACE collection strains were inoculated in liquid YPD + uridine medium and cultured at 30°C for 2 days. This culture was then diluted 10- fold in sterile water, and 5 µl of both the original culture and a 10⁻¹ dilution were spotted on SD-5FOA⁺ agar medium separately and cultured at 30°C for 6 days. For each strain, the dilution generating a few single colonies on the plate was identified and a single colony was re-cultured in liquid YPD + uridine medium for 3 days. The new YPD + uridine culture was then sequentially diluted; dilutions (10⁻¹, 10⁻², and 10⁻³) were spotted on YPD + uridine agar medium and cultured at 30°C for 2 days and then single colonies were chosen for each strain and tested for the ura- phenotype. Finally, those strains that failed to grow on SD-ura medium were collected from the corresponding YPD + uridine agar plates and transferred to liquid YPD + uridine medium to prepare the library stock. The original library stock was incubated at 30°C for two days and then was replicated by robotic plating. After incubation for 2 days at 30°C, the new library stocks were mixed with 80% glycerol to final 20% glycerol-supplemented YPD culture and were stored at -80°C in 96-well microtiter plates before use. All liquid media used in the library construction were placed in 96-well microtiter plates and all agar media used above were placed in rectangular Petri dishes.

Library validation

Candidate strains in 96-well plates were plated on fresh YPD uridine agar and incubated at 30°C for two days. Using sterile 200 µl pipet tips, a single patch of each strain was transferred to a new well of a 96-well PCR plate and the cells were dispersed in 25 µl of lysing buffer [12.5 µl of 10X PCR buffer (500 mM KCl, 100 mM Tris-HCl pH 9.0, 15 mM MgCl₂, 1% Triton X-100), 0.5 µl 50X lysis enzyme 20 unit/µl (50 mM Tris-HCl pH 8.4, 100 mM KCl, 50% V/V glycerol,

lyticase (260 unit/mg SIGMA L4025) and 12 μ l of mQ water] in order to extract DNA. PCR plates were incubated for 1h at room temperature and then 100 μ l of mQ sterile water were added to each well. Plates were placed into a thermal-cycler and heated at 95°C for 5 minutes in order to lyse cells and denature proteins. The PCR plates were then centrifuged at 3000 rpm for five minutes in a Beckman Allegra X-12R centrifuge to pellet cellular debris. To test for the loss of the transactivator module by PCR we used primers LR135F and LR135R that amplify a 1.2 kb fragment from the Act1 promoter and TetRGal4 activator. A 10 μ l aliquot of the DNA extracted as described above and rTaq polymerase were used in 50 μ l volume PCR reactions (10 nmol/ μ l dNTPs, 10 nmol/ μ l each primer, 5 U/ μ l rTaq). PCR products were verified using 1% agarose gel electrophoresis.

In the end we obtained 887 *ura3⁻*, 5-FOA resistant strains that had lost the tet transactivator and showed reasonable growth profiles (data not shown). We did loss of heterozygosity (LOH) assays by testing the derivative strains for growth on –his plates and nourseothricin plates because the 5-FOA selection process can result in a simultaneous loss of the *URA3* marker and loss of heterozygosity elsewhere in the genome [137]. The two heterozygous markers, *HIS1* and the cloNAT marker representing the two alleles of each random insertion generating the regulated gene disruption were tested using SD-his⁻ and SD-cloNat⁺ media. Out of all of the mutants, 18.7% lost the *HIS* marker, 5.1% become cloNat sensitive; no strains simultaneously lost both the *HIS1* and cloNAT markers. When these events were distributed over the *C. albicans* chromosomes, we observed the distribution of markers was somewhat correlated with chromosome size; in general, the larger chromosomes (R, 1 and 2) show higher frequencies of LOH than the smaller chromosomes (5 and 6).

Table A.1 Loss of heterozygosity of GRACE 1.0 library.

	Chr1	Chr2	Chr3	Chr4	Chr5	Chr6	Chr7	ChrR
Distribution of LOH	3.40%	4.15%	2.50%	3.00%	1.30%	1.20%	2.50%	4.00%
Chromosome Size	3.2	2.2	1.8	1.6	1.2	1	0.95	2.5

The 887 strains of the Grace 1.0 collection were arrayed in seventeen 96-well microtiter plates. The arrangement of the strains was designed to minimize artifacts due to effects of

growth on the edges of plates, and to provide an independent bar-code confirmation for each plate. All the edges are occupied by the wild-type parent strain CaSS1, and each plate has a unique barcode in the last 6 inner wells (G6 to G11) consisting of various patterns of CaSS1 and the morphologically distinct mutant *dig1/dig1* strain (Fig. A.1).

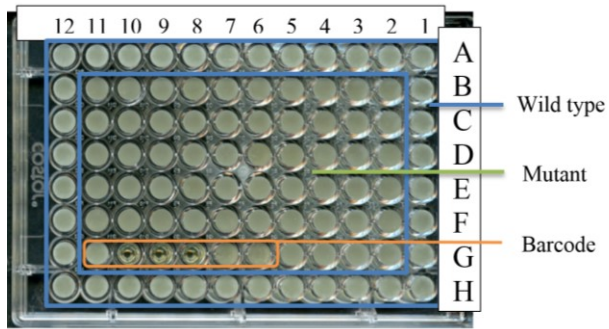


Figure A.1 Strain arrangement of GRACE 1.0 collection.

Chapter 8: References

1. NCBI. 2017. Available from:
<http://www.ncbi.nlm.nih.gov/Taxonomy/Browser/wwwtax.cgi?mode=Info&id=237561&lvl=3&lin=f&keep=1&srchmode=1&unlock>.
2. Brand A. Hyphal growth in human fungal pathogens and its role in virulence. *International journal of microbiology*. 2011;2012.
3. Schulze J, Sonnenborn U. Yeasts in the gut: from commensals to infectious agents. *Dtsch Arztebl Int*. 2009;106(51-52):837-42.
4. Truss CO. Restoration of immunologic competence to *Candida albicans*. *Journal of Orthomolecular Psychology*. 1980;9(4).
5. Denning DW. Epidemiology and pathogenesis of systemic fungal infections in the immunocompromised host. *Journal of antimicrobial chemotherapy*. 1991;28(suppl B):1-16.
6. Mårdh P-A, Rodrigues AG, Genç M, Novikova N, Martinez-de-Oliveira J, Guaschino S. Facts and myths on recurrent vulvovaginal candidosis—a review on epidemiology, clinical manifestations, diagnosis, pathogenesis and therapy. *International journal of STD & AIDS*. 2002;13(8):522-39.
7. Vincent JL, Anaissie E, Bruining H, Demajo W, El-Ebiary M, Haber J, et al. Epidemiology, diagnosis and treatment of systemic *Candida* infection in surgical patients under intensive care. *Intensive care medicine*. 1998;24(3):206-16.
8. Johnson A. The biology of mating in *Candida albicans*. *Nature Reviews Microbiology*. 2003;1(2):106-16.
9. Soll DR, Lockhart SR, Zhao R. Relationship between switching and mating in *Candida albicans*. *Eukaryotic cell*. 2003;2(3):390-7.
10. Magee B, Magee P. Induction of mating in *Candida albicans* by construction of MTL α and MTL β strains. *Science*. 2000;289(5477):310-3.
11. Hull CM, Johnson AD. Identification of a mating type-like locus in the asexual pathogenic yeast *Candida albicans*. *Science*. 1999;285(5431):1271-5.
12. Miller MG, Johnson AD. White-opaque switching in *Candida albicans* is controlled by mating-type locus homeodomain proteins and allows efficient mating. *Cell*. 2002;110(3):293-302.
13. Zordan RE, Miller MG, Galgoczy DJ, Tuch BB, Johnson AD. Interlocking transcriptional feedback loops control white-opaque switching in *Candida albicans*. *PLoS Biol*. 2007;5(10):e256.

14. Huang G, Wang H, Chou S, Nie X, Chen J, Liu H. Bistable expression of WOR1, a master regulator of white–opaque switching in *Candida albicans*. *Proceedings of the National Academy of Sciences*. 2006;103(34):12813-8.
15. Alby K, Schaefer D, Bennett RJ. Homothallic and heterothallic mating in the opportunistic pathogen *Candida albicans*. *Nature*. 2009;460(7257):890-3.
16. Hiller E, Zavrel M, Hauser N, Sohn K, Burger-Kentischer A, Lemuth K, et al. Adaptation, adhesion and invasion during interaction of *Candida albicans* with the host–focus on the function of cell wall proteins. *International Journal of Medical Microbiology*. 2011;301(5):384-9.
17. Biswas S, Van Dijck P, Datta A. Environmental sensing and signal transduction pathways regulating morphopathogenic determinants of *Candida albicans*. *Microbiology and Molecular Biology Reviews*. 2007;71(2):348-76.
18. Chandra J, Kuhn DM, Mukherjee PK, Hoyer LL, McCormick T, Ghannoum MA. Biofilm formation by the fungal pathogen *Candida albicans*: development, architecture, and drug resistance. *Journal of bacteriology*. 2001;183(18):5385-94.
19. Kennedy MJ, Rogers AL, Hanselmen LR, Soll DR, Yancey Jr RJ. Variation in adhesion and cell surface hydrophobicity in *Candida albicans* white and opaque phenotypes. *Mycopathologia*. 1988;102(3):149-56.
20. Soll DR. The role of phenotypic switching in the basic biology and pathogenesis of *Candida albicans*. *Journal of oral microbiology*. 2014;6.
21. Soll DR. High-frequency switching in *Candida albicans*. *Clinical Microbiology Reviews*. 1992;5(2):183-203.
22. Anderson J, Mihalik R, Soll DR. Ultrastructure and antigenicity of the unique cell wall pimple of the *Candida* opaque phenotype. *Journal of bacteriology*. 1990;172(1):224-35.
23. Anderson JM, Soll DR. Unique phenotype of opaque cells in the white-opaque transition of *Candida albicans*. *Journal of Bacteriology*. 1987;169(12):5579-88.
24. Guan G, Xie J, Tao L, Nobile CJ, Sun Y, Cao C, et al. Bcr1 plays a central role in the regulation of opaque cell filamentation in *Candida albicans*. *Molecular microbiology*. 2013;89(4):732-50.
25. Liang W, Guan G, Dai Y, Cao C, Tao L, Du H, et al. Lactic acid bacteria differentially regulate filamentation in two heritable cell types of the human fungal pathogen *Candida albicans*. *Molecular Microbiology*. 2016.
26. Pappas PG, Rex JH, Sobel JD, Filler SG, Dismukes WE, Walsh TJ, et al. IDSA GUIDELINES-Guidelines for Treatment of Candidiasis. *Clinical Infectious Diseases*. 2004;38(2):161-89.

27. Huang G. Regulation of phenotypic transitions in the fungal pathogen *Candida albicans*. *Virulence*. 2012;3(3):251-61.
28. Poulter R, Hanrahan V, Jeffery K, Markie D, Shepherd M, Sullivan PA. Recombination analysis of naturally diploid *Candida albicans*. *Journal of bacteriology*. 1982;152(3):969-75.
29. Lockhart SR, Pujol C, Daniels KJ, Miller MG, Johnson AD, Pfaller MA, et al. In *Candida albicans*, white-opaque switchers are homozygous for mating type. *Genetics*. 2002;162(2):737-45.
30. Tsong AE, Miller MG, Raisner RM, Johnson AD. Evolution of a combinatorial transcriptional circuit: a case study in yeasts. *Cell*. 2003;115(4):389-99.
31. Xie J, Du H, Guan G, Tong Y, Kourkoumpetis TK, Zhang L, et al. N-acetylglucosamine induces white-to-opaque switching and mating in *Candida tropicalis*, providing new insights into adaptation and fungal sexual evolution. *Eukaryotic cell*. 2012;11(6):773-82.
32. Porman AM, Alby K, Hiraakawa MP, Bennett RJ. Discovery of a phenotypic switch regulating sexual mating in the opportunistic fungal pathogen *Candida tropicalis*. *Proceedings of the National Academy of Sciences*. 2011;108(52):21158-63.
33. Hickman MA, Zeng G, Forche A, Hiraakawa MP, Abbey D, Harrison BD, et al. The/obligate diploid/'*Candida albicans* forms mating-competent haploids. *Nature*. 2013;494(7435):55-9.
34. Lachke SA, Srikantha T, Soll DR. The regulation of EFG1 in white–opaque switching in *Candida albicans* involves overlapping promoters. *Molecular microbiology*. 2003;48(2):523-36.
35. Lu H, Sun Y, Jiang Y-Y, Whiteway M. Ste18p is a positive control element in the mating process of *Candida albicans*. *Eukaryotic cell*. 2014;13(4):461-9.
36. Dohlman HG, Song J, Apanovitch DM, DiBello PR, Gillen KM, editors. Regulation of G protein signalling in yeast. *Seminars in cell & developmental biology*; 1998: Elsevier.
37. Kurjan J. The pheromone response pathway in *Saccharomyces cerevisiae*. *Annual review of genetics*. 1993;27(1):147-79.
38. Monge RA, Roman E, Nombela C, Pla J. The MAP kinase signal transduction network in *Candida albicans*. *Microbiology*. 2006;152(4):905-12.
39. Dignard D, El-Naggar AL, Logue ME, Butler G, Whiteway M. Identification and characterization of MFA1, the gene encoding *Candida albicans* a-factor pheromone. *Eukaryotic cell*. 2007;6(3):487-94.
40. Panwar SL, Legrand M, Dignard D, Whiteway M, Magee PT. MF α 1, the gene encoding the α mating pheromone of *Candida albicans*. *Eukaryotic cell*. 2003;2(6):1350-60.
41. Bennett RJ, Uhl MA, Miller MG, Johnson AD. Identification and characterization of a *Candida albicans* mating pheromone. *Molecular and Cellular Biology*. 2003;23(22):8189-201.

42. Roemer T, Jiang B, Davison J, Ketela T, Veillette K, Breton A, et al. Large - scale essential gene identification in *Candida albicans* and applications to antifungal drug discovery. *Molecular microbiology*. 2003;50(1):167-81.
43. Fonzi WA, Irwin MY. Isogenic strain construction and gene mapping in *Candida albicans*. *Genetics*. 1993;134(3):717-28.
44. Bardwell L. A walk-through of the yeast mating pheromone response pathway. *Peptides*. 2004;25(9):1465-76.
45. Merlini L, Dudin O, Martin SG. Mate and fuse: how yeast cells do it. *Open biology*. 2013;3(3):130008.
46. Banuett F. Signalling in the yeasts: an informational cascade with links to the filamentous fungi. *Microbiology and Molecular Biology Reviews*. 1998;62(2):249-74.
47. Wu W, Pujol C, Lockhart SR, Soll DR. Chromosome loss followed by duplication is the major mechanism of spontaneous mating-type locus homozygosis in *Candida albicans*. *Genetics*. 2005;169(3):1311-27.
48. Ramírez-Zavala B, Reuß O, Park Y-N, Ohlsen K, Morschhauser J. Environmental induction of white-opaque switching in *Candida albicans*. *PLoS Pathog*. 2008;4(6):e1000089-e.
49. Srikantha T, Borneman AR, Daniels KJ, Pujol C, Wu W, Seringhaus MR, et al. TOS9 regulates white-opaque switching in *Candida albicans*. *Eukaryotic cell*. 2006;5(10):1674-87.
50. Zordan RE, Galgoczy DJ, Johnson AD. Epigenetic properties of white–opaque switching in *Candida albicans* are based on a self-sustaining transcriptional feedback loop. *Proceedings of the National Academy of Sciences*. 2006;103(34):12807-12.
51. Pujol C, Daniels KJ, Lockhart SR, Srikantha T, Radke JB, Geiger J, et al. The closely related species *Candida albicans* and *Candida dubliniensis* can mate. *Eukaryotic cell*. 2004;3(4):1015-27.
52. Pendrak ML, Yan SS, Roberts DD. Hemoglobin regulates expression of an activator of mating-type locus α genes in *Candida albicans*. *Eukaryotic cell*. 2004;3(3):764-75.
53. Xie J, Tao L, Nobile CJ, Tong Y, Guan G, Sun Y, et al. White-opaque switching in natural MTL α /alpha isolates of *Candida albicans*: evolutionary implications for roles in host adaptation, pathogenesis, and sex. *PLoS Biol*. 2013;11(3):e1001525.
54. Tao L, Du H, Guan G, Dai Y, Nobile CJ, Liang W, et al. Discovery of a “white-gray-opaque” tristable phenotypic switching system in *Candida albicans*: roles of non-genetic diversity in host adaptation. *PLoS Biol*. 2014;12(4):e1001830.

55. Pande K, Chen C, Noble SM. Passage through the mammalian gut triggers a phenotypic switch that promotes *Candida albicans* commensalism. *Nature genetics*. 2013;45(9):1088-91.
56. Wellington M, Rustchenko E. 5 - Fluoro - orotic acid induces chromosome alterations in *Candida albicans*. *Yeast*. 2005;22(1):57-70.
57. Dignard D, André D, Whiteway M. Heterotrimeric G-protein subunit function in *Candida albicans*: both the α and β subunits of the pheromone response G protein are required for mating. *Eukaryotic cell*. 2008;7(9):1591-9.
58. Dignard D, Whiteway M. SST2, a regulator of G-protein signaling for the *Candida albicans* mating response pathway. *Eukaryotic cell*. 2006;5(1):192-202.
59. Willis MA, Song F, Zhuang Z, Krajewski W, Chalamasetty VR, Reddy P, et al. Structure of Ycil from *Haemophilus influenzae* (HI0828) reveals a ferredoxin - like α / β - fold with a histidine/aspartate centered catalytic site. *Proteins: Structure, Function, and Bioinformatics*. 2005;59(3):648-52.
60. Hayes RP, Lewis KM, Xun L, Kang C. Catalytic mechanism of 5-chlorohydroxyhydroquinone dehydrochlorinase from the YCII superfamily of largely unknown function. *Journal of Biological Chemistry*. 2013;288(40):28447-56.
61. Yeats C, Bentley S, Bateman A. New knowledge from old: in silico discovery of novel protein domains in *Streptomyces coelicolor*. *BMC microbiology*. 2003;3(1):3.
62. Schaefer D, Côte P, Whiteway M, Bennett RJ. Barrier activity in *Candida albicans* mediates pheromone degradation and promotes mating. *Eukaryotic cell*. 2007;6(6):907-18.
63. Tao L, Cao C, Liang W, Guan G, Zhang Q, Nobile CJ, et al. White Cells Facilitate Opposite-and Same-Sex Mating of Opaque Cells in *Candida albicans*. 2014.
64. Hnisz D, Schwarzmüller T, Kuchler K. Transcriptional loops meet chromatin: a dual - layer network controls white - opaque switching in *Candida albicans*. *Molecular microbiology*. 2009;74(1):1-15.
65. Hernday AD, Lohse MB, Fordyce PM, Nobile CJ, DeRisi JL, Johnson AD. Structure of the transcriptional network controlling white - opaque switching in *Candida albicans*. *Molecular microbiology*. 2013;90(1):22-35.
66. Lan C-Y, Newport G, Murillo LA, Jones T, Scherer S, Davis RW, et al. Metabolic specialization associated with phenotypic switching in *Candida albicans*. *Proceedings of the National Academy of Sciences*. 2002;99(23):14907-12.
67. Ene IV, Bennett RJ. The cryptic sexual strategies of human fungal pathogens. *Nature Reviews Microbiology*. 2014;12(4):239-51.

68. Lockhart SR, Daniels KJ, Zhao R, Wessels D, Soll DR. Cell biology of mating in *Candida albicans*. Eukaryotic cell. 2003;2(1):49-61.
69. Whiteway M. Yeast mating: putting some fizz into fungal sex? Current Biology. 2009;19(6):R258-R60.
70. Huang G, Yi S, Sahni N, Daniels KJ, Srikantha T, Soll DR. N-acetylglucosamine induces white to opaque switching, a mating prerequisite in *Candida albicans*. 2010.
71. Alby K, Bennett RJ. Interspecies pheromone signaling promotes biofilm formation and same-sex mating in *Candida albicans*. Proceedings of the National Academy of Sciences. 2011;108(6):2510-5.
72. Biterge B, Schneider R. Histone variants: key players of chromatin. Cell and tissue research. 2014;356(3):457-66.
73. Zunder RM, Rine J. Direct interplay among histones, histone chaperones, and a chromatin boundary protein in the control of histone gene expression. Molecular and cellular biology. 2012;32(21):4337-49.
74. Lockhart SR, Zhao R, Daniels KJ, Soll DR. α -Pheromone-induced "shmooing" and gene regulation require white-opaque switching during *Candida albicans* mating. Eukaryotic cell. 2003;2(5):847-55.
75. Odds FC, Bounoux M-E, Shaw DJ, Bain JM, Davidson AD, Diogo D, et al. Molecular phylogenetics of *Candida albicans*. Eukaryotic Cell. 2007;6(6):1041-52.
76. Miceli MH, Díaz JA, Lee SA. Emerging opportunistic yeast infections. The Lancet infectious diseases. 2011;11(2):142-51.
77. Montelone BA. Yeast mating type. eLS. 2002.
78. Haber JE. Mating-type gene switching in *Saccharomyces cerevisiae*. Annual review of genetics. 1998;32(1):561-99.
79. Srikantha T, Daniels KJ, Pujol C, Sahni N, Yi S, Soll DR. Nonsex genes in the mating type locus of *Candida albicans* play roles in α/α biofilm formation, including impermeability and fluconazole resistance. PLoS Pathog. 2012;8(1):e1002476.
80. Djordjevic S, Driscoll PC. Structural insight into substrate specificity and regulatory mechanisms of phosphoinositide 3-kinases. Trends in biochemical sciences. 2002;27(8):426-32.
81. Flanagan CA, Schnieders EA. Requirement for Yeast Cell Viability. Science. 1993;262:26.
82. Walch-Solimena C, Novick P. The yeast phosphatidylinositol-4-OH kinase *pik1* regulates secretion at the Golgi. Nature cell biology. 1999;1(8):523-5.
83. Beller M, Thiel K, Thul PJ, Jäckle H. Lipid droplets: a dynamic organelle moves into focus. FEBS letters. 2010;584(11):2176-82.

84. Currie E, Guo X, Christiano R, Chitraju C, Kory N, Harrison K, et al. High confidence proteomic analysis of yeast LDs identifies additional droplet proteins and reveals connections to dolichol synthesis and sterol acetylation. *Journal of lipid research*. 2014;55(7):1465-77.
85. Simons K, Ehehalt R. Cholesterol, lipid rafts, and disease. *The Journal of clinical investigation*. 2002;110(5):597-603.
86. Sudbery P, Gow N, Berman J. The distinct morphogenic states of *Candida albicans*. *Trends in microbiology*. 2004;12(7):317-24.
87. Vyas VK, Barrasa MI, Fink GR. A *Candida albicans* CRISPR system permits genetic engineering of essential genes and gene families. *Science advances*. 2015;1(3):e1500248.
88. S.C. Li B, Inc., personal communication. Benchling.
89. Tuch BB, Mitrovich QM, Homann OR, Hernday AD, Monighetti CK, Francisco M, et al. The transcriptomes of two heritable cell types illuminate the circuit governing their differentiation. *PLoS Genet*. 2010;6(8):e1001070.
90. Srikantha T, Tsai LK, Daniels K, Soll DR. EFG1 Null Mutants of *Candida albicans* Switch but Cannot Express the Complete Phenotype of White-Phase Budding Cells. *Journal of bacteriology*. 2000;182(6):1580-91.
91. Pujol C, Srikantha T, Park Y-N, Daniels KJ, Soll DR. Binding Sites in the EFG1 Promoter for Transcription Factors in a Proposed Regulatory Network: A Functional Analysis in the White and Opaque Phases of *Candida albicans*. *G3: Genes | Genomes | Genetics*. 2016;6(6):1725-37.
92. Database CG. 2017. Available from: http://www.candidagenome.org/cgi-bin/protein/proteinPage.pl?dbid=CAL0000199135&seq_source=C.%20albicans%20SC5314%20Assembly%2022.
93. BLAST N. 2017.
94. Browser CGO. 2017.
95. Lohse MB, Johnson AD. White–opaque switching in *Candida albicans*. *Current opinion in microbiology*. 2009;12(6):650-4.
96. Ackerman SH. Atp11p and Atp12p are chaperones for F₁-ATPase biogenesis in mitochondria. *Biochimica et Biophysica Acta (BBA)-Bioenergetics*. 2002;1555(1):101-5.
97. Penefsky HS, Cross R. Structure and mechanism of FoF₁-type ATP synthases and ATPases. *Advances in enzymology and related areas of molecular biology*. 1991;64:173-214.

98. Al-Shawi MK, Parsonage D, Senior AE. Thermodynamic analyses of the catalytic pathway of F1-ATPase from *Escherichia coli*. Implications regarding the nature of energy coupling by F1-ATPases. *Journal of Biological Chemistry*. 1990;265(8):4402-10.
99. Oldham WM, Hamm HE. Heterotrimeric G protein activation by G-protein-coupled receptors. *Nat Rev Mol Cell Biol*. 2008;9(1):60-71. PubMed PMID: 18043707.
100. Tesmer JJ. The quest to understand heterotrimeric G protein signaling. *Nat Struct Mol Biol*. 2010;17(6):650-2. Epub 2010/06/04. doi: 10.1038/nsmb0610-650. PubMed PMID: 20520658; PubMed Central PMCID: PMC2954486.
101. Sprang SR. G protein mechanisms: insights from structural analysis. *Annu Rev Biochem*. 1997;66:639-78. PubMed PMID: 9242920.
102. Hollinger S, Hepler JR. Cellular regulation of RGS proteins: modulators and integrators of G protein signaling. *Pharmacol Rev*. 2002;54(3):527-59. PubMed PMID: 12223533.
103. Dietzel C, Kurjan J. The yeast SCG1 gene: a G alpha-like protein implicated in the a- and alpha-factor response pathway. *Cell*. 1987;50(7):1001-10. PubMed PMID: 3113738.
104. Miyajima I, Nakafuku M, Nakayama N, Brenner C, Miyajima A, Kaibuchi K, et al. GPA1, a haploid-specific essential gene, encodes a yeast homolog of mammalian G protein which may be involved in mating factor signal transduction. *Cell*. 1987;50(7):1011-9. PubMed PMID: 3113739.
105. Whiteway M, Hougan L, Dignard D, Thomas DY, Bell L, Saari GC, et al. The *STE4* and *STE18* genes of yeast encode potential beta and gamma subunits of the mating factor receptor-coupled G protein. *Cell*. 1989;56(3):467-77. PubMed PMID: 2536595.
106. Bardwell L. A walk-through of the yeast mating pheromone response pathway. *Peptides*. 2005;26(2):339-50. PubMed PMID: 15690603.
107. Pryciak PM, Huntress FA. Membrane recruitment of the kinase cascade scaffold protein Ste5 by the Gbetagamma complex underlies activation of the yeast pheromone response pathway. *Genes Dev*. 1998;12(17):2684-97. PubMed PMID: 9732267.
108. Metodiev MV, Matheos D, Rose MD, Stone DE. Regulation of MAPK function by direct interaction with the mating-specific Galpha in yeast. *Science*. 2002;296(5572):1483-6. PubMed PMID: 12029138.
109. Breitreutz A, Boucher L, Tyers M. MAPK specificity in the yeast pheromone response independent of transcriptional activation. *Curr Biol*. 2001;11(16):1266-71. PubMed PMID: 11525741.
110. Butty AC, Pryciak PM, Huang LS, Herskowitz I, Peter M. The role of Far1p in linking the heterotrimeric G protein to polarity establishment proteins during yeast mating. *Science*. 1998;282(5393):1511-6. PubMed PMID: 9822386.

111. Hull CM, Raisner RM, Johnson AD. Evidence for mating of the "asexual" yeast *Candida albicans* in a mammalian host. *Science*. 2000;289(5477):307-10. PubMed PMID: 10894780.
112. Magee BB, Magee PT. Induction of mating in *Candida albicans* by construction of MTL α and MTL α strains. *Science*. 2000;289(5477):310-3. PubMed PMID: 10894781.
113. Chen J, Lane S, Liu H. A conserved mitogen-activated protein kinase pathway is required for mating in *Candida albicans*. *Mol Microbiol*. 2002;46(5):1335-44. PubMed PMID: 12453219.
114. Bennett RJ, Johnson AD. The role of nutrient regulation and the Gpa2 protein in the mating pheromone response of *C. albicans*. *Mol Microbiol*. 2006;62(1):100-19. PubMed PMID: 16987174.
115. Dignard D, Andre D, Whiteway M. Heterotrimeric G-protein subunit function in *Candida albicans*: both the alpha and beta subunits of the pheromone response G protein are required for mating. *Eukaryot Cell*. 2008;7(9):1591-9. PubMed PMID: 18658257.
116. Shpakov AO, Pertseva MN. Signaling systems of lower eukaryotes and their evolution. *Int Rev Cell Mol Biol*. 2008;269:151-282. PubMed PMID: 18779059.
117. Hsueh YP, Xue C, Heitman J. G protein signaling governing cell fate decisions involves opposing Galpha subunits in *Cryptococcus neoformans*. *Mol Biol Cell*. 2007;18(9):3237-49. PubMed PMID: 17581859.
118. Savinon-Tejeda AL, Ongay-Larios L, Valdes-Rodriguez J, Coria R. The KIGpa1 gene encodes a G-protein alpha subunit that is a positive control element in the mating pathway of the budding yeast *Kluyveromyces lactis*. *J Bacteriol*. 2001;183(1):229-34. PubMed PMID: 11114921.
119. Kawasaki L, Savinon-Tejeda AL, Ongay-Larios L, Ramirez J, Coria R. The Gbeta(KISte4p) subunit of the heterotrimeric G protein has a positive and essential role in the induction of mating in the yeast *Kluyveromyces lactis*. *Yeast*. 2005;22(12):947-56. PubMed PMID: 16134098.
120. Navarro-Olmos R, Kawasaki L, Dominguez-Ramirez L, Ongay-Larios L, Perez-Molina R, Coria R. The beta subunit of the heterotrimeric G protein triggers the *Kluyveromyces lactis* pheromone response pathway in the absence of the gamma subunit. *Mol Biol Cell*. 2010;21(3):489-98. Epub 2009/12/18. doi: 10.1091/mbc.E09-06-0472. PubMed PMID: 20016006; PubMed Central PMCID: PMC2814793.
121. Soll DR. Mating - type locus homozygosity, phenotypic switching and mating: a unique sequence of dependencies in *Candida albicans*. *Bioessays*. 2004;26(1):10-20.
122. Whiteway M, Hougan L, Thomas DY. Overexpression of the *STE4* gene leads to mating response in haploid *Saccharomyces cerevisiae*. *Mol Cell Biol*. 1990;10(1):217-22. PubMed PMID: 2104659.
123. Huang G, Yi S, Sahni N, Daniels KJ, Srikantha T, Soll DR. N-acetylglucosamine induces white to opaque switching, a mating prerequisite in *Candida albicans*. *PLoS Pathog*. 2010;6(3):e1000806. Epub

2010/03/20. doi: 10.1371/journal.ppat.1000806. PubMed PMID: 20300604; PubMed Central PMCID: PMC2837409.

124. Dignard D, El-Naggar AL, Logue ME, Butler G, Whiteway M. Identification and characterization of MFA1, the gene encoding *Candida albicans* a-factor pheromone. *Eukaryot Cell*. 2007;6(3):487-94. PubMed PMID: 17209123.

125. Murad AM, Lee PR, Broadbent ID, Barelle CJ, Brown AJ. Clp10, an efficient and convenient integrating vector for *Candida albicans*. *Yeast*. 2000;16(4):325-7. Epub 2000/02/12. doi: 10.1002/1097-0061(20000315)16:4<325::AID-YEA538>3.0.CO;2-#. PubMed PMID: 10669870.

126. Dignard D, Whiteway M. SST2, a regulator of G-protein signaling for the *Candida albicans* mating response pathway. *Eukaryot Cell*. 2006;5(1):192-202. PubMed PMID: 16400182.

127. Srikantha T, Borneman AR, Daniels KJ, Pujol C, Wu W, Seringhaus MR, et al. TOS9 regulates white-opaque switching in *Candida albicans*. *Eukaryot Cell*. 2006;5(10):1674-87. PubMed PMID: 16950924.

128. Cote P, Whiteway M. The role of *Candida albicans* FAR1 in regulation of pheromone-mediated mating, gene expression and cell cycle arrest. *Mol Microbiol*. 2008;68(2):392-404. PubMed PMID: 18346117.

129. Hirschman JE, Jenness DD. Dual lipid modification of the yeast ggamma subunit Ste18p determines membrane localization of Gbetagamma. *Mol Cell Biol*. 1999;19(11):7705-11. PubMed PMID: 10523659.

130. McIntire WE. Structural determinants involved in the formation and activation of G protein betagamma dimers. *Neurosignals*. 2009;17(1):82-99. PubMed PMID: 19212142.

131. Sondek J, Bohm A, Lambright DG, Hamm HE, Sigler PB. Crystal structure of a G-protein beta gamma dimer at 2.1A resolution. *Nature*. 1996;379(6563):369-74. PubMed PMID: 8552196.

132. Gautam N, Downes GB, Yan K, Kisselev O. The G-protein betagamma complex. *Cell Signal*. 1998;10(7):447-55. PubMed PMID: 9754712.

133. Cote P, Sulea T, Dignard D, Wu C, Whiteway M. Evolutionary reshaping of fungal mating pathway scaffold proteins. *MBio*. 2011;2(1):e00230-10. Epub 2011/01/21. doi: 10.1128/mBio.00230-10. PubMed PMID: 21249169; PubMed Central PMCID: PMC3023161.

134. Yi S, Sahni N, Daniels KJ, Lu KL, Huang G, Garnaas AM, et al. Utilization of the mating scaffold protein in the evolution of a new signal transduction pathway for biofilm development. *MBio*. 2011;2(1):e00237-10. Epub 2011/01/12. doi: 10.1128/mBio.00237-10. PubMed PMID: 21221248; PubMed Central PMCID: PMC3018282.

135. Xie K, Allen KL, Kourrich S, Colon-Saez J, Thomas MJ, Wickman K, et al. Gbeta5 recruits R7 RGS proteins to GIRK channels to regulate the timing of neuronal inhibitory signaling. *Nat Neurosci.* 2010;13(6):661-3. Epub 2010/05/11. doi: 10.1038/nn.2549. PubMed PMID: 20453851; PubMed Central PMCID: PMC2876203.
136. Fox SJ, Shelton BT, Kruppa MD. Characterization of genetic determinants that modulate *Candida albicans* filamentation in the presence of bacteria. *PloS one.* 2013;8(8):e71939.
137. Staab JF, Datta K, Rhee P. Niche-specific requirement for hyphal wall protein 1 in virulence of *Candida albicans*. *PloS one.* 2013;8(11):e80842.